Article

Invention of MK-8262, a Cholesteryl Ester Transfer Protein (CETP) Inhibitor Backup to Anacetrapib with Best-in-Class Properties

Petr Vachal,* Joseph L. Duffy, Louis-Charles Campeau, Rupesh P. Amin, Kaushik Mitra, Beth Ann Murphy, Pengcheng P. Shao, Peter J. Sinclair, Feng Ye, Revathi Katipally, Zhijian Lu, Debra Ondeyka, Yi-Heng Chen, Kake Zhao, Wanying Sun, Sriram Tyagarajan, Jianming Bao, Sheng-Ping Wang, Josee Cote, Concetta Lipardi, Daniel Metzger, Dennis Leung, Georgy Hartmann, Gordon K. Wollenberg, Jian Liu, Lushi Tan, Yingju Xu, Qinghao Chen, Guiquan Liu, Robert O. Blaustein, and Douglas G. Johns

Cite This: https://doi.org/10.1021/acs.jmedchem.1c00959

Read Online

ACCESS | Metrics & More | Article Recommendations | Supporting Information

ABSTRACT: Cholesteryl ester transfer protein (CETP) represents one of the key regulators of the homeostasis of lipid particles, including high-density lipoprotein (HDL) and low-density lipoprotein (LDL) particles. Epidemiological evidence correlates increased HDL and decreased LDL to coronary heart disease (CHD) risk reduction. This relationship is consistent with a clinical outcomes trial of a CETP inhibitor (anacetrapib) combined with standard of care (statin), which led to a 9% additional risk reduction compared to standard of care alone. We discuss here the discovery of MK-8262, a CETP inhibitor with the potential for being the best-in-class molecule. Novel in vitro and in vivo paradigms were integrated to drug discovery to guide optimization informed by a critical understanding of key clinical adverse effect profiles. We present preclinical and clinical evidence of MK-8262 safety and efficacy by means of HDL increase and LDL reduction as biomarkers for reduced CHD risk.
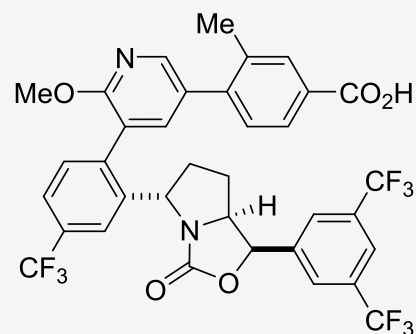
MK-8262

INTRODUCTION

Cardiovascular disease represents a major and persistent global health risk, accounting for approximately 31% of all deaths worldwide in 2019. Significant gains have been made toward reversing this risk, including standard-of-care pharmaceuticals such as statins and β blockers. Additional successful interventions include the surgical implantable cardioverter defibrillator (ICD) devices—with and without resynchronization therapy—and improved lifestyle choices due to increased health awareness. However, cardiovascular disease, mainly coronary heart disease (CHD) and stroke, remains the leading cause of death.[1] Additional clinically relevant mechanisms combined with current standard of care bear the potential for dramatically impacting human mortality caused by cardiovascular disease. One of the key contributors to cardiovascular disease is CHD caused in part by atherogenic lipoprotein deposition and inflammatory infiltration. As such, the further reduction of CHD presents an attractive intervention for the reduction of overall cardiovascular disease risk.

The primary rationale for pursuing cholesteryl ester transfer protein (CETP) as a target to combat CHD was rooted in epidemiological evidence associating elevated HDL cholesterol (HDL-C) with reduced cardiovascular risk.[2−6] Studies on HDL particle biology over the past few decades have demonstrated anti-atherogenic functionalities of HDL,[7−11] supporting the notion that increasing HDL-C, or increasing the number of circulating HDL particles, could confer cardiovascular protection. Epidemiological studies and numerous statin clinical trials strongly demonstrated that elevated LDL-cholesterol (LDL-C) was positively associated with elevated cardiovascular risk. Figure 1 depicts the role of CETP in mediating transfer of neutral lipids (i.e., cholesteryl ester and triglycerides) between HDL and LDL particle types. One hypothesized mode of CETP's mediation of neutral lipid transfer is that CETP serves as a "tunnel" through which these particles migrate.[12] When this tunnel is closed, as when CETP is inhibited, cholesteryl ester and triglycerides can no longer equilibrate. Inhibition of CETP then results in an increase in the cholesteryl ester content of HDL particles (manifest as an increase in plasma HDL-C) and in a concomitant decrease in the level of circulating LDL-C. Since the emergence of the earliest clinical-stage CETP inhibitors (i.e., torcetrapib), further genetic evidence supported the potential for CETP inhibition, and this may have fueled the development

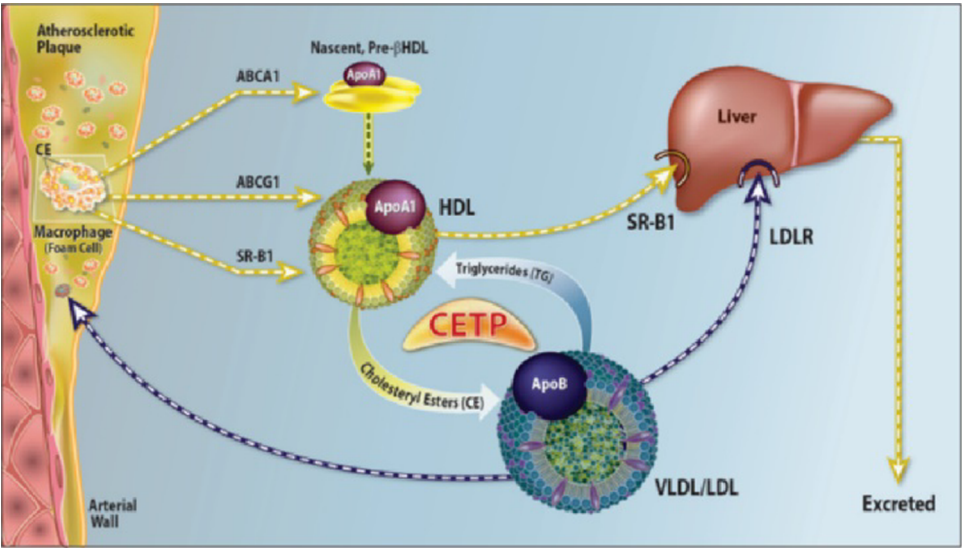**Figure 1.** HDL and LDL metabolism; reverse cholesterol transport. Only LDL can deposit into macrophages but both HDL and LDL are cleared through the liver. CETP facilitates equilibration between HDL and LDL; CETP inhibition leads to a significant increase of circulating HDL-C and reduction of LDL-C.

Table 1. Summary of Clinical Results for CETP Inhibitors

Row	Clinical CETPi	Torcetrapib	Dalcetrapib	Evacetrapib	Obicetrapib	Anacetrapib
1	Company	Pfizer	Roche DalCor	Lilly	Amgen, Dezima, Mitsubishi-Tanabe, New Amsterdam Pharma	Merck & Co., Inc.
2	Chemical structure					
3	Status in 2010	Discontinued	Ph-3 in progress	Ph-2b completed	Ph-1 completed	Ph-3 (REVEAL) in progress
4	Clinical trial	Ph-3 ILLUMINATE	Ph-3 Dal-OUTCOMES Dal-genE	Ph-3 ACCELERATE	Ph-2 TULIP	Ph-3 DEFINE Ph-3 REVEAL
5	LDL-C	-25%	-2%	-40%	-40%	-40%
	HDL-C	+72%	+31%	+132%	+138%	+138%
6	Current Status	Discontinued (safety)	Dal-OUTCOMES discontinued Dal-genE in progress[24]	Discontinued (futility)[25]	Completed Ph-2[26] Ph-3 initiating 2021[27]	Completed; 9% additional risk reduction[16,17] Strategic suspension

of additional CETP candidates, including dalcetrapib, evacetrapib, and anacetrapib.[13−15]

The clinical outcomes trials of CETP inhibitors were designed to test whether the elevation of HDL-C and/or the added reduction of LDL-C beyond statin therapy would further reduce the risk of CHD. At the time of the initiation of the backup molecule for anacetrapib, the CETP outcomes trials had either failed (torcetrapib) or were in progress. However, we now have

better insight into the beneficial effect of CETP inhibition beyond standard of care. The results of the REVEAL outcomes trial demonstrated that the addition of the CETP inhibitor anacetrapib to atorvastatin for a median duration of 4.1 years yielded an additional 9% relative reduction in CHD compared to atorvastatin therapy alone.[16,17]

Table 1 summarizes key clinical results for CETP inhibitors[18] with two notable time points: row 6 of Table 1 shows current development status, while row 3 shows the status at the time when we were initiating a program aimed at improving on anacetrapib, providing for relevant context to the discovery program described therein. At the start of this backup program, Pfizer had terminated Phase 3 clinical trial (ILLUMINATE) due to statistically significant adverse effects (AEs) as measured by an excess of cardiovascular (CV) deaths that may have been due to blood pressure and plasma aldosterone.[19] It was not clear at that time whether the safety findings from the ILLUMINATE trial resulted from inhibition of CETP and therefore were mechanism-based or were compound-specific. At the same time, Roche was conducting a Phase 3 cardiovascular outcomes trial (dal-OUTCOMES)[20] with dalcetrapib, dubbed a CETP "modulator" rather than "inhibitor" due to presumed covalent, irreversible modification of one or more cysteine residues of the CETP target.[21] Lilly had just completed a Phase 2b trial for evacetrapib but the results were not yet publicly disclosed. Mitsubishi-Tanabe (TA-8995) was holding off further development of their clinical candidate, now known as obicetrapib, after completing Phase 1. The asset TA-8995 has since been acquired, first by Dezima (DEZ-001), then later by Amgen (AMG-899), and most recently by New Amsterdam Pharma. Our clinical candidate anacetrapib was being studied in the first of two Phase 3 trials (DEFINE)[22] aimed at demonstrating the safety of CETP inhibition given the safety signal noted with torcetrapib. A combination of additional preclinical characterization and data from the DEFINE trial provided support to the notion that torcetrapib-related adverse events (AEs) were not CETP mechanism-based, paving a safe path to a larger Phase 3 trial for anacetrapib (REVEAL)[23] aimed at comparing clinical outcomes. The Phase 3 results for other CETP inhibitors are also presented in Table 1.[24−27]

A meaningful backup molecule would need to maintain the full CETP inhibition observed clinically for anacetrapib (DEFINE) and evacetrapib (ACCELERATE). The backup candidate must also differentiate from torcetrapib on safety (ILUMINATE) as well as from dalcetrapib on both mechanism of action and absorption, distribution, metabolism and excretion (ADME). Additionally, evidence was emerging that the long terminal half-life in plasma of anacetrapib seen after the drug was discontinued may have resulted from its accumulation into, and slow washout from adipose tissue.[28−32] Despite these pharmacokinetic concerns, anacetrapib appeared safe in preclinical toxicity evaluations. In clinical studies, anacetrapib was well tolerated with no significant AEs in the two phase 3 clinical trials (DEFINE and REVEAL), which together enrolled over 30 000 patients. Nevertheless, we postulated that a viable backup molecule should be devoid of extended tissue accumulation and retention. Additionally, the ideal backup molecule would show no change in drug exposure between fed and fasted subjects (food effect). The backup should be amenable to conventional formulation enabling fixed-dose combination with a range of statins, which are the standard of care for CHD and on top of which CETP inhibitors would ideally be co-administered. We hypothesized that compounds

that maintained the positive attributes of anacetrapib but are designed with a lower log D would be devoid of significant adipose retention, provide a more tractable terminal half-life, afford similar oral exposure in the fed or fasted state, and be more amenable to conventional formulation. Finally, the backup molecule should utilize multiple pathways for in vivo metabolism and excretion as well as be devoid of pregnane X receptor (PXR) inhibition to avoid drug−drug interaction (DDI) potential. It is noteworthy that anacetrapib inhibited PXR with an IC_{50} of 3.5 μM in vitro. This finding provided the rationale for conducting an early safety clinical study aimed at de-risking the potential for DDI with anacetrapib. This safety trial, as well as any of the subsequent large clinical trials, including Phase 3 trials REVEAL and DEFINE, did not reveal any DDI-related issues for anacetrapib.[33]

■ RESULTS AND DISCUSSION

Figure 2 shows an assay funnel (aka, research operating plan, ROP) designed to enable triage and optimization of molecules
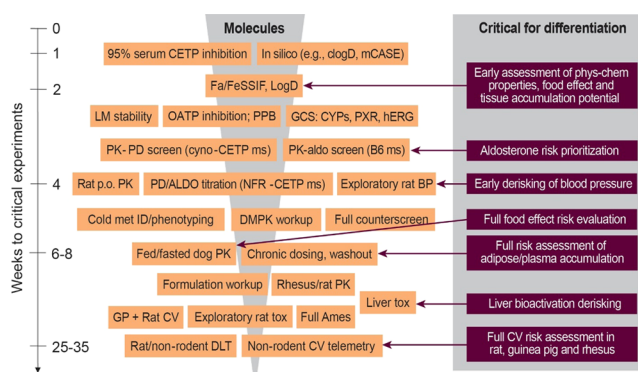
Figure 2. Bioassay hierarchy, aka Research Operating Plan (ROP), for optimization and triage of molecules.

toward the ideal profile defined above. Of note are the following features: first, early Tier 2 high throughput in vitro assessment of physical−chemical properties was demonstrated to correlate well with more sophisticated, lower throughput in vivo food effect and tissue accumulation assays (Tier 7). Early de-risking of the blood pressure signal in a single-dose Tier 5 assay provided a relatively high-throughput early triage well before the formal safety dose-dependent risk assessment in Tier 10, saving a significant amount of time and resources for key molecules. A gene-signature-based risk assessment for drug-induced liver injury (DILI)[34] was performed for key molecules in Tier 8−9.

Structurally diverse CETP inhibitors have shown clinical efficacy for elevation of HDL and reduction of LDL (Table 1). Additional distinct preclinical lead series have been reported from multiple laboratories, including our own.[35,36] We concurrently advanced the structure−activity relationship (SAR) study of the oxazolidinone class of CETP inhibitors characterized by anacetrapib to determine whether further improvements in this class were attainable toward a best-in-class profile.

Anacetrapib has established an outstanding preclinical and clinical safety profile, and robust translational pharmacokinetics. In clinical lipid studies, the efficacy profile is consistent with several other maximally efficacious candidates (Table 1). Our clinical experience with anacetrapib, however, identified features of the profile that could be further improved. Anacetrapib is a

polyfluorinated lipophilic compound with poor aqueous solubility (<1 μM in pH 2 and pH 7 phosphate buffer) and very low calculated total polar surface area (TPSA = 44 Å^2).[37] The log D for the molecule is too high to be accurately measured by an isocratic high-performance liquid chromatography (HPLC) method at pH 7.3. Consistent with these properties, anacetrapib exhibits a positive food effect, with significantly enhanced oral bioavailability when administered with a high-fat meal.[38] The low aqueous solubility of anacetrapib requires clinical formulation as a 12% active pharmaceutical ingredient in a hot-melt extrusion, which could impede a more convenient fixed-dose combination with statin drugs.[39] Anacetrapib is metabolized primarily by the CYP3A4 enzyme in humans, and was found to induce CYP3A4 when incubated with human hepatocytes.[40] Therefore, a compound with diminished agonism of the CYP-inducing PXR would be optimal.[41] Finally, anacetrapib distributes into white adipose tissue in both preclinical species and in humans.[42,43] This biodistribution leads to a biphasic pharmacokinetic elimination profile with a long terminal half-life. We hypothesized that the advantageous profile of the oxazolidinone CETP inhibitor class could be further improved by an anacetrapib derivative that preserved the potency of anacetrapib while exhibiting decreased lipophilicity as measured by TPSA and log D.

A recent review has summarized the SAR strategy that led to the discovery of anacetrapib.[44] This SAR experience guided our lipophilicity investigation toward four regions of the molecule as outlined in Figure 3.[45,46] The 3,5-bistrifluoromethyl substituent
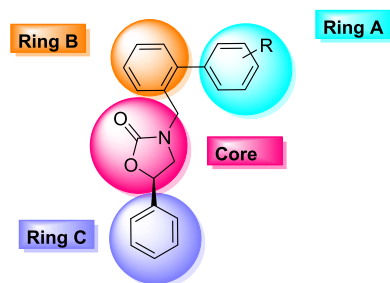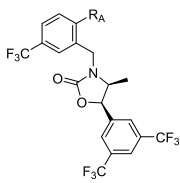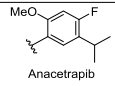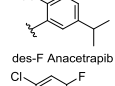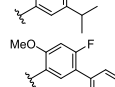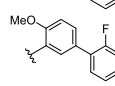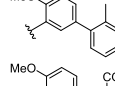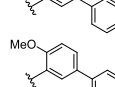

Figure 3. Labeled regions of the oxazolidinone lead class investigated for further optimization to explore improvements on anacetrapib.

in Ring C is common to several reversible CETP inhibitors that have been pursued in the clinic (Table 1), and this substituent was maintained for the first round of investigation. The oxazolidinone "Core" constrains the pharmacophore substituents as a rigid scaffold and was also left intact for the initial investigation. We reasoned that the Ring B and Ring A regions could be amenable to incorporation of more hydrophilic substituents while preserving CETP inhibitory activity.

A broad substitution investigation of the Ring A region was carried out, and representative compounds from this study are provided in Table 2. The compounds were tested for their ability to inhibit CETP-mediated cholesterol ester transfer in 2% human serum using a fluorogenic inhibition assay (CE$_F$) that has been described previously.[47] The compounds were also evaluated for their ability to activate PXR, both for their inflection point (EC$_{50}$) and maximal activation at 10 μM. As the HPLC log D for anacetrapib and close analogues are too high to be accurately measured by isocratic HPLC methods, the molecules were evaluated for the substituent impact on the calculated TPSA as a surrogate for log D.

Table 2. Modification of Ring A (R$_A$) Substituents on Oxazolidinone CETP Inhibitors[b]

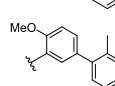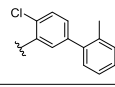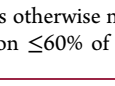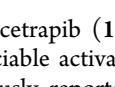| Cpd. #	R$_A$–R	CE$_F$ transfer inhibition		PXR Activation		TPSA
		IC$_{50}$ (nM)[a]	% max at 10 μM	EC$_{50}$ (μM)	% max (10 μM)	Å^2
1	(MeO, F, isopropyl) Anacetrapib	17	> 99	3.9	41	44
2	(MeO, isopropyl) des-F Anacetrapib	7.0	95	2.6	38	44
3	(Cl, F, isopropyl)	30.4	95	7.5	24	32
4	(MeO, F, phenyl)	501[b]	87	> 30	4	41
5	(MeO, 2'-F-phenyl)	41.8[b]	98	> 30	10	43
6	(MeO, 2'-methyl-phenyl)	29.4[b]	94	> 30	20	42
7	(MeO, 2'-CO$_2$H-phenyl)	3,060[b]	96	> 30	3	85
8	(MeO, 4'-CO$_2$H-phenyl)	82.0	> 99	--	--	84
9	(MeO, methyl, CO$_2$H-phenyl)	9.0	> 99	> 30	0	83
10	(Cl, methyl, CO$_2$H-phenyl)	12.7	> 99	> 30	12	74

[a]Unless otherwise noted, IC$_{50}$ values are from >2 assays with standard deviation ≤60% of the reported mean. [b]Single assay determination.

Anacetrapib (**1**) is a potent inhibitor of CETP but retains appreciable activation of PXR and low TPSA. We utilized the previously reported des-F anacetrapib (**2**) as a surrogate for anacetrapib (**1**) for novel experiments during these studies due to the ongoing clinical evaluation of anacetrapib. Replacement of the methoxy substituent with Cl (**3**) diminished PXR activity, but also CETP potency and TPSA. Replacement of the isopropyl substituent with a phenyl (**4**) as substituent "R" significantly reduced the CETP potency, but also fully ablated PXR activity. We found that CETP inhibitory activity could be restored by the addition of an ortho-fluoro substituent (**5**) or methyl (**6**) on the R-phenyl ring without a concomitant increase in activation of PXR. The TPSA was significantly increased by the incorporation of an ortho carboxylic acid (**7**), but with significant loss of CETP potency. The increased TPSA was retained and CETP potency was partially restored by trans-position of the carboxylate to the para position (**8**). Further incorporation of the ortho methyl substituent provided **9**, which improved on anacetrapib in several key parameters. This

Table 3. Solubility, Pharmacokinetics in C57Bl/6 Mice, and Pharmacodynamics in B6-TG Mice

Cpd[a] #	soly pH 7 (μM)[b]	dose IV/PO[c] (mg/kg)	C_{max} (μM)	oral AUC_N (μM·h·kg/mg)	IV CL_b[d] (mL/min/kg)	IV $t_{1/2}$ (h)	F (%)	$\Delta \uparrow$HDL-C[e] (mg/dL)
1	<1	0.6/2	0.28	0.36	11	3.6	15	35
2	<1	1/2	0.16	0.29	19	4.9	17	22
9	16	1/2	0.43	0.86	18	2.5	65	31
10	43	1/2	0.39	1.8	5.6	6.2	43	30

[a]Each value is the mean from at least two mice, with standard deviation (SD) < 30% of the mean. [b]Solubility was measured in pH 7 phosphate buffer. [c]IV dose formulated in DMSO:PEG:water (10:55:35); by mouth dose formulated in DMSO:chremophor:saline (2:4:94). [d]Whole blood total clearance. [e]Mean increase in HDL cholesterol in B6-TG (CETP) mice following BID oral doses at 10 mg/kg.

compound exhibited excellent CETP potency, significantly higher TPSA, and was devoid of PXR activation. Replacement of the ortho methoxy group in **9** with a chloro-substituent (**10**) retained CETP potency in contrast to the decrease observed between the analogous **1** and **3**. The higher calculated TPSA values for **9** and **10** translated to measurable isocratic HPLC log D values of 5.5 and 6.2, respectively.

The carboxyl derivatives **9** and **10** were further profiled. Anacetrapib (**1**), des-fluoro anacetrapib (**2**), as well as both **9** and **10** were devoid of significant inhibitory activity against ion channels Na_v 1.5 and Ca_v1.2 located in the heart and vasculature. However, both **9** and **10** exhibited concerning human Ether-à-go-go-Related Gen (hERG) block, with IC_{50} values of 10 and 5.0 μM, respectively.[48] The compounds **1**, **2**, **9**, and **10** have an undetectable free fraction in plasma from mouse, rat, and human. The pharmacokinetic properties were evaluated in C57Bl/6 mice, and the results are shown in Table 3. In these studies, **10** exhibited the lowest total clearance following an intravenous (iv) dose and a highest oral dose-normalized area under the curve (AUC_N). The compounds were also evaluated for their ability to elevate HDL cholesterol in transgenic C57Bl/6 mice expressing cyno CETP (B6-transgenic, B6-TG mice), using a BID protocol described previously.[46] In this pharmacodynamic screening assay, both **9** and **10** showed comparable efficacy to anacetrapib (**1**) and were slightly superior to des-fluoro anacetrapib (**2**). Compound **10** afforded higher aqueous solubility at neutral pH, which could aid in eventual formulation studies. Therefore, this analogue was evaluated in greater depth.

We postulated that **10**, with a higher TPSA than anacetrapib (**1**), would result in relatively lower tissue accumulation. This was tested by comparing the terminal half-life of **1** and **10** following 7-day dosing in lean B6-TG mice. The compounds were administered orally on a once-a-day basis (QD; anacetrapib at 200 mg/kg/day, and **10** at 100 mg/kg/day to match final plasma concentrations). The blood levels of the compounds were measured for 240 h following the final dose. The results are illustrated in Figure 4. From this experiment, the $t_{1/2}$ of anacetrapib (**1**) was extrapolated to approximately 121 ($\pm$36) h, whereas the $t_{1/2}$ of **10** was 83 ($\pm$46) h. This experiment indicated that CETP inhibitors with reduced lipophilicity may provide a simplified clinical elimination profile as compared to anacetrapib (**1**).[43] However, compounds with even lower lipophilicity would be required to fully establish this relationship.

A significant concern in the clinical development of CETP inhibitors has been the potential for off-target elevation in plasma aldosterone as seen with torcetrapib.[49] We therefore evaluated candidate compounds for aldosterone release in a preclinical screening assay. We optimized a mass-spectrometry (MS)-based assay of mouse plasma to quantify circulating
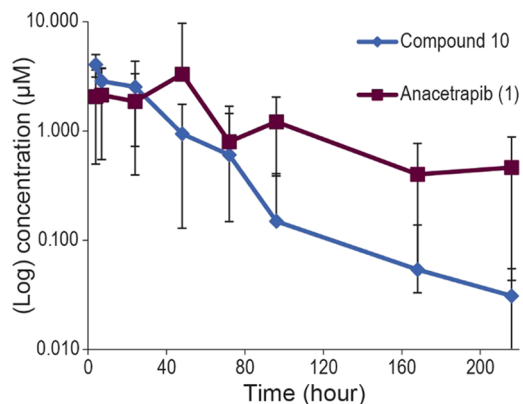

Figure 4. Blood levels of **1** and **10** in C57Bl/6 mice following 7 days of oral dosing at 200 mg/kg for anacetrapib (**1**) ($n = 10$) and 100 mg/kg/day for **10** ($n = 12$).

aldosterone 60 min after an oral dose of CETP inhibitor (see the Supporting Materials (SI)). This assay was used to quantify the exposure window between the no-effect level (NOEL) for aldosterone release relative to the minimum efficacious dose (MED) for full plasma CETP inhibition in CETP transgenic mice. We define this window as the preclinical aldosterone margin (ALDO margin). Note that 100% CETP inhibition is not thought to be achievable due to the ex vivo nature of the CETP activity assays, which rely on measurement of labeled lipid enrichment in exogenously added lipoprotein fractions.[50] Therefore, we identify >75% plasma CETP inhibition in the ex vivo assay as full inhibition. For control experiments, we collected results from preclinical studies with torcetrapib and des-fluoro anacetrapib (**2**), and the aggregated results are illustrated graphically in Figure 5. Following a 100 mg/kg dose, torcetrapib afforded maximal CETP inhibition in mice expressing human CETP, where expression is driven by the natural flanking region promoter (NFR-TG mice).[51] Following a 30 mg/kg dose, torcetrapib exhibited significant aldosterone elevation in B6 mice, providing no margin for efficacy over aldosterone release. This is consistent with the clinical observation for torcetrapib from the ILLUMINATE trial.[52] On the other hand, **2** exhibited no significant aldosterone release at plasma levels of 8.2 μM (100 mg/kg oral dose), whereas maximal plasma CETP inhibition (in cyno-TG mice) could be achieved at plasma levels of 1.1 μM (1 mg/kg dose), affording an aldosterone margin of greater than 7.5×.

The use of cynomolgus transgenic (cyno-TG) mice or NFR-TG mice for control experiments (Torcetrapib or **2**) was determined by the availability of TG mice at the time of profiling but does not impact the interpretation of maximum CETP inhibition. For the investigation of novel compounds, the aldosterone margin experiment was harmonized to utilize
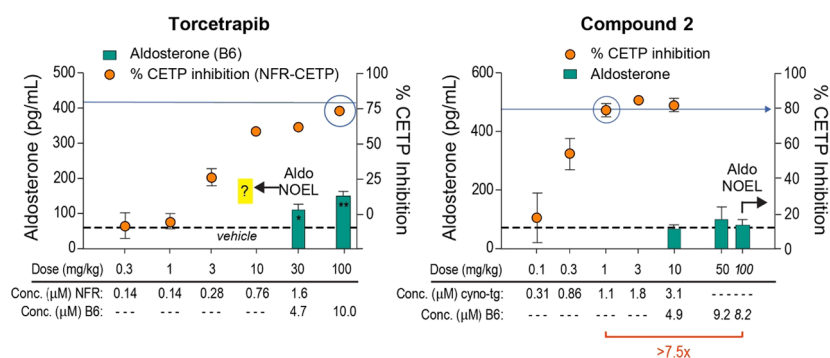
Figure 5. Definition of Aldosterone (ALDO) margin: Plasma concentration ratio of the no-effect level (NOEL) for compound-induced aldosterone elevation (μM) divided by the plasma concentration (μM) at which maximal compound-induced CETP inhibition was observed, in the indicated species (NFR transgenic mice, cyno-tg mice, or C57/B6 mice).
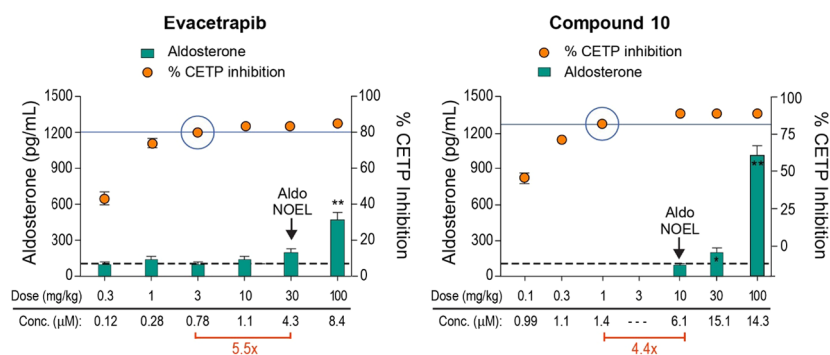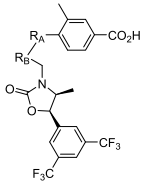

Figure 6. ALDO margin in NFR mice for evacetrapib and **10**.

CETP-TG mice for exposure, aldosterone measurements, and plasma CETP inhibition in a single animal. Using this standard protocol, evacetrapib exhibited an aldosterone margin of 5.5× between the NOEL for aldosterone release and maximal CETP inhibition (Figure 6). These results are consistent with recent clinical data showing no significant elevation of aldosterone following fully efficacious doses of evacetrapib in the ACCELERATE trial.[53] Compound **10** exhibits a lower aldosterone margin than evacetrapib of approximately 4.4×. During the optimization studies outlined here, we used the aldosterone margin as a relative measure to prioritize molecules but not necessarily as an absolute numeral. Given the observed clinical safety of evacetrapib, however, we sought to significantly exceed the 5.5× aldosterone margin observed with this inhibitor in any optimized backup compound to anacetrapib.

The discovery of **9** and **10** established that compounds from the oxazolidinone class with significantly greater solubility and TPSA could maintain the favorable CETP potency and improve the pharmacokinetic (PK) properties of anacetrapib (**1**). We sought to further extend these findings by incorporating heterocycles into the Ring A and Ring B regions of the molecule. The results of these studies are shown in Table 4. For this phase of the program, we improved the primary CETP inhibition assay to the ^{3}[H]-CE transfer method (CE$_T$) that has been described.[54] This method allowed the evaluation of compounds in the presence of 95% human serum, and **1**, **2**, and **10** are included in Table 4 with this method for comparison. The hERG inhibitory potency is also listed, as this activity needed to be further reduced compared to **10**. Finally, the compounds were evaluated for the elevation of aldosterone in NFR-TG mice 60 min following an oral dose. The NOEL for statistically significant aldosterone elevation is provided in terms of both

dose and blood level for the compound. In several cases, a further dose-titration was completed to the point of significant aldosterone elevation. In these experiments, the aldosterone percent increase (as compared to vehicle), dose, and exposure are also provided for the lowest dose affording a significant aldosterone increase (effect level).

Incorporating the 2-methyl-4-carboxyphenyl substituent "R" from **10** into the compounds effectively mitigated the PXR activation for all new entities (EC$_{50}$ > 30 μM), and that substituent was included in all compounds in this series. We discovered that heteroatoms could be incorporated into the R$_B$–R$_A$ region of the molecule without significant loss of intrinsic potency. Incorporation of a pyridyl nitrogen in the 3-position of R$_B$ provided **11**, which maintained CETP potency while significantly reducing the log D and hERG activity. The compound also afforded no significant aldosterone release at higher exposure than the effect level for **10**. Transposition of the pyridyl nitrogen to the 5-position afforded **12**, which was a more potent CETP inhibitor but also significantly more potent for aldosterone release in mice. The R$_A$ pyridyl isomer **13** also maintained CETP potency but was a potent inhibitor of hERG. A combination of the pyridyl regioisomers provided **14**–**16**. The derivative **14** was the most potent CETP inhibitor of the series, but also maintained activity as an hERG inhibitor. Derivatives **15** and **16** exhibited lower potency as CETP inhibitors but were devoid of hERG inhibition. The pyrimidine derivatives **17** and **18** were also somewhat less potent CETP inhibitors but were also devoid of significant hERG inhibition. The amino-pyrimidine derivatives **19**–**23** maintained the lower log D values from this series as well. The most active of these, dimethylaminopyrimidine **19**, is a potent CETP inhibitor and exhibited the highest ALDO NOEL of this series of compounds

Table 4. Heterocycle Incorporation in Ring A−B (R_{A-B}) Substituents on Oxazolidinone CETP Inhibitors[e]

Cpd. #	R =	CE$_T$ transfer inhibition[a] IC$_{50}$ (nM)	% max (10 μM)	hERG block[c] IC$_{50}$ (μM)	LogD HPLC, pH 7.3	Aldost. NOEL[d] μM (mg/kg)	Aldost. % incr. μM (mg/kg)
1 Anacetrapib	[structure]	45	94	> 30	> 6.9	--	--
2 Des-F anacetrapib	[structure]	25[b]	94	> 30	> 6.9	> 9.2[e] (> 100)	--
10	[structure]	43[b]	92	5.0	6.2	6.1 (10)	194 % 15.1 (30)
11	[structure]	54	96	> 30	4.7	> 26 (> 30)	--
12	[structure]	23[b]	92	> 30	5.3	1.0 (1)	109 % 9.5 (10)
13	[structure]	34[b]	>99	0.44	5.4	--	--
14	[structure]	20[b]	>99	2.5	5.1	11 (30)	330 % 12 (100)
15	[structure]	84	91	> 30	5.7	19 (30)	540 % 32 (100)
16	[structure]	134	97	> 30	4.5	> 40 (> 30)	--
17	[structure]	69[b]	> 99	> 30	4.9	28 (30)	389 % 41 (100)
18	[structure]	145[b]	96	> 30	4.9	--	--
19	[structure]	30	91	16	4.8	> 126 (> 100)	--
20	[structure]	46[b]	96	--	--	> 19 (> 100)	--
21	[structure]	94[b]	96	19	4.6	18[e] (30)	305 % 38[e] (100)
22	[structure]	97[b]	95	> 30	5.2	64 (30)	406 % 83 (100)
23	[structure]	170[b]	89	11	4.8	> 52 (10)	--
24	[structure]	82[b]	94	> 30	4.2	27 (10)	65 % 32 (30)
25	[structure]	42[b]	95	19	4.5	> 23 (> 10)	--
26	[structure]	49[b]	93	> 30	4.6	45 (30)	356 % 61 (100)

[a]Unless otherwise noted, IC$_{50}$ values are from >2 assays with standard deviation ≤40% of the reported mean. [b]Single assay determination.

Table 4. continued

[c]hERG inhibition was measured by binding displacement of ^{35}S-labeled MK-0499, a well-characterized hERG blocker. [d]Measured in NFR-TG mice, with standard deviation <40% of the mean ($n = 8$). [e]Measured in cyno-TG mice ($n = 8$).

(>91 μM whole blood exposure), albeit with some hERG activity as well. The methoxypyrimidine 24 was the most hydrophilic compound of the series, with a log D of 4.2. The ethylpyrimidine derivative 25 was relatively more potent as a CETP inhibitor, but also exhibited some hERG inhibition. The hERG inhibition was mitigated by incorporating the electron-withdrawing difluoroethyl substituent (26), which maintained the potency as a CETP inhibitor.

Key compounds from each subseries in Table 4 were profiled further to determine the concentration required for full CETP inhibition in NFR-TG mice, and the results are provided in Table 5. This potency was used with the NOEL for aldosterone release (Table 4) to provide the aldosterone margin. The 24 h shake-flask solubility of the compounds was also evaluated in a pH 7 phosphate buffer to provide an early indication of formulation feasibility. Additionally, we recognized that the aliphatic carboxylic acid substituent incorporated from 10 could be a pharmacophore recognized by the organic anion transporting polypeptides (OATP) transporter. The isoform OATP1B1 is known to transport atorvastatin, and inhibition of this isoform by a CETP inhibitor could result in drug−drug interactions on coadministration.[55] Therefore, several compounds were assessed for OATP1B1 inhibition.

From the compounds listed in Table 5, all achieved maximal CETP inhibition in vivo in NFR-TG mice. The least potent compounds, 10, 17, and 24, required roughly 1 μM blood exposure for complete inhibition, and this was similar to des-fluoro anacetrapib 2. While 12 and 14 exhibited high levels of in vivo CETP potency, the compounds induced significant aldosterone elevation at low exposure as well (10 and 12 μM, respectively, Table 4). Compounds 15, 21, and 26 maintained potent CETP inhibition in vivo and afforded a wide aldosterone margin. The methoxypyrimidine derivative 24 afforded the lowest log D (Table 4) and highest solubility (Table 5) of this series, and inhibited CETP in vivo. Of these final three compounds, 15 and 26 were devoid of hERG inhibition as well. However, we found that all of the carboxyl-containing compounds tested exhibited similar potency for OATP1B1 inhibition in vitro; the significance of this finding is discussed further below.

The R_B−R_A dimethylaminopyrimidine scaffold represented by 19 was utilized for further investigation, owing to the superior exposure, solubility, efficacy, and aldosterone margin of this compound compared to others in the series above. Using this pharmacophore, we next sought to further reduce the lipophilic burden caused by the bis(trifluoromethyl)phenyl moiety present in anacetrapib (Ring C in Figure 3). Substantial effort was devoted to this SAR, and representative compounds are shown in Table 6, where the comparable data for 19 are represented for comparison.

As compared to 19, compounds 27−37 were successful in reducing lipophilicity while maintaining significant CETP inhibition. For example, the pyridyl derivative 36 reduced the HPLC log D by 1.6 as compared to 19, while maintaining CETP inhibition only 3× below anacetrapib 1 (Table 4). Compounds 27 and 31−33 maintained CETP inhibitory activity comparable

Table 5. Solubility, CETP Inhibition and ALDO Margin in NFR-TG Mice, and OATP1B1 Inhibition for CETP Inhibitors

Cpd #	max CETP Inh		Δ ↑HDL-C[a]		ALDO margin	soly pH 7 (μM)[c]	OATP1B1 % Inh at 500 nM
	% Inh[b]	μM (mg/kg)	mg/dL	μM			
2	80[d]	1.1 (1)	36	1.0	≥8.2×	<2	0
10	81	1.4 (1)			4.4×	43	
12	86	≤0.30 (≤0.3)			≥3.2×	29	
14	70	0.13 (0.15)			85×	9	
15	75	≤0.15 (≤0.1)			≥130×	5	67
17	76	0.87 (1)			32×	6	65
19	78	0.24 (0.1)	52	1.3	25×	43	79
21	80	≤0.28 (≤0.3)	28	1.4	≥130×	8	68
24	66[e]	0.90 (0.3)	36	2.0	≤30	52	83
26	80	≤0.40 (≤0.3)			≥110×	20	72

[a]Measured in B6 cyno-TG mice 4 h after a single 30 mg/kg oral dose, with standard deviation ≤10% of the mean (n = 9). [b]CETP inhibition was determined in NFR-TG mice 60 min following an oral dose, as compared to vehicle, with standard deviation ≤40% of the mean (n = 8). [c]Solubility was determined by 24 h shake-flask method in phosphate buffer at 25 °C. [d]Measured in B6 cyno-TG mice (n = 8). [e]Compound CETP inhibition was only examined at 0.3 mg/kg in vivo.

to **19**, but also maintained a comparable block of hERG. Unfortunately, compared to **19**, all derivatives exhibited an increased stimulation of the aldosterone signal at comparable plasma concentration. Importantly, the trifluoromethoxy regioisomer **29** maintained comparable aldosterone stimulation to **28**, despite the complete lack of CETP inhibitory potency of **29**. These results narrowed the prospects of being able to replace the lipophilic bis(trifluoromethyl)phenyl substituent and refocused the SAR effort to balance the CETP activity, aldosterone risk and physical−chemical properties to other parts of the pharmacophore. Therefore, our further evaluation compared compounds that maintained the bis(trifluoromethyl)-phenyl substituent present in anacetrapib.
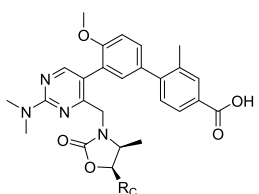
The most advanced molecule, **15**, has been extensively profiled in a panel of preclinical safety assessment assays: no significant safety signal was detected, and the molecule provided a wide aldosterone margin (>130×), as well as a clean off-target profile. As such, compared to close anacetrapib analogues, **15** represents the most advanced preclinical derivative of the series with improved physical−chemical properties. However, **15** maintained a few potential risks common to both itself and anacetrapib, which are discussed below.

Anacetrapib is a very effective CETP inhibitor suitable for QD dosing with a clean off-target profile. Only a few potential liabilities have been identified; physical−chemical properties were the presumed root cause for several concerns for anacetrapib. The food effect observed preclinically and clinically and the potential for tissue accumulation, most notable in adipose tissue, began to emerge from chronic dosing studies. Low solubility and crystallinity posed an additional challenge for development. Ideally, to enable the option of weekly dosing (QW) without the risk of accumulation, an improved molecule would have an extended half-life with no tissue accumulation. Furthermore, anacetrapib exhibited a modest level of PXR inhibition; it is noteworthy, however, that in vitro PXR activity of anacetrapib did not translate into any adverse effects in the clinic. We reasoned that all of these properties may be addressed by further rigidifying the modestly flexible central core pharmacophore conformation of anacetrapib. We postulated that, if the productive conformation responsible for CETP inhibition is favored, a lower overall dose may be sufficient for maintaining full intrinsic inhibition. At the same time, off-target PXR inhibition had been correlated to structural flexibility of the inhibitor and hence a more rigid core was less likely to display

the off-target activity. Theoretically, as depicted in Figure 7, there are three ways to rigidify the core of anacetrapib. We synthesized several examples of each design and found that two of the three designs (Designs A and B) were detrimental to the CETP activity, and several corresponding derivatives lost virtually all inhibitory activity. However, Design C proved to be tolerated for CETP inhibitory properties. The mixture of stereoisomers of Design C were determined to be active in the CETP inhibition assay. Subsequent extensive purification established that the observed activity was solely due to a single stereoisomer of Design C while all of the remaining 7 stereoisomers were inactive. Since our computational approaches were unable to predict the desired stereochemistry in silico, we resorted to synthesizing and separating all 8 isomers to identify the single one that was active (**38**). Isomer **38** inhibited CETP in vitro at levels comparable to anacetrapib (85 vs 45 nM, respectively). But unlike anacetrapib, **38** lacked the undesired PXR inhibition (>30 vs 3 μM, respectively). The first unoptimized fit-for-purpose synthesis of the complex bicyclic Design C utilized to prepare each of the 8 isomers is outlined in Scheme 1.

Encouraged by the initial data on **38**, we explored isosteric derivatives of the novel rigid bicyclic pharmacophore core. Several designs are represented in Figure 8 (see the Supporting Information for detailed synthetic procedures for each derivative). Formal substitution of oxygen for sulfur-generated molecule **46** with an in vitro CETP inhibition of 170 nM, which is less than half as potent as **38**. Other modifications turned out to be more detrimental to CETP inhibition. Lactam **47**, lactone **50**, and thiazolidinone **51** only displayed moderate to low CETP inhibition in vitro. Both urea and sulfonylurea derivatives **48** and **49** warranted further investigation and are the subject of a separate communication. However, overall, neither derivative proved to be advantageous over **38**.[56] A series of spiro-analogues, represented here by **52**, was designed with the idea of invoking central core rigidity through conformational rather than structural constraints. Spiro-analogue **52** displayed good CETP activity in vitro; however, we deprioritized **52** due to increased PXR activity in vitro compared to **38** (PXR EC$_{50}$ for **52** was 2.6 μM while no significant activity was observed for **38** up to 30 μM). We speculate that lesser overall structural rigidity of **52** compared to **38** was the underlying reason for residual PXR off-target activity consistent with monocyclic-core series. In conclusion, none of the central core substitutions led to an

## Table 6. Replacements for Ring C in Oxazolidinone CETP Inhibitors[e]

Cpd. #	R_C	CE_T transfer inhibition[a]		hERG block[b]	LogD	Aldost.	Aldost.
		IC$_{50}$ (nM)	% max (10 µM)	IC$_{50}$ (µM)	HPLC, pH 7.3	% vs. veh.[c]	µM[d]
19	3,5-bis(CF$_3$)phenyl	30	91	16	4.8	62 % (n.s.)	126[e]
27	3-CF$_3$	55	87	9.6	4.1	309 %	84
28	3-OCF$_3$	133	91	17	4.3	243 %	89
29	4-OCF$_3$	10,000	50	3.8	4.3	336 %	68
30	3-Cl	112	90	15	4.0	N/A	N/A
31	CF$_3$, Cl	25	94	20	4.6	416 %	195[e]
32	CF$_3$, F	51	92	25	4.3	197 %	106
33	Cl, Cl	19	96	16	4.6	381 %	99
34	F, F	161	87	11	3.8	327 %	90
35	pyridine, CF$_3$	246	88	> 30	3.3	N/A	N/A
36	pyridine, CF$_3$	143	87	> 30	3.2	347 %	124
37	pyridine, CF$_3$	582	74	22	3.8	811 %	52[e]

[a]Unless otherwise noted, IC$_{50}$ values are from >2 assays with standard deviation ≤40% of the reported mean. [b]hERG inhibition was measured by binding displacement of ^{35}S-labeled MK-0499, a well-characterized hERG blocker. [c]Percent circulating aldosterone vs vehicle (100%) measured in C57/B6 mice 1 h after a 100 mg/kg dose. [d]Whole blood exposure measured 1 h after dose. [e]Compound was dosed 2 × 100 mg/kg at t = 0, 1 h, with aldosterone and exposure measured 1 h after final dose, to achieve comparable exposure.

improvement over 38, prompting a narrowing of our focus on this bicyclic oxazolidinone core.

The fit-for-purpose synthetic route (Scheme 1) utilized for the preparation of 38 and its isomers was not suitable for broader SAR investigation. The cumbersome route limited material supply for 38 and its key analogues, hindering further SAR optimization and profiling deeper into the ROP. We strive for chemical synthesis to ensure that we never restrain drug discovery cycle times. A significant effort was devoted to devise a flexible, high-yielding synthesis that would be divergent at a late-stage and therefore allow derivatization of an advanced common intermediate. Scheme 2 outlines the fruits of this effort. The second-generation synthesis represents a notable improvement over the racemic, low-yielding, nonselective, first-generation fit-for-purpose route (Scheme 1). Starting from commercially

available aldehyde 53, this approach takes advantage of two stereoselective transformations: Ellman diastereoselective alkylation[57] yielding the desired amine 55 in 4:1 selectivity, followed by a highly enantioselective, albeit low-yielding, Shi epoxidation.[58] The final cyclization of the synthetic route led to a partial epimerization of the benzylic stereocenter of 58. While 58 could easily be isolated as a single isomer, a combination of low-yielding Shi epoxidation and epimerization in the final step led to a significant yield erosion. Nevertheless, the second-generation route provided access to a highly functionalized advanced intermediate 58 in 6 steps and a 10% overall yield. This route enabled an initial SAR of the bicyclic pharmacophore as well as a scale-up of 38 needed for additional profiling in vitro and in vivo in the ROP.
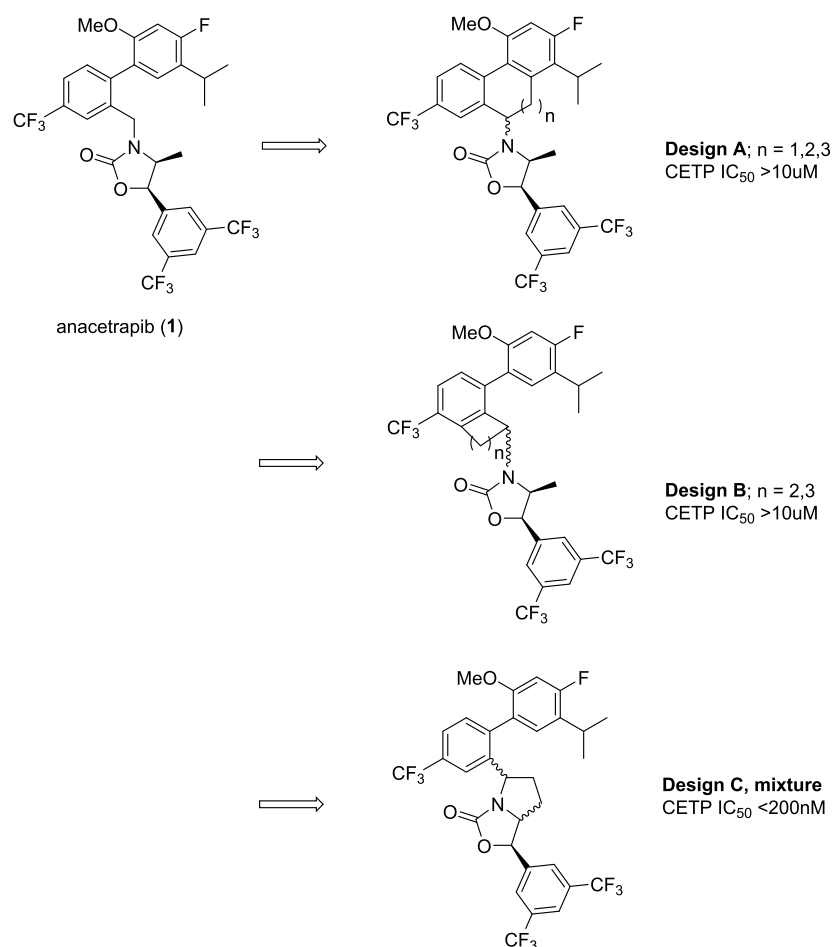
Figure 7. Strategy to increase the rigidity of the anacetrapib pharmacophore aimed at increasing the prevalence of active conformation, reducing the predicted human dose, and limiting PXR off-target activity.

The third-generation approach that was designed to access intermediate **58** with high selectivity starts with a racemic addition of vinyl Grignard to the same commercially available aldehyde **53**, and subsequently to benefit from a catalytic double-stereodifferentiation kinetic resolution promoted by Hartwig[59] or Helmchen[60] iridium catalysts using chiral **60**, yielding a highly functionalized single enantiomer **61** in nearly quantitative yield. A Schrock-[61] or Grubbs-type[62] (Zhan 1B[63]) catalyst-mediated ring-closing metathesis (RCM) of **61**, followed by hydrogenation of olefin **62** with Wilkinson[64] catalyst yielded **58** in just four linear steps, a 40% overall yield, and with full control of enantio- and stereo-selectivity in all steps. Versatile bromide **58** can be readily converted to final candidates under Suzuki conditions with the desired boronic-acid—coupling partner. The third-generation synthetic approach is an outstanding example of synthetic chemistry innovation on the critical path, ultimately enabling drug discovery within a synthetically challenging but pharmacologically preferred scaffold. It was also the basis for the first larger-scale delivery (>10 g) of several key analogues, including **38**.

Equipped with the highly efficient third-generation synthesis, we were able to rapidly generate the SAR of the bicyclic pharmacophore by simply substituting the starting material aldehyde **53** for the desired substitution pattern of ring R_B (Figure 1) within the third-generation synthetic route (Scheme 2c). This approach enabled us to generate numerous advanced cyclic oxazolidinone analogues of **58** and to use an aldehyde

library for modular SAR exploration. Initially, for simplicity of synthesis and with the knowledge of the modular additivity of the SAR established for the monocyclic series, we generated the basic SAR scan in the context of anacetrapib analogues. We eventually envisioned converting the leading set of molecules into their respective ring R_A carboxylic acids, analogous to the anacetrapib and **15** pair in the monocyclic series. We found a reasonable correlation of the CETP activity between the bicyclic and monocyclic series (Table 7). The bicyclic series was less sensitive than the monocyclic analogues to changes of the bottom, highly lipophilic, aromatic ring R_C substitutions, as evidenced by comparing **38** to **63−67**. The bicyclic series also exhibited sensitivity to substitution of the left-hand-side ring R_B with another substituent (**68**), or with a heterocycle, as **70−72** afforded diminished potency compared to trifluoromethylbenzene analogue **38**. The only exception is the equipotent pyridine **69**, which featured the dimethylamino substituent as a potential metabolic liability. In summary, the initial scan suggested that the left-hand-side trifluoromethyl benzene pharmacophore may be preferred but is not unique, while the bottom aromatic ring SAR might be more flexible compared to the monocyclic series (Table 7).

We next turned our attention to the terminal, right-hand-side carboxylic acid moiety of the molecule. We reasoned that with higher intrinsic CETP inhibition and a better off-target profile of the bicyclic series, modification of the carboxylic acid portion of the molecule is a suitable strategy for reducing the overall

Scheme 1. First Fit-for-Purpose Synthesis of Bicyclic Design C (Figure 7) Was Utilized to Prepare Each of the Eight Possible Isomers, Including the Single Active CETP Inhibitor Isomer 38[a]
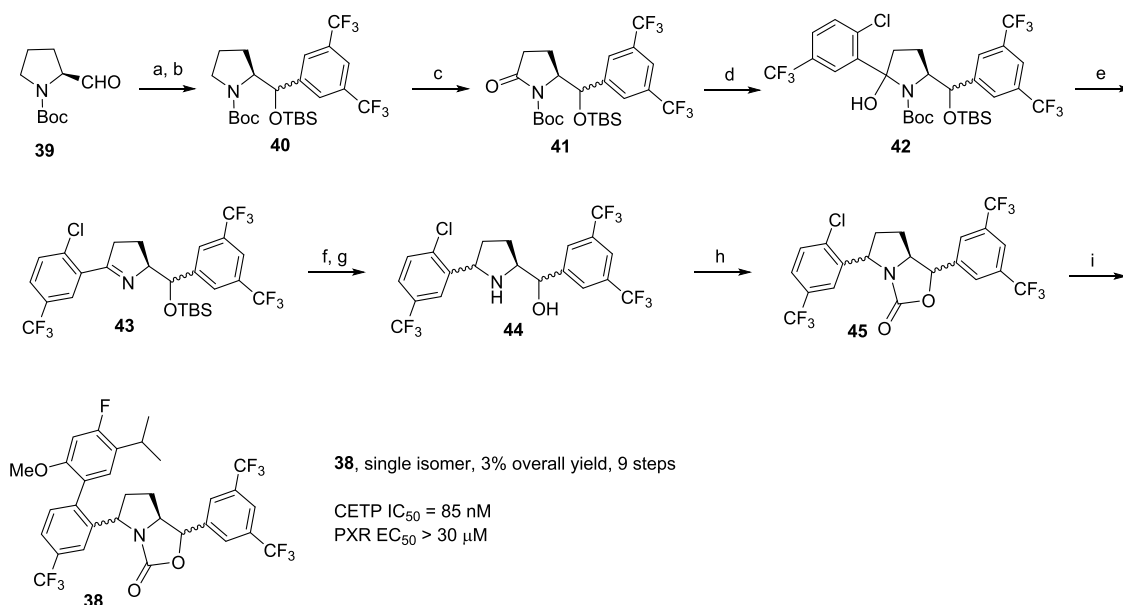
^{a}Reagents, conditions, isolated yield: (a) 1-bromo-3,5-bis(trifluoromethyl)benzene, nBuLi, tetrahydrofuran (THF), −78 °C, 5 min; (b) TBSOTf, 43% (2 steps); (c) $NaIO_4$, $RuCl_3 \cdot H_2O$ EtOAc/water, 22 °C, 15 h, 67%; (d) 2-bromo-1-chloro-4-(trifluoromethyl)benzene, iPrMgCl THF at −78 to 22 °C, 15 h, 71%; (e) trifluoroacetic acid (TFA), dichloromethane (DCM), 22 °C, 30 min; (f) $NaCNBH_4$, methanol, 0 °C, 2 h; (g) tetra-n-butylammonium fluoride (TBAF), 22 °C, 2 h, 39% of mixture of isomers (3 steps); (h) phosgene, toluene, 22 °C, 30 min, 84% (mixture of isomers); (i) (4-fluoro-5-isopropyl-2-methoxyphenyl)boronic acid, $PdOAc_2$, DtBPF, K_3PO_4, THF and water, 70 °C, 15 h, 61% (mixture of isomers separated by chiral chromatography).
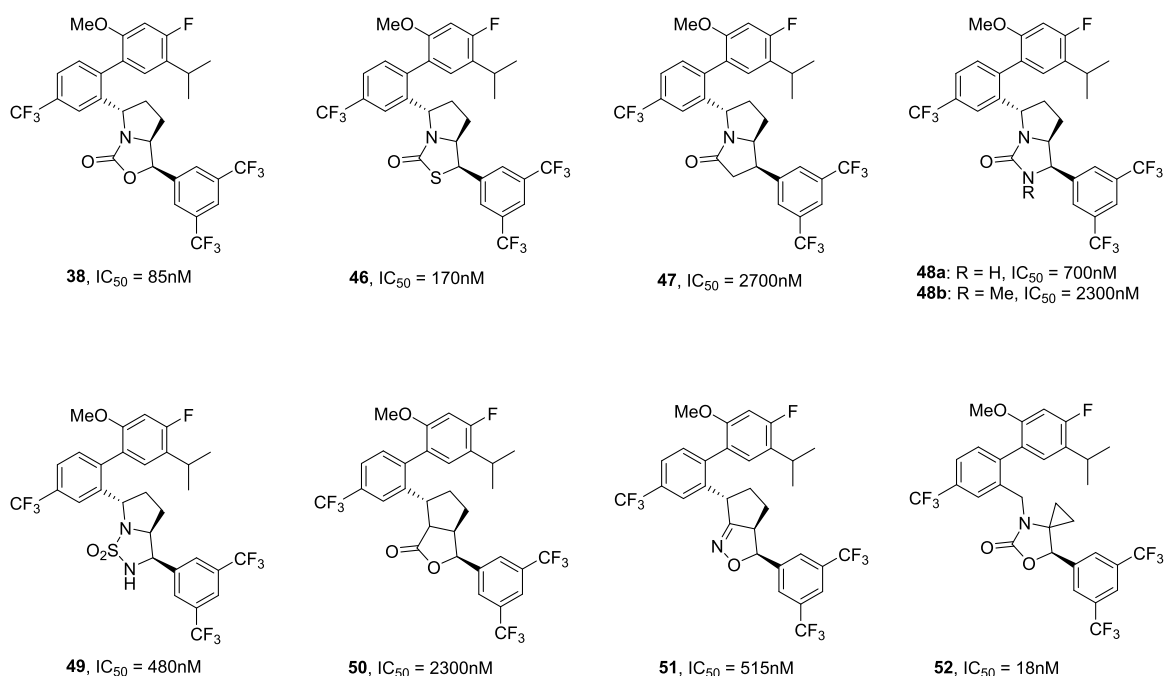
Figure 8. SAR of the central rigid bicyclic core; **46−52** are selected derivatives of **38**.

lipophilicity. We established that calculated log D (clog D) correlated well with experimentally measured log D, which in turn was a good predictor of experimentally measured solubility, pharmacokinetic profiles, food effect and the propensity to be retained in adipose tissue. Proposed permutations of key pharmacophores were assessed computationally for a favorable predicted clog D. Of these, approximately 100 derivatives were

synthesized for in vitro and in vivo profiling. Selected examples of the active CETP inhibitors synthesized in this campaign with key on- and off-target profiles in vitro and in vivo are summarized in Tables 8 and 9.

Compounds **73−91** represent a general design in which the established privileged bis-trifluoromethyl phenyl bicyclic oxazolidinone is substituted with several preferred aryl and

Scheme 2. (b) Second- and (c) Third-Generation Synthetic Strategies for Enabling a Detailed SAR Investigation of the Bicyclic Core Series[a]

(a) **First-Generation route** (not pictured, see Scheme 1): 9 steps, racemic, 3% overall yield to **38**.

(b) **Second-Generation route:** Enantioselective, 6 steps to to Suzuki reaction bromide **58**; 10% overall yield:
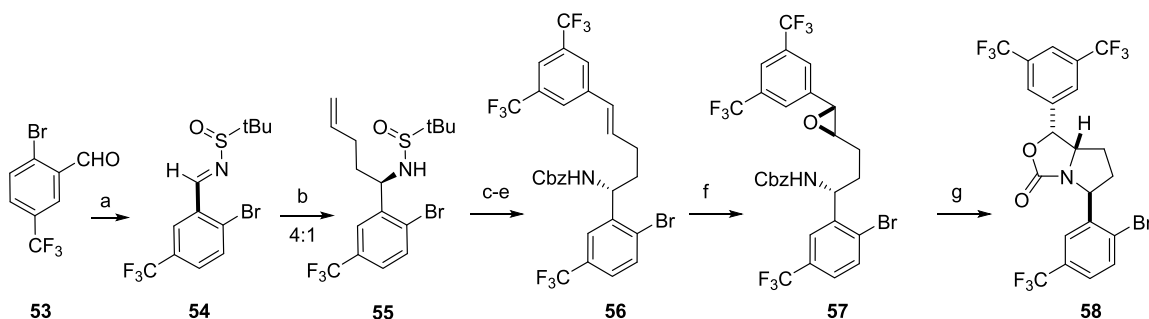
(c) **Third-Generation route:** Double stereodifferentiating kinetic resolution, 4 steps to Suzuki reaction bromide **58**; 40% overall yield:
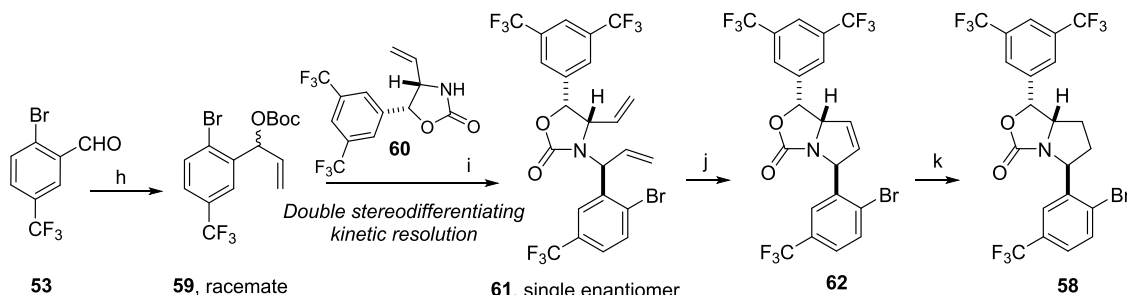
[a]Reagents, conditions, isolated yield: (a) (R)-(+)-2-methyl-2-propanesulfinamide, Ti(OEt)₄, 40 °C, 1 h, 84%; (b) prop-3-en-1-ylmagnesium bromide, DCM, THF, 22 °C, 1 min, 67%; (c) HCl in dioxane, MeOH, 22 °C, 30 min; (d) N,N-diisopropylethylamine (DIEA), DCM, CBZ-Cl, 0 °C, 30 min, 72% (2 steps); (e) 1,3-bis(trifluoromethyl)-5-vinylbenzene, Zhan catalyst (RC301), DCM, 60 °C, 55 min, 90%; (f) sodium tetraborate decahydrate, aqueous ethylenediaminetetraacetic acid disodium salt dihydrate solution, Bu₄NHSO₄ D-Epoxone, CH₃CN and EtOAc, Oxone, 0 °C, 1.5 h, 30% conversion, 67% yield based on recovered starting material; (g) DBU, N,N-dimethylformamide (DMF), microwave 200 °C, 3 min, 68% (mixture of isomers separated by chiral chromatography); (h) vinyl magnesium bromide, THF, 0 °C, 30 min, 67%; (i) (11bS)-N,N-bis((R)-1-phenylethyl)dinaphtho[2,1-d:1′,2′-f][1,3,2]dioxaphosphepin-4-amine, [Ir(COD)Cl]2, DBU, THF, 33 °C, 48 h, 48% based on racemic **59** in kinetic resolution = equivalent of 96% based on **60** (2 steps); (j) 1,3-bis(2,4,6-trimethylphenyl)-4,5-dihydroimidazol-2-ylidene[2-(i-propoxy)-5-(N,N-dimethylaminosulfonyl)phenyl]methyleneruthenium(II) dichloride, toluene, 60 °C, 2 h, 85%; (k) RhCl(PPh₃)₃, 40 psi H₂, ethanol, 22 °C, 15 h, >99%.
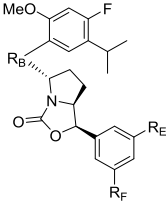
heteroaryl rings (R_B, Table 8). These rings are in turn ortho-substituted by a series of bi-heteroaryl and bi-aryl carboxylic acids R_A. The observed log D (measured by HPLC at pH 7.3), an important in vitro predictor of desired in vivo properties, is generally within the predicted range of 5−6, a notable improvement over log D > 7 for anacetrapib. Log D variability within the range of molecules **73−91** appears to best correlate with the overall polarity and pK_a properties of the heterocycle. With the notable exceptions of compounds **80−81**, **83**, and **86**, derivatives of this design generally exhibited a very clean off-target profile with no activity against a range of ion channels, Cytochrome P450 enzymes (CYPs; neither acutely nor in a time-dependent manner) and PXR (Table 8, "Key off-target findings" column; unless stated otherwise, no significant off-target findings in vitro). One notable exception for the entire structural class was the relatively strong inhibition of the OATP-family of transporters in vitro (in the absence of plasma), which correlated to the presence of the carboxylic acid.

Compounds **92−95** exemplify an effort to further lower the log D by reducing the overall polarity and molecular weight. The hypothesis proved to be correct as each of the four examples

shown in Table 8 further reduced the measured log D compared to their aromatic equivalents, while a high level of CETP inhibition was still observed. Unfortunately, with added flexibility of the carboxylic acid side chain, several off-target findings were noted, including CYP inhibition and ion channel interference. Additionally, and somewhat surprisingly, three of the four derivatives displayed poor aqueous solubility at low pH, reduced further from the observed solubility of the closest aromatic comparator **73**.

The guiding principle for the design of analogues **96−101** was the desire to de-risk the liability of carboxylic acid for the OATP inhibition. While nonacidic derivatives **96−101** generally did not inhibit OATP in vitro, they suffered from a range of undesirable off-target findings, ranging from CYP inhibition to strong ion channel liabilities in vitro. Most importantly, the physical−chemical properties of these molecules deteriorated significantly, consistent with a significant increase in log D. These changes ultimately resulted in an overall dramatic loss in aqueous solubility at both low and high pH. It was reasonable to assume that in addition to the solubility, **96−101** would also

Table 7. Initial SAR Scan of the Bicyclic Pharmacophore of the Leading Molecule 38[c]

Cpd. #	R_B	R_E, R_F	CE_T transfer inhibition[a]		LogD
			IC_{50} (nM)	% max (10 μM)	HPLC, pH 7.3
38[b]	(3,4-bis-CF₃ phenyl)	CF₃, CF₃	82	91	7.1
63	(3,4-bis-CF₃ phenyl)	CF₃, Me	56	95	7.0
64	(3,4-bis-CF₃ phenyl)	CF₃, Cl	150	91	6.5
65	(3,4-bis-CF₃ phenyl)	CF₃, H	22	93	6.1
66	(3,4-bis-CF₃ phenyl)	CF₃, F	71	94	6.3
67	(3,4-bis-CF₃ phenyl)	Cl, Cl	213	89	6.1
68	(F-phenyl)	CF₃, CF₃	470	84	7.0
69	(Me₂N-pyridyl)	CF₃, CF₃	108	87	7.0
70	(Me₂N-pyridyl)	CF₃, CF₃	900	82	6.9
71[c]	(Cl-pyridyl)	CF₃, CF₃	>10000	15	N.D.
72	(Me₂N-pyrimidyl)	CF₃, CF₃	1100	77	7.0

[a]Unless otherwise noted, IC_{50} values are from >2 assays with standard deviation ≤40% of the reported mean. [b]20% not significant increase of circulating aldosterone vs vehicle (100%) measured in C57/B6 mice 1 h after a 30 mg/kg dose. [c]Single assay determination.

likely carry a liability for food effect and tissue retention in vivo and would therefore be unsuitable for further development.

Finally, the most promising permutations of the aryl/heteroaryl R_B (Table 8) ortho-substituted bi-heteroaryl/bi-aryl carboxylic acids R_A were combined with several modifications of the bottom bis-trifluoromethylphenyl ring in the attempt to lower the overall lipophilicity, i.e., the variation of R_E and R_F. Deleting one or both trifluoromethyl substituents led to a significant loss of functional activity (107). However, compared to their bistrifluoromethyl analogues 73, 87, and 91, respectively, substitution of a single trifluoromethyl with fluorine or methyl yielded strong CETP inhibition in vitro, exemplified by 102–106, with the additional benefit of reducing $\log D$. Despite the improvement in physical–chemical properties, methyl derivatives suffered from decreased stability in liver microsome homogenate in vitro as well as decreased aqueous solubility relatively to their trifluoromethyl analogues. Several of these analogues also registered a moderate increase in Nav1.5 off-target activity.

The aggregate of potent CETP inhibition in vitro, lack of off-target activity and favorable $\log D$ guided selection of key derivatives for in vivo evaluation. These compounds were profiled for aldosterone margin determination, rodent pharmacokinetics and telemetrized rat blood pressure evaluation. Compounds 74, 75, 90, 91, and 99 all failed to provide an

acceptable aldosterone margin (Table 8, ALDO column) of at least 10x above the full CETP inhibition in vivo. While 73 and 104 exhibited improved an aldosterone margin of 10× and 85×, respectively, a statistically significant increase in blood pressure (Δ10 mm of mercury) was detected in rats at 15 and 50 mg/kg, respectively, both of which correlated to an approximate 25× margin over the projected plasma exposure needed for a full CETP efficacy in vivo (Table 9). The blood pressure signal for a chronic indication, disqualified both 73 and 104 from consideration for further development, especially given the history of blood pressure signals observed with torcetrapib, which was withdrawn from clinical development.

Compound 87 represents the single molecule in Table 8 meeting the very stringent criteria for a drug candidate intended for chronic dosing: high CETP inhibition in vitro and in vivo at low dose, very clean off-target profile in vitro[65] with no statistically significant blood pressure signal in vivo (Table 9), relatively high 24× aldosterone margin, and good stability profile with no significant cross-species variability in vitro. Compound 87 was selected for a full preclinical safety assessment and larger quantities of this molecule were required. An optimized synthesis specifically tailored to preparation of 87 was developed. Scheme 3 shows the approach that allowed synthesis of 87 in 35% overall yield and seven linear steps from inexpensive commercially available materials. Convergent

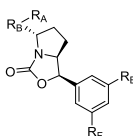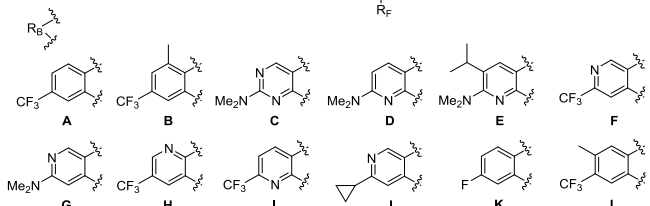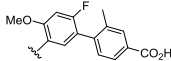## Table 8. Detailed SAR Investigation of the Bicyclic Pharmacophore[h]
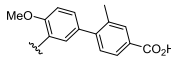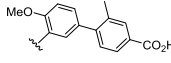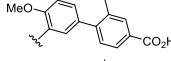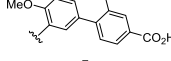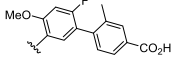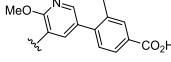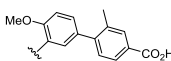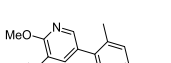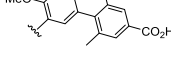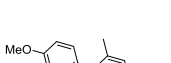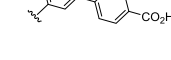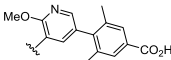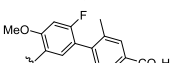
Cpd #	R_A	R_B	R_E / R_F	LogD pH 7.3	CETPi IC$_{50}$ nM[a]	CETPi MED Mg/kg[b]	ALDO	Key off-target findings[c]
73	structure (MeO, F biphenyl, CO$_2$H)	A	CF$_3$ / CF$_3$	5.5	54	1	10x	Nav1.5 = 22µM; Cav 1.2 = 17µM; CYP2C8 = 8 µM; OATP < 1µM, rat BP[d]
74	structure (MeO biphenyl, CO$_2$H)	B	CF$_3$ / CF$_3$	6	87	1	<10x	OATP < 1µM
75	structure (MeO biphenyl, CO$_2$H)	C	CF$_3$ / CF$_3$	5.3	432	10	<1x	OATP < 1µM
76	structure (MeO biphenyl, CO$_2$H)	D	CF$_3$ / CF$_3$	5.8	714			Low stability in LM[e]; OATP N/D
77	structure (MeO biphenyl, CO$_2$H)	E	CF$_3$ / CF$_3$	6.6	182			Low aq. solubility at all pH
78	structure (MeO, F biphenyl, CO$_2$H)	F	CF$_3$ / CF$_3$	4.8	191			Low aq. solubility at low pH; OATP N/D
79	structure (MeO pyridyl, CO$_2$H)	F	CF$_3$ / CF$_3$	4.6	141			CYP2C9 = 21µM; OATP < 1µM
80	structure (MeO biphenyl, CO$_2$H)	G	CF$_3$ / CF$_3$	4.6	276			CYP2C9 = 9µM; MK499 = 2µM, Cav 1.2 = 17µM; OATP < 1µM
81	structure (MeO pyridyl, CO$_2$H)	H	CF$_3$ / CF$_3$	4.5	188			Nav1.5 = 17µM; Cav 1.2 = 7µM; CYP2C8 = 4µM; OATP < 1µM
82	structure (MeO pyridyl, CO$_2$H)	H	CF$_3$ / CF$_3$	4.8	750			CYP2C8 = 11µM; OATP < 1µM
83	structure (MeO biphenyl, CO$_2$H)	H	CF$_3$ / CF$_3$	4.6	427			CYP3A4 = 9µM; CYP2D6 = 9µM; CYP2C9 = 5µM; CYP2C8 = 4µM; OATP < 1µM
84	structure (MeO pyridyl, CO$_2$H)	I	CF$_3$ / CF$_3$	5.8	560			N/D
85	structure (MeO, F biphenyl, CO$_2$H)	J	CF$_3$ / CF$_3$	4.8	614			N/D
86	structure (MeO biphenyl, CO$_2$H)	K	CF$_3$ / CF$_3$	5.1	229			Nav1.5 = 14µM; Cav 1.2 = 16µM; CYP2C9 = 6µM; OATP < 1µM
87[f]	structure (MeO pyridyl, CO$_2$H)	A	CF$_3$ / CF$_3$	5.3	53	0.3	24x	OATP < 1µM

Table 8. continued

Cpd #	R_A	R_B	R_E / R_F	LogD pH 7.3	CETPi IC$_{50}$ nM[a]	CETPi MED Mg/kg[b]	ALDO	Key off-target findings[c]
88	(structure)	L	CF$_3$ / CF$_3$	6	120			Nav1.5 = 5µM; OATP N/D
89	(structure)	L	CF$_3$ / CF$_3$	5.8	106			Low aq. solubility at low pH; OATP N/D
90	(structure)	B	CF$_3$ / CF$_3$	5.7	124	1	<10x	Low aq. solubility at low pH; Nav1.5 = 10µM; OATP N/D
91	(structure)	A	CF$_3$ / CF$_3$	5.4	60	1	7x	OATP < 1µM; rat BP[d]
92	(structure)	A	CF$_3$ / CF$_3$	4.7	128			CYP2C9 = 9µM; CYP2C8 = 2µM; MK499 = 12µM, Cav 1.2 = 7µM; OATP = 2µM
93[g]	(structure)	A	CF$_3$ / CF$_3$	5	154			Low aq. solubility at low pH; CYP2C9 = 9µM; OATP N/D
94	(structure)	A	CF$_3$ / CF$_3$	5.1	97			Low aq. solubility at low pH; CYP2C9 = 3µM; CYP2C8 = 4µM; CYP3A4 = 6µM; MK499 = 4µM, Cav 1.2 = 4µM; OATP N/D
95	(structure)	A	CF$_3$ / CF$_3$	5.6	242			Low aq. solubility at low pH; OATP N/D
96	(structure)	A	CF$_3$ / CF$_3$	5.7				Low aq. solubility at all pH; MK499 = 1.4µM, Cav 1.2 = 7µM; PXR = 7µM; OATP N/D
97 a-d[h]	(structure)	A	CF$_3$ / CF$_3$	5.9	184-607[i]			Low aq. solubility at all pH; PXR 0.3- 5µM; MK499 = 0.2-10µM
98 a-d[h]	(structure)	A	CF$_3$ / CF$_3$	5.5	89-450[i]			Low aq. solubility at all pH; Nav 1.5 = 6µM; MK499 = 5µM; PXR=13µM; OATP >20µM
99[g]	(structure)	A	CF$_3$ / CF$_3$	5.7	246	30	5x	Low aq. solubility at all pH; PXR 2µM; MK499 = 1.2µM; OATP >20µM
100	(structure)	A	CF$_3$ / Me	6.6	95			Low aq. solubility at all pH; MK499 = 200nM; OATP N/D
101	(structure)	A	CF$_3$ / Me	6.9	167			Low aq. solubility at all pH; MK499 = 2.3µM; OATP N/D

O

Table 8. continued

Cpd #	R_A	R_B	R_E R_F	LogD pH 7.3	CETPi IC$_{50}$ nM[a]	CETPi MED Mg/kg[b]	ALDO	Key off-target findings[c]
102	MeO— (structure, F, Me, CO$_2$H)	A	CF$_3$ Me	5.1	85			Low aq. solubility at all pH; low stability in LM; Nav 1.5 12μM; OATP < 1μM
103	MeO— (structure, F, CO$_2$H)	A	CF$_3$ F	5	126		25x	Nav 1.5 = 6μM; CYP2C9 = 16μM; CYP2C8 = 3μM; OATP < 1μM
104	MeO— (structure, N, CO$_2$H)	A	CF$_3$ F	4.8	120		25x	Nav 1.5 = 13μM; CYP2C9 = 27μM; CYP2C8 = 3μM; OATP < 1μM, rat BP[d]
105	MeO— (structure, N, CO$_2$H)	A	CF$_3$ F	4.9	76	0.3	85x	Low aq. solubility at all pH; low stability in LM; CYP2C8 = 3μM; OATP < 1μM
106	MeO— (structure, F, CO$_2$H)	A	CF$_3$ Me	5.3	45			Low aq. solubility at all pH; low stability in LM; Nav 1.5 14μM; CYP2C9 = 9μM; CYP2C8 = 3μM OATP < 1μM
107	MeO— (structure, N, CO$_2$H)	A	CF$_3$ H	4.7	860			N/D

[a]In vitro—unless otherwise noted, IC$_{50}$ values are from >2 assays with standard deviation ≤40% of the reported mean. [b]In vivo—MED, minimum efficacious dose, to maximum CETP inhibition in vivo in NFR-TG-mouse at a dose (mg/kg). [c]Key off-target findings: unless otherwise noted, the following are all in vitro off-target IC$_{50}$ > 30 μM: Cav1.2, Nav1.5, MK499 = Ikr, CYP3A4, 2D6, 2C9, 2C8, PXR, OATP; no TDI signal. [d]Telemetrized rat blood pressure, IV dosing—see Table 9 for details. [e]LM, liver microsome, stability of parent molecule in LM homogenate in vitro. [f]No statistically significant increase in telemetrized rat blood pressure vs vehicle after 50 mg/kg IV dose; see Table 9. [g]Single isomer, absolute stereochemistry not determined. [h]All four isomers isolated, range of on- and off-target activity for all four shown in the entry, log D determined for the most active isomer.

Table 9. Rodent In Vivo Profile of Key Compounds: Mouse Pharmacokinetics and Telemetrized Rat Blood Pressure

Cpd #	mouse pharmacokinetics[a]					rat blood pressure[b]	
	AUCN	MRT	Cl	Vd	F	dose	compound vs vehicle
	(μM/h)	(h)	(mL/min/kg)	(L/kg)	(%)	(mg/kg)	(Δmm Hg)
73	3.4	5.8	6.6	2.3	60	15	10
75	0.7	2.8	33	5.6	140		
87	9.2	6.0	2.6	0.95	43	50	not statistically significant
91						50	10

[a]An average of two experiments per arm, dosed at 1 mg/kg IV and 2 mg/kg by mouth, respectively. [b]Three experiments, dosed at 15 or 50 mg/kg IV, statistically significant blood pressure increase vs vehicle dosed to the same subject over identical time period prior to the administration of the compound.

Suzuki coupling of 114 and 119 was retained; however, the synthesis of chiral fragment 114 was revamped to eliminate the need for chiral separation of building blocks and to reduce cycle times. An approach using readily available pyroglutamic acid derivative 108 was developed in which an anti-organometallic addition to a hemi-aminal 109 proceeded with very high diastereoselectivity setting the two chiral centers across the pyrrolidine ring, yielding 110. The final chiral center was also set via substrate control with a DIBAL reduction of the aryl ketone 111. Deprotection and carbamate formation provided compound 114, which was then ready for end-game coupling. Conditions for the final coupling were optimized for the Cl-coupling partner 114, which was necessary, given that the new

approach made it impossible to carry the bromide (58, Scheme 2) through the sequence. This was readily accomplished using a third-generation XPhos precatalyst.[66]

The mouse aldosterone margin has served as an effective tool for prioritizing molecules across diverse chemical series because it is independent of the absolute value of the on- and off-target activities. The experiment directly correlates two plasma concentrations for the same molecule; the minimum concentration needed for full CETP inhibition (MED) vs the maximum concentration lacking significant aldosterone elevation (NOEL). However, the translation of these preclinical findings to the clinical profile of CETP inhibitors (Table 1) was still hypothetical. Torcetrapib represented a positive control for the

Scheme 3. Optimized Synthetic Strategy for the Scale-Up of Safety Assessment Candidate 87
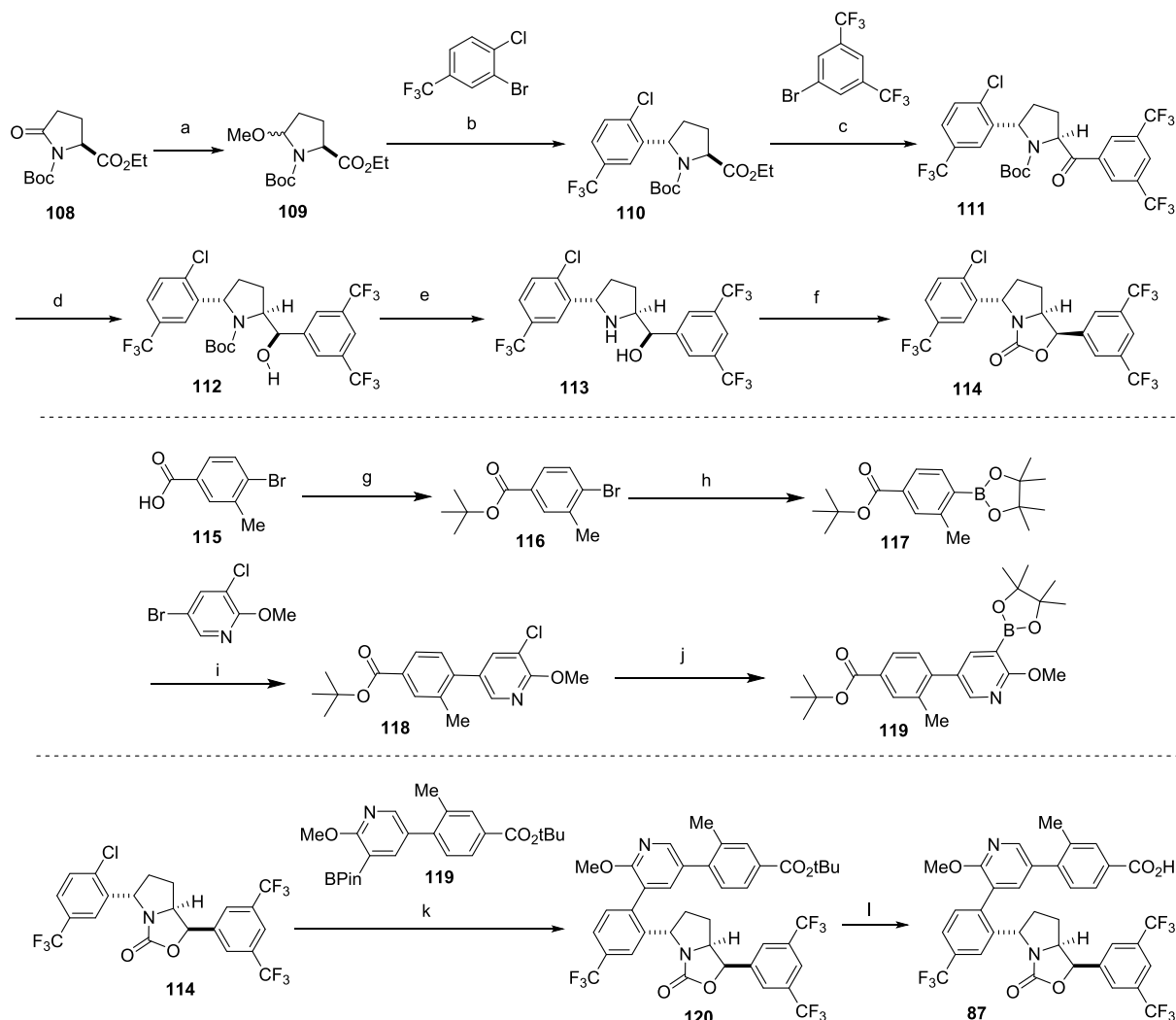
[a]Reagents, conditions, isolated yield. (a) LiBHEt$_3$, pTSA, PhMe-THF, −35 °C, 90%; (b) iPrMgBr, CuBr-Me$_2$S, THF −25 °C, 70%; (c) BuLi, MTBE, −90 °C 72%; (d) DiBAL-H, THF, −5 °C, 93%; (e) HCl, EtOAc, 20 °C, 84%; (f) triphosgene, DCM, 30 °C, 90%; (g) Boc$_2$O, 4-dimethylaminopyridine (DMAP), t-BuOH/MTBE, 40 °C, 92%; (h) Pd(dppf)Cl$_2$, B$_2$Pin$_2$, dioxane, 120 °C, 80%; (i) Pd(dppf)Cl$_2$, PhMe/water, 85 °C; (j) XPhos-Palladium Generation 3 precatalyst, B$_2$Pin$_2$, dioxane, 85 °C, 90%; (k) XPhos-Palladium Generation 3 precatalyst, K$_3$PO$_4$, THF/water, 60 °C, 92%; (l) TFA, toluene, 55 °C, 97%.
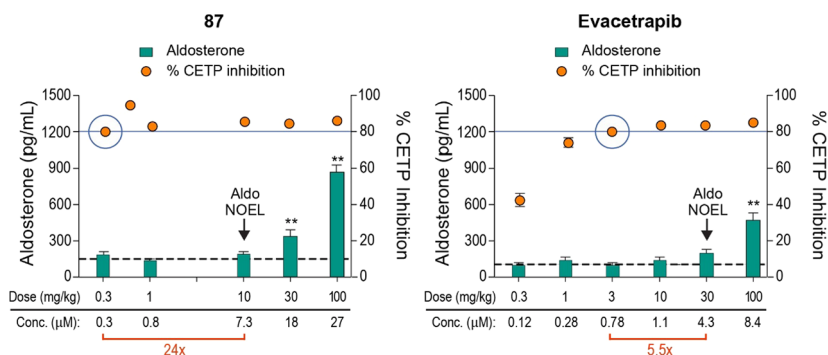
Figure 9. Side-by-side comparison of **87** to evacetrapib: a correlation of preclinical margin to clinical results for evacetrapib, which serves as a negative clinical control of lesser preclinical margin, cf. **87**.

correlation, as it exhibited no preclinical aldosterone margin and clinical aldosterone-related AEs. Anacetrapib could not be used as a robust negative control for the correlation. The compound exhibited >8× preclinical aldosterone margin with no clinical

AEs, but anacetrapib was exposure limited at higher potential margins due to suboptimal physical−chemical properties and solubility. Fortunately, when **87** was selected as a preclinical safety assessment candidate, evacetrapib had already completed
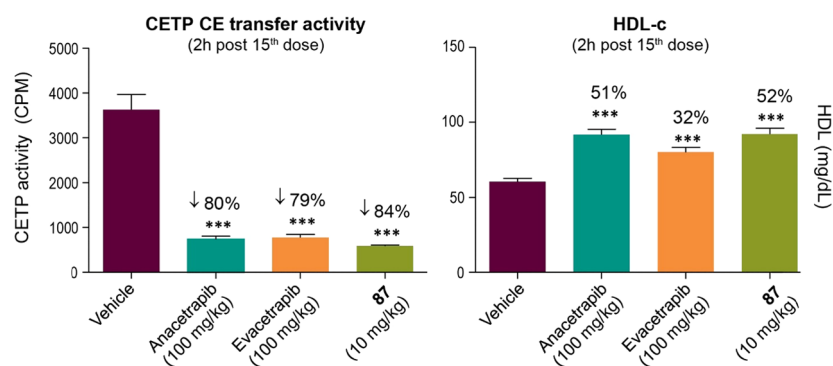
Figure 10. Chronic efficacy in transgenic CETP mice: CETPi and HDL cholesterol efficacy in vivo. Side-by-side comparison of **87** at 10 mg/kg to evacetrapib and anacetrapib at 100 mg/kg; *** $P < 0.001$ vs vehicle (one-way analysis of variance (ANOVA), Dunnett's multiple comparison test); cholesteryl ester (CE), counts per minute (CPM).

Table 10. Preclinical Pharmacokinetics of 87 in CD1 Mice, WH Rats, Beagle Dogs, and Rhesus Monkeys Following a Single Oral or IV Dose

	mouse	rat	dog	monkey
IV dose (mg/kg)	1	1	0.5	0.5
Cl_p (mL/min/kg)	2.6 ± 0.58	3.1 ± 0.27	0.52 ± 0.17	0.39 ± 0.18
Vd_{ss} (L/kg)	0.95 ± 0.38	2.4 ± 0.32	0.54 ± 0.08	1.3 ± 0.2
$t_{1/2}$ terminal (h)	4.4 ± 1.1	8.1 ± 1.5	15 ± 2.9	50 ± 8.8
$t_{1/2}$ MRT (h)	6.0 ± 1.0	13 ± 2.5	18 ± 3.5	60 ± 16
P.O. (mg/kg)	2	2	2	2
C_{max} (μM)	0.43 ± 0.31	0.4 ± 0.04	0.69 ± 0.52	0.22 ± 0.09
T_{max} (h)	2.7 ± 1.2	4.0 ± 0.0	1.7 ± 0.6	6.7 ± 1.2
$AUC_{0-\infty}$ (μM·h)	7.9 ± 1.7	9.7 ± 2.6	13 ± 12	11 ± 2.3
F (%)	43	65	14 ± 13	8.4 ± 1.8

the Phase 2 clinical trials with no significant compound-related effects on aldosterone release or blood pressure and therefore could serve a viable negative control for the ALDO-margin-to-clinic correlation. Figure 9 makes a side-by-side comparison of evacetrapib to 87. Evacetrapib exhibits approximately 5× preclinical aldosterone margin while 87 shows a 24× margin over the maximum CETP efficacy in vivo. We postulated that a 24× preclinical aldosterone margin should be sufficient for advancing 87 into clinical trials with reduced risk of AEs at high exposure.

To fully profile the comparative efficacy of 87, the compound was examined in a 2-week chronic treatment of CETP transgenic mice alongside anacetrapib and evacetrapib, and the results are provided in Figure 10. The compounds were administered QD at the minimal dose needed to provide maximal CETP inhibitions, and this was demonstrated in Figure 10a. Two hours following the final dose, maximal CETP inhibition resulted in a significant HDL cholesterol increase in vivo for 87, which was comparable to both positive controls, anacetrapib and evacetrapib. It is noteworthy that 87 at 10 mg/kg reaches the same level of maximum efficacy as both evacetrapib and anacetrapib at 100 mg/kg dose.

The full pharmacokinetic profile of 87 was assessed in several preclinical species, and the results are presented in Table 10. Following a single IV dose to wild-type (WT) CD1 mouse, Wistar-Han (WH) rats, Beagle dogs, and Rhesus monkeys, plasma clearance and volume of distribution of 87 were low (Cl_p, 0.39–3.1 mL/min/kg; Vd_{ss}, 0.54–2.4 L/Kg). Consistent with low plasma clearance values, terminal half-lives in all species were long (ranging from 4.4 h in mouse to 50 h in monkeys).

Compound 87 displayed low to moderate bioavailability (8.4–65% across species).

The elimination half-life of 87 from plasma, liver, and adipose tissue was investigated in several mouse strains to thoroughly differentiate the compound from anacetrapib.[67] In one study, 87 was administered orally to NFR-TG mice in a single dose at 10 mg/kg in 0.5% methocellulose, and serial samples were collected over a period of 72 h. The plasma half-life of 87 in this study was 12 h (Table 11). Next, the compounds were administered orally

Table 11. Half-Lives of 87 from Plasma, Liver, and Adipose Tissue in Lean and DIO Wild-Type and Lean NFR-TG Mice Following Single Dose and 40-Day QD Dose (10 mg/kg)

	single dose of 87 NFR-TG	multiple dose of 87		
		lean wt	DIO wt	lean NFR-TG
plasma	12 ± 0.5 h	0.8 ± 0.1 d	2.8 ± 0.9 d	12 ± 5.5 d
liver	N/A	1.5 ± 1.6 d	3.2 ± 1.0 d	2.9 ± 0.9 d
adipose	N/A	0.8 ± 0.2 d	3.6 ± 2.0 d	1.5 ± 1.0 d

for 14 days at 10 mg/kg (in 0.5% methocellulose) to examine the potential for accumulation. Terminal samples were collected on days 1, 7, 14, 28, and 40, following the last dose. It was found that plasma half-lives in lean, diet-induced obesity (DIO) and NFR-TG mice were progressively longer (MD $t_{1/2}$ 0.8, 2.8, and 12 days, respectively), indicating the increased influence of fat content and CETP-binding to plasma elimination kinetics. A similar trend was also observed for liver and adipose tissue (Table 11). Importantly, in lean NFR-TG mice, the plasma $T_{1/2}$ was approximately 24× longer following the multi-day dosing than was the single dose. Together, these two studies nicely
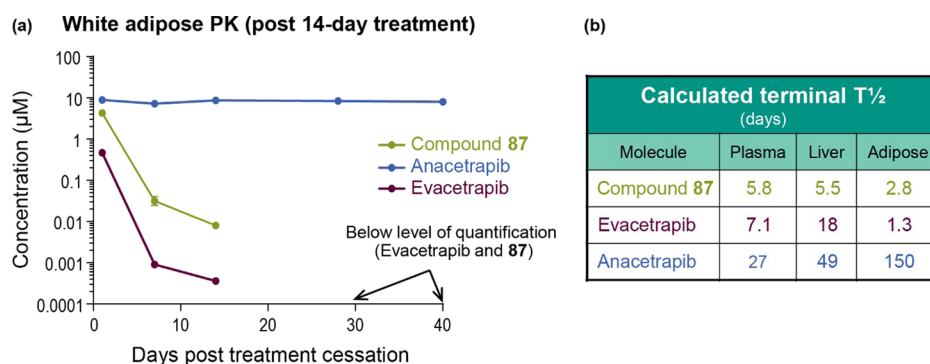
Figure 11. (a) Time course of parent molecule elimination from white adipose tissue of DIO-NFR-TG-mice after the cessation of 2-week dosing (Anacetrapib 100 mg/kg/day; Evacetrapib 30 mg/kg/day; **87** 10 mg/kg/day; dosed orally once daily in 0.5% methylcellulose vehicle). (b) Calculated half-life of parent molecule in plasma, liver, and adipose tissues.

demonstrated the effect of multiple dosing, adipose tissue distribution, and CETP-binding on the half-life of **87**. Notably, in all strains, elimination rates of **87** from adipose tissue were roughly equal or lesser than that of plasma, suggesting that **87** did not accumulate in the adipose compartment (Table 11).

Using the results from Table 11, we sought to compare the adipose retention of **87** with the clinical CETP inhibitors anacetrapib and evacetrapib following multiple-dose 14-day treatment. For this study, NFR-TG mice were fed to induce the diet-induced obese (DIO) state. Figure 11 compares the tissue retention characteristics of the CETP inhibitors. From Figure 11a the time course of parent molecule elimination from white adipose tissue of DIO-NFR-TG mice is shown after the cessation of 2-week dosing, which illustrates the comparatively lower tissue retention of **87** and evacetrapib as compared to anacetrapib. Figure 11b shows the calculated half-life of the parent molecule in plasma, liver, and adipose tissues from this study. Notably, **87** is eliminated from all tissues, including the adipose, at a rate comparable to evacetrapib and at a significantly higher rate compared to anacetrapib. It is noteworthy that the kinetics displayed in Figure 11 only account for the elimination of the parent molecule and not any metabolites. Evacetrapib undergoes extensive metabolism in vitro and in vivo, producing additional entities that might extend drug-related exposure post-parent elimination due to long-lived circulating and/or covalently bound metabolites.[68]

The mouse served as the primary preclinical species model to predict a human dose and investigate the PK of **87**. The advantages of this species include the availability of lean WT and DIO strains that do not express CETP, as well as the NFR transgenic CD1 strain that does express human CETP. Following single and multiple oral dosing to WT mice, **87** showed plasma half-life values of 0.18 and 0.8 days, respectively. The 4x greater half-life at steady state upon multiple dosing was hypothesized to result from increased adipose tissue distribution. In comparison, single- and multiple-dose half-life values in NFR-TG mice were 12 h and 12 days, respectively, suggesting that binding to CETP significantly increased the compound half-life as well. A third factor contributing to the elimination of **87** is the relative fat content of the subject, as evidenced by the 4x longer half-life in the DIO WT strain (2.8 d) as opposed to lean WT mice (0.8 d). It is important to note that, although **87** was distributed to adipose tissue, which extended its half-life somewhat, it did not accumulate in the adipose compartment. This is evidenced by the fact that the elimination rate of **87** from adipose tissue was roughly parallel to that of plasma in both lean

(0.8 d for both plasma and tissue) and DIO (2.8 d from plasma, 3.6 d from tissue) strains. In the NFR-TG mouse, **87** shows faster elimination from tissue (1.5 d) than from plasma (12 d), confirming the lack of tissue accumulation in another animal strain. Preclinical data suggested that **87** would have a shorter human half-life relative to anacetrapib because of the lack of tissue accumulation, which represented a clear advantage (Table 11).

The effect of food on the PK parameters of **87** was investigated next in dogs. The compound was dosed at 1 mg/kg in fed (high-fat diet) and fasted arms in 0.5% methocel and Imwitor/Tween formulations. In these studies, no significant difference in plasma $AUC_{0-24\ h}$ exposure was observed between the fed and fasted states (Table 12).

Table 12. Food Effect on 87 Pharmacokinetics in Dogs

dosing vehicle fasted/ fed dogs	0.5% methocel		Imwitor/Tween	
	fasted	fed	fasted	fed
normalized $AUC_{0-72\ h}$ ($\mu M \cdot h \cdot kg/mg$)	6.5 ± 0.4	4.2 ± 1.7	24 ± 8	22 ± 7
C_{max} (μM)	0.5 ± 0.1	0.3 ± 0.1	1.5 ± 0.8	1.3 ± 0.5
estimated %F_{oral}	14%	9%	53%	48%
food effect (ratio $AUC_{0-72\ h}$) fed/ fasted)	0.6×		0.9×	

Mindful of the risk stemming from the existence and potential clinical relevance of the long-lived metabolites observed for torcetrapib,[69] elimination pathways of **87** in WH rats and rhesus monkeys were investigated following a single oral dose of $^3[H]$ **87** to bile-duct-cannulated (BDC) subjects. Table 13 summarizes the findings for both species. Irrespective of route of administration, the only species observed in bile, feces, urine, and plasma were either parent **87**, a glucuronide of **87**, or in one case a minor amount of taurine conjugate of **87**. The major route of excretion of **87** included elimination of the parent or its glucuronide. In plasma, the parent was the major drug-related material at 2-, 4-, 8-, and 24-h post-dose with trace amounts of parent glucuronide. No long-lived or circulating metabolites were observed for **87** in either species, which provided a level of confidence that the risk of metabolite-related AEs is low.

The effects of **87** on measures of cardiac conduction and repolarization were assessed both in vitro and in vivo (anesthetized guinea pigs and conscious telemetered monkey models). The observed ion channel IC_{50} values with **87** were

Table 13. Elimination Pathways of 87 in WH Rats and Rhesus Monkeys Were Investigated Following a Single Oral Dose of [^{3}H] 87 to Bile-Duct-Cannulated Subjects

		RAT			
				relative % of total recovered	
dosing		% total radioactivity	87-parent	87-glucoronide	87-taurine c.
PO	recovered total bile	>99%	<2	>98	0
	recovered total feces composition	46%	>98		
	recovered total urine	0%			
IV	recovered total bile	67%		>98	
	recovered total feces	15%	>98		
	plasma composition T = 2 h		>96	<4	
	plasma composition T = 24 h		>99		

		RHESUS MONKEY			
				relative % of total recovered	
dosing		% total radioactivity	87-parent	87-glucoronide	87-taurine c.
PO	recovered total bile	>99%	<1	>96	3
	recovered total feces composition	60%	95	5	
	recovered total urine	7%	>99		
	plasma composition T = 2 h		>99		
	plasma composition T = 24 h		>99		

>30 μM for hERG, I_{Ks}, and I_{Ca}. The IC$_{50}$ for inhibition of I_{Na} was 4.1 μM. These values in the context of the unbound plasma concentration at C_{max} of 87 (free fraction of 87 in plasma is below 0.1%) suggest a low risk for effects on cardiac conduction or proarrhythmia. Consistent with these data, there was a lack of any test-article-related effects on PR, QRS, QT, or QTc intervals with 87 up to 47 μM (~118-fold above the predicted clinical C_{max}) in an exploratory IV cardiovascular study in anesthetized guinea pigs or in conscious telemetrized rhesus monkeys at oral doses up to 25 mg/kg (C_{max} = 29 μM) providing an exposure multiple of ~73-fold above the predicted clinical C_{max}. Additionally, there were no test-article-related hemodynamic changes in non-human primate (NHP) at these exposures. For all safety species, the safety margin for 87 was either equivalent to or exceeded those of the remaining comparator clinical-stage CETP inhibitors, none of which were causing any cardiovascular AEs in Phase 1−3 clinical trials.[70] Compound 87 was also assessed for potency to a full panel of over 110 known pharmacology targets in a Eurofins Panlabs panel, and showed no activity exceeding 50% at 10 μM.

Compound 87 was assessed for its potential to undergo "bioactivation" to potentially reactive intermediates as an approach to inform the potential for any increase in the risk of drug-induced clinical liver injury (DILI). For the in vitro study, HEK293/CYP cell lines expressing human CYP1A2, CYP2E1, CYP2D6, CYP2C8, CYP2B6, CYP3A4, CYP2C19, or CYP2C9 were exposed to different concentrations of 87 up to a maximal concentration of 25 μM limited by effects on cell viability. Compound 87−induced cytotoxicity was assessed +/− the presence of a particular human CYP enzyme and +/− the presence of buthionine sulfoximine, a depleter of glutathione. Cell lysates were also probed via Western blot for the level of human CYP remaining at the end of the incubation. A reduction in the amount of human CYP remaining is believed to reflect the amount of covalent modification of the CYP and its subsequent elimination in the proteasome. Cell lysates were also evaluated by Western blot for protein concentration of Nrf2, a biomarker of oxidative stress. Compound 87 reduced cell viability in a dose-dependent manner beginning at ~10 μM in all 8 cell lines regardless of human CYP expression or glutathione depletion.

The compound had no effect on human CYP protein concentration or Nrf2 activation in any of the 8 cell lines. Overall, there was no evidence of 87 undergoing CYP-dependent bioactivation in HEK293/human CYP cells. Notably, in contrast to the findings with 87, evacetrapib demonstrated an increased potential for bioactivation by human CYP3A4 and dalcetrapib was subject to bioactivation mediated by human CYP2B6, CYP2C9, and CYP2C19 as well as through another CYP-independent pathway in the HEK293/human CYP cell-based assays.

For in vivo studies to assess tolerability and drug-induced bioactivation in the liver, rats were treated with 87 at 750 mg/kg/day for 7 days in an exploratory dose-limiting toxicity study, after which RNA samples from their livers were extracted, purified, and assessed for the induction of an in vivo rat bioactivation signature indicative of the generation of drug-related reactive metabolites.[71] Compound 87 did not elicit any prominent bioactivation signal in rat liver; these transcriptional analyses indicated no concerning risk for bioactivation and demonstrated a profile similar to compounds in the clinic that have no known DILI. In contrast to the findings with 87, evacetrapib and dalcetrapib were positive for bioactivation based on analogous studies and their transcriptional profiles, which supported the conclusion of a notable increase in generation of reactive metabolites in the rat similar to compounds tested in rats that are known to have a DILI in clinic.[35] Although 750 mg/kg/day was not tolerated in a subsequent 2-week rat study, 87 was shown to be well tolerated up to 50 mg/kg/day (~50-fold over anticipated human clinical exposures) when administered to rats for 3 months, demonstrating only very slight to slight changes in a few monitorable biochemical and hematologic parameters and no adverse histomorphologic changes. Additionally, doses up to 20 mg/kg/day (~42-fold the projected clinically efficacious exposure) for up to 3 months in NHP showed no adverse antemortem or postmortem findings with changes limited to expected pharmacologic effects on lipid parameters, as demonstrated by an approximate 50% increase in high-density lipoproteins and an approximate 50% decrease in low-density lipoproteins at the 5 mg/kg/day dose after 2 weeks of treatment. Further, the potential developmental toxicity of 87

Table 14. Comparison of MK-8262 to Other CETP Inhibitors: A List of Selected Properties That Represent a Differentiation among the Comparators

	MK-8262	anacetrapib	dalcetrapib	evacetrapib
log D	5.3	7.1	6.5	6.7
PXR (μM)	>30 μM	9.1 μM	9.4 μM	4.5 μM
TDI[a] index	1.0	N/A	N/A	4.6
clinical dose	QD: 1−3 mg (p)[b]	100 mg	600 mg	130 mg
	QW: 50 mg (p)[b]			
dose number	<1 (QD)	133 (QD)	240 (QD)	43 (QD, Ph2)
	<5 (QW)			
tissue accumulation (NFR-TG-ms)	no accumulation	accumulation	N/A	no accumulation
food effect	0.6−1.3× dog	8× dog	N/A	1.4× dog
	1× human	6× human		
aldosterone margin	24×	>8×	N/A	5×
DILI[35]	negative	N/A	positive	positive

[a]TDI, time-dependent inhibition of CYPs. [b]Projected (p) from a Ph1 SAD study. [c]For the full table, see the Supporting Information.
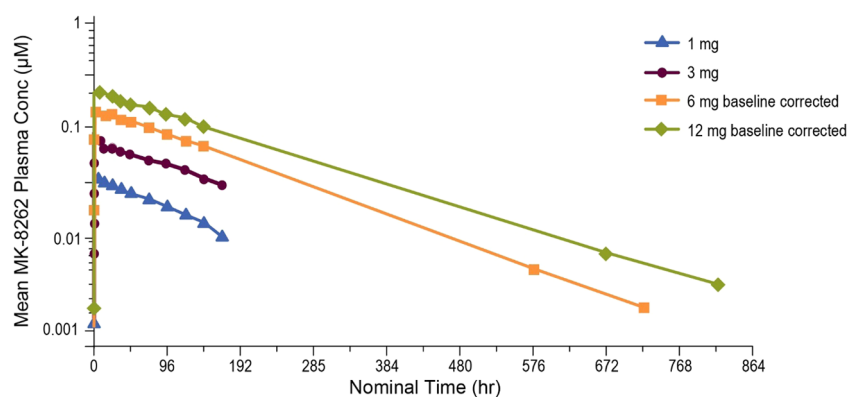
Figure 12. MK-8262 SAD Ph1 clinical results, pharmacokinetics: MK-8262 displayed a biphasic PK profile, with a half-life of approximately 5 days, and no evidence of tissue accumulation.

was tested in a rat whole embryo culture (WEC) assay using gestation day 9 embryos.[72] The embryos were exposed to different concentrations of **87** ranging from 3 to 173 μM for 48 h, representing a sensitive window of organogenesis. No effects were observed in this assay with **87** up to 22 μM, and the WEC-predictive model ranked developmental toxicity potential lower for **87** than for evacetrapib and dalcetrapib (dalcetrapib > evacetrapib > **87**).

After a thorough absorption, distribution, metabolism, and excretion (ADME) process, stability, in vitro counter screening, in vivo pharmacokinetics and pharmacodynamics, and pre-clinical safety assessment, **87** was deemed suitable for clinical development and was designated as MK-8262.

Single-compartment allometric analysis of Cl_p values from WH rats, beagle dogs, and rhesus monkeys, derived from single-dose IV studies, provided a projected human Cl_p of 0.2 mL/min/kg. Low turnover of MK-8262 in vitro precluded the use of in vitro in vivo correlation (IVIVC) methodology for this assessment. Detailed preclinical work indicated the influence of dosing frequency, fat content and CETP-binding in determining the half-life of the compound. Preclinical models are not available to quantitatively measure the impact of these variables to accurately estimate a human plasma half-life. To predict a clinical dose, the half-life was approximated to be 62 h from allometrically scaled Cl_b of 0.2 mL/min/kg and mean Vd_{ss} of 1.4 L/kg. Assuming an effective steady-state trough concentration of 0.3 μM, the clinical dose was projected to be 70 mg (with a conservative bioavailability value of 10%) with steady-state C_{max}

and $AUC_{0-24\ h}$ values of 0.4 μM and 8.0 μM·h, respectively. However, accounting for better bioavailability, the human dose of MK-8262 to achieve maximum CETP inhibition for first-in-human studies was estimated to be 1−3 mg of QD, or 50 mg of QW. The improved physical−chemical properties of MK-8262 allowed its dosing as an amorphous suspension in Phase 1 clinical studies rather than the hot-melt extrusion formulation needed for anacetrapib.

Table 14 shows a side-by-side comparison of key properties of MK-8262 with those of other CETP inhibitors being tested in clinical trials while MK-8262 was being developed (see the Supporting Information for a more comprehensive list). Acknowledging the different stages of clinical development for MK-8262 (Ph1) vs anacetrapib, evacetrapib, and dalcetrapib (all progressed into Ph3), MK-8262 nevertheless stands out for its potential to be a best-in-class molecule, from several perspectives. The overall physical−chemical properties of MK-8262 are superior to the rest of the class, basically represented by the log D value of the molecule (log D = 5.3). Generally, a certain level of lipophilicity may be required for strong in vivo inhibition of a protein like CETP, which interacts with plasma lipids; excessive lipophilicity can result in additional liabilities, including prolonged tissue retention. The significantly lower log D of MK-8262 as compared to all other molecules is consistent with the de-risked adipose retention outlined in Table 11 and with a range of additional superior properties in Table 14, including the lack of food effect in the clinic and a good excretion profile. The projected human dose required for maximum CETP
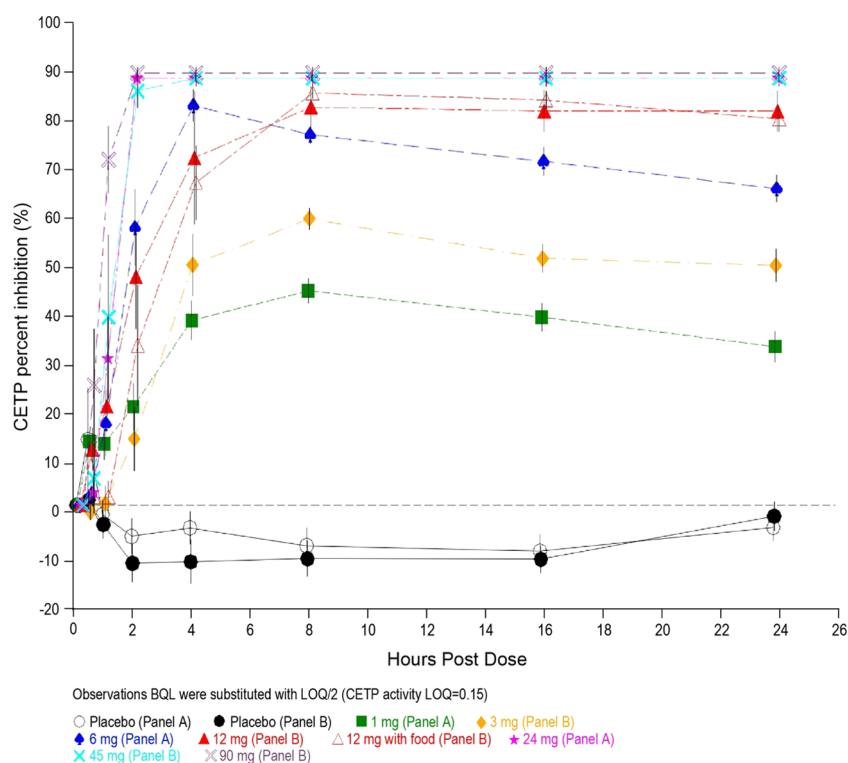
Figure 13. MK-8262 SAD Ph1 clinical results: percentage of CETP inhibition achieved following administration of a single oral dose of MK-8262 in healthy young subjects ($N = 6$/panel); BQL (below quantification limit); limit of quantification (LOQ).

inhibition—and, therefore, full LDL PD effect—is approximately $100\times$ lower than the doses required for all other compounds (the projected efficacious human dose of MK-8262 is 1−3 mg of QD). A low projected dose in combination with inherit superior physical−chemical properties renders the very low dose number, a critical indicator of developability of a once-a-day or once-weekly monotherapy. Additionally, such a favorable dose number virtually assures the option to combine MK-8262 with statins, the standard of care on top of which CETP inhibitors are to be administered, either co-administered or as a fix-dose-combination single pill with a statin. MK-8262 is clearly differentiated in the absence of a DILI[35] signal for liver bioactivation as well as exceptional aldosterone margin vs comparators. In summary, the aforementioned data positioned MK-8262 for clinical development.

A randomized, placebo-controlled, double-blind phase I clinical trial was performed in normal healthy volunteers to determine the safety, tolerability, pharmacokinetics, and pharmacodynamics (inhibition of CETP activity) of single oral doses of MK-8262 (1, 3, 6, 12, 24, 45, 90 mg) in human subjects (Figure 12). MK-8262 was generally well tolerated at single doses up to 90 mg. MK-8262 displayed a biphasic PK profile, with a half-life of approximately 120 h, affording the potential for QW dosing. No evidence of a significant food effect was seen. In a comparable study, anacetrapib displayed a single-dose terminal half-life between 9−62 h in normal healthy volunteers, with a positive food effect that increased exposure 2- to 3-fold with a low fat meal, and 6- to 8-fold with a high-fat meal, compared to fasted subjects.[73] Importantly, the single-dose PK of anacetrapib underestimated the extremely prolonged plasma terminal half-life observed with chronic administration, which was attributed to distribution into and slow egress of anacetrapib from adipose tissue,[44] an effect which was ruled out for MK-8262 preclinically. In this single-dose Ph1 study in humans,

doses of MK-8262 above 12 mg were associated with maximum inhibition of baseline CETP activity (Figure 13). Taken together with the single-dose PK results, the effect of MK-8262 on CETP activity suggests a once-daily dose of ≤1 mg. Due to the progression of the lead molecule anacetrapib through its Phase 3 cardiovascular outcomes trial, a decision was made to suspend further development of MK-8262. Importantly, the decision was due to strategic reasons rather than any nonclinical or clinical safety findings, or any aspect of performance of the molecule.

CONCLUSIONS

After decades of CETP-mechanism-related drug discovery efforts, recent clinical outcomes have demonstrated that a combination of CETP inhibition and statins has the potential to reduce CHD risk by as much as additional 9% compared to statins alone.[16,17] Here, we reported the invention of **87**, a unique CETP inhibitor with the potential for being the best-in-class molecule. We have presented the method by which we optimized for the desired on-target profile and de-risked the potential for AEs that had been clinically demonstrated for several other CETP inhibitors. Our discovery and optimization methods were based on standard safety de-risking paradigms as well as novel approaches, balancing on-target efficacy with the potential for elevations in plasma aldosterone and related cardiovascular biomarkers. Based on its established preclinical profile and its potential to be the best-in-class CETP inhibitor, **87** was designated as the development candidate MK-8262. The single-ascending dose clinical studies of MK-8262 demonstrated the validity of our approach, rendering the candidate as safe and fully efficacious at a very low dose, projected at or below 1 mg of QD, for a full CETP inhibition. The efficacy for CETP inhibition invoked by MK-8262, along with its safety profile, exhibits a

clear potential for reducing the overall cardiovascular risk due to the modulation of cholesterol and lipoprotein biology.

EXPERIMENTAL SECTION

General. All procedures were carried out under a nitrogen atmosphere using commercially available solvents that were used without further purification. Starting materials were obtained from commercial sources and were used without further purification. Normal-phase column chromatography was carried out using prepacked silica gel cartridges on a Combiflash Rf separation system by Teledyne ISCO. Reversed-phase HPLC purification was carried out using YMC C18 column on a Gilson HPLC system utilizing a gradient of 0.05% TFA in water/acetonitrile as the eluent. NMR spectra were recorded using Varian Inova 500 spectrometers. The reported compounds are of ≥95% purity, unless otherwise noted. Purity analysis was carried out by LC-Mass analysis using an Agilent 1100 system fitted with Waters Micromass.

Modular synthesis of **2−37** was achieved by assembling various building blocks for quick SAR on different parts of target molecules colored by rings was applied. The synthesis is exemplified by the preparation of **10**.

*Step i: (4S, 5R)-5-[3,5-Bis(trifluoromethyljpheny1]-3-[2-iodo-5-(trifluoromethyl)benzyl-4-methyl-l,3-xazo-lidin-2-one (**Intermediate 3**).* A solution of (4S,5R)-5-[3,5-bis(trifluoromethylphenyl)-4-methyl-1,3-oxazolidin-2-one (**Intermediate 1**, 3.13 g, 10.0 mmol) in dry THF (93 mL) was added dropwise via cannula to a stirred suspension of sodium hydride (60% dispersion in mineral oil) (0.317 mL, 9.50 mmol) in dry THF (93 mL) at 0 °C under N$_2$. The reaction was stirred at 25 °C for 30 min. A solution of 2-(bromomethyl)-L-iodo-4-(trifluoromethyl)benzene (**Int 2**, 3.65 g, 10.00 mmol) in dry THF (46.5 mL) was added dropwise via cannula, and the reaction mixture was stirred overnight at 25 °C. Water (100 mL) was added, and the reaction mixture was extracted with EtOAc (3 × 100 mL). The combined extracts were dried (MgSO$_4$) and concentrated in vacuo to give the crude product. The crude was purified by flash chromatography (Biotage Horizon, 65i, Si, ~85−90 mL/min, 100% hexanes for 360 mL, gradient to 20% EtOAc in hexanes over 2400 mL, gradient to 50% EtOAc in hexanes over 1224 mL) to afford desired product (4S,5R)-5-[3,5-bis(trifluoromethyl)phenyl]-3-[2-iodo-5-(trifluoromethyl)-benzyl]-4-methyl-l,3-oxazolidin-2-one (**Int 3**, 5.16 g, 8.64 mmol, 86% yield), as a colorless solid. LCMS (ESI) calcd for C$_{20}$H$_{13}$F$_9$INO$_2$ [M + H]$^+$: 598.0, found: 598.0. ^{1}H NMR (CDCl$_3$, 500 MHz): δ 8.06 (d, J = 8.2 Hz, 1H), 7.93 (s, 1H), 7.82 (s, 2H), 7.61 (s, 1H), 7.33 (dd, J = 8.2, 1.4 Hz, 1H), 5.79 (d, J = 7.8 Hz, 1H), 4.91 (d, J = 16 Hz, 1H), 4.40 (d, J = 16 Hz, 1H), 4.16−4.06 (m, 1H), 0.83 (d, J = 6.4 Hz, 3 H) ppm.

*Step ii: (4S,5R)-5-[3,5-Bis(trifluoromethyl)phenyl]-3-{[2'-chloro-5,-nitro-4-(trifluoromethyl) biphenyl-2-yl]methyl}-4-methyl-1,3-oxazolidin-2-one (**Intermediate 5**).* A mixture of (4S,5R)-5-[3,5-bis(trifluoromethyl)phenyl]-3-[2-iodo-5-(trifluoromethyl)-benzyl]-4-methyl-l,3-oxazolidin-2-one (**Intermediate 3**, 1.5 g, 2.51 mmol), 2-chloro-5-nitro phenyl boronic acid (**Intermediate 4**, 0.740 g, 3.67 mmol), tetrakis(triphenylphosphine) palladium (430 mg, 0.372 mmol), and sodium carbonate (0.532 g, 5.02 mmol) in 50 mL of water/EtOH/toluene (1:2:4) was heated to reflux for 4 h. Thin-layer chromatography (TLC) (CH$_2$Cl$_2$:hexane/l:l) showed that the reaction was complete. The solvents were removed. Water (30 mL) was added. The organic was extracted with methylene chloride (3 × 40 mL). The combined methylene chloride layers were washed with brine and dried over sodium sulfate. Flash column using CH$_2$Cl$_2$:hexane/6:4 as the eluent afforded (4S,5R)-5-[3,5-bis(trifluoromethyl)phenyl]-3-{[2'-chloro-5,-nitro-4-(trifluoromethyl)biphenyl-2-yl]methyl}-4-methyl-1,3-oxazolidin-2-one (**Intermediate 5**, 0.96 g, yield 62.2%) as a colorless solid. LCMS (ESI) calcd for C$_{26}$H$_{16}$ClF$_9$N$_2$O$_4$ [M + H]$^+$: 627.1, found: 627.0. ^{1}H NMR (CDCl$_3$, 500 MHz): δ 1:1 mixture of roamers 8.16−8.31 (m, 1H), 8.21 (d, J = 2.5 Hz, l/zH), 8.16 (d, J = 2.5 Hz, VzH), 7.90 (s, 1H), 7.71−7.78 (m, 5H), 7.42−7.46 (m, 1H), 5.66 (d, J = 4.5 Hz, % H), 5.64 (d, J = 4.5 Hz, VzH), 4.93 (d, J=15.5 Hz, VzH), 4.79 (d, J = 16 Hz, VzH), 4.03 (d, J = 16 Hz, VzH), 3.94 (m, 1H), 3.91 (d, J = 15.5 Hz, VzH), 0.70 (d, J = 6.5 Hz, 1.5H), 0.64 (d, J = 6.5 Hz, 1.5H) ppm.

*Steps iii, iv: (4S,5R)-5-[3,5-Bis(trifluoromethyl)phenyl]-3-{[2'-chloro-5'-iodo-4-(trifluoromethyl)biphenyl-2-yl]methyl}-4-methyl-l,3-oxazolidin-2-one (**Intermediate 6**).* To a solution of (4S,5R)-5-[3,5-bis(trifluoromethyl)phenyl]-3-{[2'-chloro-5,-nitro-4-(trifluoromethyl)biphenyl-2-yl]methyl}-4-methyl-1,3-oxazolidin-2-one (**Intermediate 5**, 1.14 g, 1.82 mmol) in EtOH (20 mL) at room temperature was added SnCl$_2$·H$_2$O (5 equiv). The solution was stirred at room temperature for 4 h. TLC (CH$_2$Cl$_2$:hexane/l:l) showed that the reaction was completed. EtOAc (50 mL) was added. The mixture was washed with water (2 × 20 mL), brine, and dried over sodium sulfate. The solvent was removed under reduced pressure, and the residue was diluted with chloroform (30 mL). *n*-Pentyl nitrite (0.36 mL, 2.73 mmol) and iodine (0.55 g, 2.18 mmol) were added. The mixture was stirred under refluxing for 1 h. The mixture was diluted with methylene chloride (30 mL), and the purple solution was washed with saturated sodium thiosulfate solution, brine, and dried over sodium sulfate. Flash column using EtOAc:hexane/2:98 as the eluent afforded (4S,5R)-5-[3,5-bis(trifluoromethyl)phenyl]-3-{[2'-chloro-5'-iodo-4-(trifluoromethyl)biphenyl-2-yl]methyl}-4-methyl-l,3-oxazolidin-2-one (**Intermediate 6**, 650 mg, yield 50%). LCMS (ESI) calcd for C$_{26}$H$_{16}$ClF$_9$INO$_2$ [M + H]$^+$: 707.0, found: 707.0. ^{1}H NMR (CDCl$_3$, 500 MHz): δ a mixture of 1:1 atopoisomers 7.90 (s, 1H), 7.77 (s, 1H), 7.70−7.75 (m, 4H), 7.65 (d, J = 2.5 Hz, VzH), 7.61 (d, J = 2.5 Hz, 1/2 H), 7.40 (m, 1H), 7.28 (m, 1H), 5.66 (d, J = 8Hz, 1/2 H), 5.64 (d, J = 8 Hz, 1/2 H), 4.85 (d, J = 15.5 Hz, 1/2 H), 4.82 (d, J = 14 Hz, 1/2 H), 4.02 (d, J = 16 Hz, 1/2 H), 3.96 (m, 1/2 H), 3.95 (d, J = 15.5 Hz, 1/2 H), 3.79 (m, 1/2 H), 0.64 (d, J = 6.5 Hz, 1.5H), 0.57 (d, J = 6.5 Hz, 1.5H) ppm.

Step v. Methyl 2″-(((4S,5R)-5-(3,5-Bis(trifluoromethyl)phenyl)-4-methyl-2-oxooxazolidin-3-yl)methyl)-4'-chloro-2-methyl-4″-(trifluoromethyl)-[1,1':3',1″-terphenyl]-4-carboxylate. A mixture of (4S,5R)-5-[3,5-bis(trifluoromethyl)phenyl]-3-{[2'-chloro-5'-iodo-4-(trifluoromethyl)biphenyl-2-yl]methyl}-4-methyl-l,3-oxazolidin-2-one (**Intermediate 6**, 0.490 g, 0.692 mmol), methyl 3-methyl-4-(4,4,5,5-tetramethyl-1,3,2-dioxaborolan-2-yl)benzoate (**Intermediate 7**, 0.382 g, 1.385 mmol), tetrakis(triphenylphosphine) palladium (40 mg, 5% mol) and sodium carbonate (0.220 g, 2.077 mmol) in 14 mL of water/EtOH/toluene (1:2:4) was heated to reflux for 2 h. TLC (CH$_2$Cl$_2$:hexane/8:2) showed that the reaction was over. The solvents were removed. Water (10 mL) was added. The organic was extracted with methylene chloride (3×20 mL). The combined methylene chloride layers were washed with brine and dried over sodium sulfate. methyl 2″-(((4S,5R)-5-(3,5-bis(trifluoromethyl)phenyl)-4-methyl-2-oxooxazolidin-3-yl)methyl)-4'-chloro-2-methyl-4″-(trifluoromethyl)-[1,1':3',1″-terphenyl]-4-carboxylate (0.386 mg, yield 76%) was obtained after purification with preparative TLC using 18% EtOAc in hexane as the eluent. MS ESI: calcd for C$_{35}$H$_{25}$ClF$_9$NO$_4$ [M + H]$^+$ 730.13, found 730.13. ^{1}H NMR (CDCl$_3$, 500 MHz): δ 1:1 mixture of atropisomers: 8.03 (2H, s), 7.97 (1H, s), 7.90 (1H, d, J = 7.5 Hz), 7.87 (1H, s), 7.69−7.73 (2H, m), 7.48 (1/2 H, d, J = 7.9 Hz), 7.45 (1/2 H, d, J = 8.0 Hz), 7.37 (1H, m), 7.35 (1H, d, J = 1.9 Hz), 7.31 (1H, d, J = 9.2 Hz), 7.25 (1H, d, J = 1.9 Hz), 7.21 (1H, d, J = 2.1 Hz), 5.63 (1H, m), 5.00 (1/2 H, d, J = 15 Hz), 4.80 (1/2 H, d, J = 16 Hz), 4.08 (1/2 H, d, J = 16 Hz), 4.00 (1/2 H, d, J = 15.3 Hz), 3.94 (3H, s), 3.90 (1H, m), 2.91 (3H, s), 2.89 (3H, s), 2.37 (1.5H, s), 2.36 (1.5 H, s), 0.62 (1.5 H, d, J = 6.5 Hz), 0.60 (1.5 H, d, J = 6.5 Hz) ppm.

*Step vi: 2″-(((4S,5R)-5-(3,5-Bis(trifluoromethyl)phenyl)-4-methyl-2-oxooxazolidin-3-yl)methyl)-4'-chloro-2-methyl-4″-(trifluoromethyl)-[1,1':3',1″-terphenyl]-4-carboxylic Acid (**10**).* Methyl 2″-({(4S,5R)-5-[3,5-bis(trifluoromethyl)phenyl]-4-methyl-2-oxo-l,3-oxazolidin-3-yl}methyl)-4,-chloro-2-methyl-4″-(trifluoromethyl)-1, T:3', 1-terphenyl-4-carboxylate (25 mg, 0.034 mmol), aqueous potassium hydroxide (300 mL, 3 M, 0.90 mmol) and ethanol (2 mL) were stirred at 20 °C overnight. Volatiles were removed under reduced pressure. The resulting residue was treated with brine followed by extraction with ethyl acetate. The combined extracts were dried over Na$_2$SO$_4$ followed by filtration and concentration in vacuo to afford an oil. This oil was purified by preparative TLC on SiO$_2$ (eluted with 50% EtOAc in hexanes) to afford a clear glass. The glass was further purified by reversed-phase preparative HPLC (Kromasil 100-5C18, 100 × 21.1

mm) eluting by a MeCN (0.1% TFA, v/v)/H_2O (0.1% TFA, v/v) gradient mixture affording 2″-({(4S,5R)-5-[3,5-bis(trifluoromethyl)-phenyl]-4-methyl-2-oxo-l,3-oxazolidin-3-yl}methyl)-4,-chloro-2-meth-yl-4″-(trifluoromethyl)-l,l,:3,l″-terphenyl-4-carboxylic acid (**10**, 22 mg, yield 90%). MS ESI: calcd for $C_{34}H_{23}ClF_9NO_4$ [M + H]$^+$ 716.12, found 716.12. ^{1}H NMR signals are doubled because of atropisomerism 'H NMR (CDCl$_3$, 500 MHz) δ 7.99 (d, J = 8.0 Hz, 1H), 7.92 (d, J = 8.5 Hz, 1H), 7.85 (d, J = 5 Hz, 1H), 7.72−7.68 (m, 1,5H), 7.67−7.60 (m, 2.5H), 7.47−7.36 (m, 2H), 7.32 (d, J = 8.0 Hz, 0.5H), 7.28 (d, J = 8.0 Hz, 0.5H), 7.15 (s, 1H), 7.08 (dd, J = 8.5, 7.0 Hz, 1H), 5.58 (d, J = 8.0 Hz, 0.5H),5.29 (d, J = 6.5 Hz, 0.5H), 4.97 (d, J = 15.5 Hz, 0.5H), 4.94 (d, J = 14 Hz, 0.5H), 4.16 (d, J = 16 Hz, 0.5H), 3.96 (d, J = 15.5 Hz, 0.5H), 3.87 (s, 3H), 3.83−3.74 (m, 1H), 2.38, 2.33 (s, 3H), 0.55 (d, J = 6.5 Hz, 1.5H), 0.42 (d, J = 7 Hz, 1.5H) ppm.

Using this process with appropriate subunits, the following compounds were prepared as representative of **2**−**37**.

(4S,5R)-5-(3,5-Bis(trifluoromethyl)phenyl)-3-((6′-methoxy-4-(tri-fluoromethyl)-[1,1′:3′,1″-terphenyl]-2-yl)methyl)-4-methyloxazoli-din-2-one (4). ^{1}H NMR (CDCl$_3$, 500 MHz): δ 1:1 mixture of atropisomers 7.88 (s, IH), 7.74 (s, IH), 7.72 (s, IH), 7.67 (t, J = 7 Hz, IH), 7.62 (s, IH), 7.54 (m, IH), 7.31−7.34 (m, IH), 6.90−6.93 (m, IH), 5.63 (d, J = 8 Hz, 0.5H), 5.25 (d, J = 8 Hz, 0.5H), 4.98 (d, J = 15.5 Hz, 0.5H), 4.88 (d, J = 16 Hz, 0.5H), 4.12 (d, J = 15.5 Hz, 0.5H), 3.88 (d, J = 16.5 Hz, 0.5H), 3.84 (s, 3H), 3.81 (s, 3H), 3.73 (m, IH), 0.59 (d, J = 6.5 Hz, 1.5H), 0.45 (d, J = 6.5 Hz, 1.5H) ppm. MS ESI: calcd for $C_{33}H_{24}F_9NO_3$ [M + H] 654.16, found 654.2.

2″-(((4S,5R)-5-(3,5-Bis(trifluoromethyl)phenyl)-4-methyl-2-ox-ooxazolidin-3-yl)methyl)-4′-methoxy-2-methyl-4″-(trifluorometh-yl)-[1,1′:3′,1″-terphenyl]-4-carboxylic Acid (9). ^{1}H NMR signals are doubled because of atropoisomerism. ^{1}H NMR (CDCl$_3$, 500 MHz) δ 7.99 (d, J = 8.0 Hz, IH), 7.92 (d, J = 8.5 Hz, IH), 7.85 (d, J = 5 Hz, IH), 7.72−7.68 (m, 1.5H), 7.67−7.60 (m, 2.5H), 7.47−7.36 (m, 2H), 7.32 (d, J = 8.0 Hz, 0.5H), 7.28 (d, J = 8.0 Hz, 0.5H), 7.15 (s, IH), 7.08 (d, J = 8.5, 7.0 Hz, IH), 5.58 (d, J = 8.0 Hz, 0.5H), 5.29 (d, J = 6.5 Hz, 0.5H), 4.97 (d, J = 15.5 Hz, 0.5H), 4.94 (d, J = 14 Hz, 0.5H), 4.16 (d, J = 16 Hz, 0.5H), 3.96 (d, J = 15.5 Hz, 0.5H), 3.87 (s, 3H), 3.83−3.74 (m, IH), 2.38, 2.33 (s, 3H), 0.55 (d, J = 6.5 Hz, 1,5H), 0.42 (d, J = 7 Hz, 1,5H). MS ESI: calcd for $C_{35}H_{26}F_9NO_5$ [M + H]$^+$ 712.16, found 712.10.

3′-(4-(((4S,5R)-5-(3,5-Bis(trifluoromethyl)phenyl)-4-methyl-2-ox-ooxazolidin-3-yl)methyl)-6-(trifluoromethyl)pyridin-3-yl)-4′-me-thoxy-2-methyl-[1,1′-biphenyl]-4-carboxylic Acid (11). ^{1}H NMR (500 MHz, CD$_3$OD) ppm δ 8.59 (1H, s), 7.99 (1H, d, J = 2.3 Hz), 7.84−7.94 (5H, m), 7.51 (1H, dd, J = 8.4, 2.0 Hz), 7.25−7.36 (3H, m), 5.80 (1/2 H, d, J = 8.4 Hz), 5.55 (1/2 H, d, J = 7.9 Hz), 4.78 (1H, d, J = 16.4 Hz), 4.42 (1/2 H, d, J = 16.2 Hz), 4.24 (1/2H H, d, J = 16.4 Hz), 4.02 (1H, m), 3.90 (3H, s), 2.38 (1.5 H, s), 2.35 (1.5 H, s), 0.56 (1.5 H, d, J = 7.5 Hz), 0.52 (1.5 H, d, J = 7.5 Hz). MS ESI: calcd for $C_{34}H_{25}F_9N_2O_5$ [M + H] 713.16, found 713.24.

3′-(2-(((4S,5R)-5-(3,5-Bis(trifluoromethyl)phenyl)-4-methyl-2-ox-ooxazolidin-3-yl)methyl)-6-(trifluoromethyl)pyridin-3-yl)-4′-me-thoxy-2-methyl-[1,1′-biphenyl]-4-carboxylic Acid (12). ^{1}H NMR (500 MHz, CD$_3$OD) ppm δ 7.98 (1H, s), 7.84−7.93 (5H, m), 7.81 (1H, br), 7.47 (1H, dd, J = 18.5, 2.2 hz), 7.34 (1H, d, J = 7.7 Hz), 7.24−7.30 (2H, m), 4.86 (1/2 H, br), 4.81 (1/2 H, br), 4.81 (3H, s), 4.30−4.33 (1H, m), 3.89 (3H, s), 2.36 (3H, s), 0.69 (3H, s), MS ESI: calcd for $C_{34}H_{25}F_9N_2O_5$ [M + H] 713.16, found 713.12.

4-(5-(2-(((4S,5R)-5-(3,5-Bis(trifluoromethyl)phenyl)-4-methyl-2-oxooxazolidin-3-yl)methyl)-4-(trifluoromethyl)phenyl)-6-methoxy-pyridin-3-yl)-3-methylbenzoic Acid (13). ^{1}H NMR (500 MHz, CDCl$_3$) ppm δ 8.30 (1H, s), 8.08 (1H, s), 8.01 (1H, d, J = 7.9 Hz), 7.91 (1H, s), 7.74 (2H, d, J = 10.4 Hz), 7.71 (2H, d, J = 7.6 Hz), 7.54 (1H, s), 7.46 (1H, d, J = 8.0 Hz), 7.38 (1H, d, J = 7.0 Hz). MS ESI: calcd for $C_{34}H_{25}F_9N_2O_5$ [M + H] 713.16, found 713.10.

4-(2′-(((4S,5R)-5-(3,5-Bis(trifluoromethyl)phenyl)-4-methyl-2-ox-ooxazolidin-3-yl)methyl)-2-methoxy-6′-(trifluoromethyl)-[3,3′-bi-pyridin]-5-yl)-3-methylbenzoic Acid (14). ^{1}H NMR (500 MHz, CD$_3$OD) ppm δ 8.28 (1H, 2.3 Hz), 7.98 (1H, s), 7.96 (1H, d, J = 8.1 Hz), 7.94 (1H, d, J = 8.1 Hz), 7.90 (3H, m), 7.84 (1H, d, J = 8.0 Hz), 7.77 (1H, d, J = 2.0 Hz), 7.41 (1H, d, J = 7.9 Hz), 5.49 (1H, br), 4.83 (1H, m), 4.32−4.40 (2H, m), 4.02 (3H, s), 2.40 (3H, s), 0.73 (3H, d, J

= 6.6 Hz). MS ESI: calcd for $C_{33}H_{24}F_9N_3O_5$ [M + H] 714.16, found 714.10.

4-(2′-(((4S,5R)-5-(3,5-Bis(trifluoromethyl)phenyl)-4-methyl-2-ox-ooxazolidin-3-yl)methyl)-2,6′-dimethoxy-5′-(trifluoromethyl)-[3,3′-bipyridin]-5-yl)-3-methylbenzoic Acid (15). ^{1}H NMR (500 MHz, CDCl$_3$) ppm δ 8.30 (d, J = 2.3 Hz, 1H), 8.07 (s, 1H), 8.03 (d, J = 8.0 Hz, 1H), 7.92 (s, 1H), 7.79 (s, 1H), 7.77 (s, 2H), 7.57 (s, 1H), 7.39 (d, J = 7.9 Hz, 1H), 6.0 (br, 1H), 5.73 (d, J = 8.4 Hz, 1H), 4.85 (br, 1H), 4.40 (br, 1H), 4.11 (s, 3H), 4.04 (s, 3H), 3.99 (br, 1H), 2.42 (s, 3H), 0.80 (br, 3H); MS ESI: calcd for $C_{36}H_{33}F_6N_5O_6$ [M + H] 744.17, found 744.07.

2,2,2-Trifluoroacetic Acid-4-(4′-(((4S,5R)-5-(3,5-bis-(trifluoromethyl)phenyl)-4-methyl-2-oxooxazolidin-3-yl)methyl)-2-methoxy-6′-(trifluoromethyl)-[3,3′-bipyridin]-5-yl)-3-methylben-zoic Acid (16). ^{1}H NMR (500 MHz, CD$_3$OD) ppm δ 8.63 (1H, s), 8.30 (1H, d, J = 2.3 Hz), 7.98−8.00 (2H, m), 7.80−7.92 (S, m), 7.41 (1H, d, J = 7.9 Hz), 5.80 (1/2 H, br), 5.72 (1/2 H, br), 4.81 (1H, br), 4.40 (2H, br), 4.03 (3H, s), 2.40 (3H, s), 0.62 (3H, d, J = 6.5 hz); MS ESI: calcd for $C_{33}H_{24}F_9N_3O_5$ [M + H] 714.16, found 714.29.

3′-(4-(((4S,5R)-5-(3,5-Bis(trifluoromethyl)phenyl)-4-methyl-2-ox-ooxazolidin-3-yl)methyl)-2-(trifluoromethyl)pyrimidin-5-yl)-4′-me-thoxy-2-methyl-[1,1′-biphenyl]-4-carboxylic Acid (17). ^{1}H NMR (500 MHz, DMSO-d_6) ppm δ 8.83 (1H, s), 8.01 (1H, s), 7.95 (1H, s), 7.93 (2H, s), 7.89 (1H, d, J = 8.1 Hz), 7.58 (1H, d, J = 8.0 Hz), 7.41 (1H, s), 7.39 (1H, d, J = 7.6 hz), 7.32 (1H, d, J = 7.8 Hz), 5.82 (1H, br), 4.81 (1H, m), 4.38−4.48 (2H, m), 3.93 (3H, s), 2.39 (3H, s), 0.72 (3H, d, J = 6.3 Hz); MS ESI: calcd for $C_{33}H_{24}F_9N_3O_5$ [M + H] 714.16, found 714.02.

4-(5-(4-(((4S,5R)-5-(3,5-Bis(trifluoromethyl)phenyl)-4-methyl-2-oxooxazolidin-3-yl)methyl)-2-(trifluoromethyl)pyrimidin-5-yl)-6-methoxypyridin-3-yl)-3-methylbenzoic Acid (18). ^{1}H NMR (500 MHz, CD$_3$OD) ppm δ 8.91 (1H, s), 8.37 (1H, s), 8.03 (1H, s), 8.01 (1H, s), 7.95 (2H, s), 7.93 (1H, m), 7.88 (1H, s), 7.42 (1H, dd, J = 7.9, 1.5 Hz), 5.87 (1H, d, 9.0 Hz), 4.81 (1H, m), 4.40−4.12 (2H, m), 4.03 (3H, s), 2.40 (3H, s), 0.78 (2H, d, J = 6.7 Hz); MS ESI: calcd for $C_{32}H_{23}F_9N_4O_5$ [M + H] 715.15, found 715.07.

3′-(4-(((4S,5R)-5-(3,5-Bis(trifluoromethyl)phenyl)-4-methyl-2-ox-ooxazolidin-3-yl)methyl)-2-(dimethylamino)pyrimidin-5-yl)-4′-me-thoxy-2-methyl-[1,1′-biphenyl]-4-carboxylic Acid (19). ^{1}H NMR (600 MHz, CDCl$_3$) ppm δ 8.22 (s, 1H), 8.01 (s, 1H), 7.95 (d, J = 8.9 Hz, 1H), 7.87 (s, 1H), 7.72 (s, 2H), 7.32−7.36 (m, 2H), 7.15 (s, 1H), 7.05 (d, J = 8.7 Hz, 1H), 5.61 (br, 1H), 4.79 (br, 1H), 4.34 (br, 1H), 4.10 (br, 1H), 3.86 (s, 3H), 3.25 (s, 6H), 2.37 (s, 3H), 0.68 (br, 3H); ^{13}C NMR (125 MHz, CDCl$_3$) ppm δ 171.13, 161.59, 161.30, 158.50, 157.61, 146.08, 138.38, 135.69, 133.59, 132.41, 132.19, 131.96, 131.74, 131.44, 130.18, 129.99, 128.23, 127.68, 126.41, 124.25, 123.85, 122.52, 122.05, 120.24, 117.61, 110.70, 77.28, 77.21, 77.00, 76.79, 55.56, 54.29, 44.74, 37.18, 20.55, 14.51; MS ESI: calcd for $C_{34}H_{30}F_6N_4O_5$ [M + H] 689.21, found 689.34.

3′-(2-(Azetidin-1-yl)-4-(((4S,5R)-5-(3,5-bis(trifluoromethyl)-phenyl)-4-methyl-2-oxooxazolidin-3-yl)methyl)pyrimidin-5-yl)-4′-methoxy-2-methyl-[1,1′-biphenyl]-4-carboxylic Acid (20). ^{1}H NMR (500 MHz, CDCl$_3$) ppm δ 8.22 (s, 1H), 8.01 (s, 1H), 7.95 (d, J = 8.9 Hz, 1H), 7.87 (s, 1H), 7.78 (s, 2H), 7.34−7.38 (m, 2H), 7.19 (s, 1H), 7.05 (d, J = 8.7 Hz, 1H), 5.61 (br, 1H), 4.82 (br, 1H), 4.39 (br, 1H), 4.25 (m, 4H), 4.10 (br, 1H), 3.86 (s, 3H), 2.42 (m, 2H), 2.39 (s, 3H), 0.68 (br, 3H); MS ESI: calcd for $C_{35}H_{30}F_6N_4O_5$ [M + H] 701.20, found 701.30.

3′-(4-(((4S,5R)-5-(3,5-Bis(trifluoromethyl)phenyl)-4-methyl-2-ox-ooxazolidin-3-yl)methyl)-2-(3-fluoroazetidin-1-yl)pyrimidin-5-yl)-4′-methoxy-2-methyl-[1,1′-biphenyl]-4-carboxylic Acid (21). ^{1}H NMR (500 MHz, CDCl$_3$) ppm δ 8.22 (s, 1H), 8.01 (s, 1H), 7.95 (d, J = 8.9 Hz, 1H), 7.89 (s, 1H), 7.78 (s, 2H), 7.32−7.36 (m, 2H), 7.19 (s, 1H), 7.05 (d, J = 8.7 Hz, 1H), 5.61 (br, 1H), 5.41−5.58 (m, 1H), 4.79 (br, 1H), 4.55 (m, 2H), 4.39 (br, 1H), 4.38 (m, 2H), 4.10 (br, 1H), 3.86 (s, 3H), 2.40 (s, 3H), 0.68 (br, 3H); MS ESI: calcd for $C_{35}H_{29}F_7N_4O_5$ [M + H] 719.20, found 719.30.

3′-(4-(((4S,5R)-5-(3,5-Bis(trifluoromethyl)phenyl)-4-methyl-2-ox-ooxazolidin-3-yl)methyl)-2-(pyrrolidin-1-yl)pyrimidin-5-yl)-4′-me-thoxy-2-methyl-[1,1′-biphenyl]-4-carboxylic Acid (22). ^{1}H NMR (500 MHz, CDCl$_3$) ppm δ 8.39 (s, 1H), 7.98 (s, 1H), 7.95 (s, 1H), 7.92

(d, J = 8.9 Hz, 1H), 7.78 (s, 2H), 7.42 (d, J = 8.5 Hz, 1H), 7.32 (d, J = 8.6 Hz, 1H), 7.22 (s, 1H), 7.10 (d, J = 8.7 Hz, 1H), 5.71 (d, J = 9.0 Hz, 1H), 4.82 (br, 1H), 4.39 (br, 1H), 4.15 (br, 1H), 3.86 (s, 3H), 3.75−3.85 (br, 4H), 2.15 (br, 4H), 2.39 (s, 3H), 0.78 (br, 3H); MS ESI: calcd for $C_{36}H_{32}F_6N_4O_5$ [M + H] 715.23, found 715.22.

3′-(4-(((4S,5R)-5-(3,5-Bis(trifluoromethyl)phenyl)-4-methyl-2-ox-ooxazolidin-3-yl)methyl)-2-morpholinopyrimidin-5-yl)-4′-me-thoxy-2-methyl-[1,1′-biphenyl]-4-carboxylic Acid (23). ¹H NMR (500 MHz, CDCl₃) ppm δ 8.24 (1H, s), 8.03 (1H, s), 7.98 (1H, dd, J = 8.0, 2.1 Hz), 7.88 (1H, s), 7.74 (2H, s), 7.40 (1H, dd, J = 8.0, 2.0 Hz), 7.37 (1H, d, J = 8.1 Hz), 7.18 (1H, s), 7.08 (1H, d, J = 8.2 Hz), 5. 58 (1H, br), 4.83 91H, br), 4.22 (1H, br), 4.0 (1H, br), 3.8−3.93 (7H, m), 2.40 (3H, s), 0.65 (3H, br); MS ESI: calcd for $C_{36}H_{32}F_6N_4O_6$ [M + H] 731.22, found 731.27.

3′-(4-(((4S,5R)-5-(3,5-Bis(trifluoromethyl)phenyl)-4-methyl-2-ox-ooxazolidin-3-yl)methyl)-2-morpholinopyrimidin-5-yl)-4′-me-thoxy-2-methyl-[1,1′-biphenyl]-4-carboxylic Acid (24). ¹H NMR (500 MHz, CDCl₃) ppm δ 9.0−9.4 (br, 1H), 8.30 (s, 1H), 8.01 (s, 1H), 7.98 (d, J = 8.6 Hz, 1H), 7.89 (s, 1H), 7.72 (s, 2H), 7.42 (d, J = 8.6 Hz, 1H), 7.38 (d, J = 8.7 Hz, 1H), 7.18 (s, 1H), 7.15 (d, J = 8.7 Hz, 1H), 5.61 (br, 1H), 4.85 (br, 1H), 4.25 (br, 1H), 4.18 (br, 1H), 3.91 (br, 3H), 3.8−3.9 (m, 8H), 2.39 (s, 3H), 0.60-0.80 (br, 3H); MS ESI: calcd for $C_{36}H_{32}F_6N_4O_6$ [M + H] 731.22, found 731.55.

3′-(4-(((4S,5R)-5-(3,5-Bis(trifluoromethyl)phenyl)-4-methyl-2-ox-ooxazolidin-3-yl)methyl)-2-ethylpyrimidin-5-yl)-4′-methoxy-2-methyl-[1,1′-biphenyl]-4-carboxylic Acid (25). ¹H NMR (500 MHz, CDCl₃) ppm δ 8.60 (s, 1H), 8.02 (s, 1H), 7.98 (d, J = 8.9 Hz, 1H), 7.89 (s, 1H), 7.78 (s, 2H), 7.45 (d, J = 8.8 Hz, 1H), 7.38 (d, J = 8.7 Hz, 1H), 7.21 (s, 1H), 7.15 (d, J = 9.0 Hz, 1H), 5.65 (br, 1H), 4.95 (br, 1H), 4.40 (br, 1H), 4.20 (br, 1H), 3.91 (s, 3H), 3.16 (q, J = 7.0 Hz, 2H), 2.39 (s, 3H), 1.41 (t, J = 7.1 Hz, 3H), 0.79 (br, 3H); MS ESI: calcd for $C_{34}H_{29}F_6N_3O_5$ [M + H] 674.20, found 674.22.

3′-(4-(((4S,5R)-5-(3,5-Bis(trifluoromethyl)phenyl)-4-methyl-2-ox-ooxazolidin-3-yl)methyl)-2-(1,1-difluoroethyl)pyrimidin-5-yl)-4′-methoxy-2-methyl-[1,1′-biphenyl]-4-carboxylic Acid (26). ¹H NMR (500 MHz, CD₃OD) ppm δ 8.78 (s, 1H), 8.01 (s, 1H), 7.98 (m, 3H), 7.85 (d, J = 8.7 Hz, 1H), 7.55 (d, J = 8.7 Hz, 1H), 7.39 (m, 2H), 7.28 (d, J = 8.8 Hz, 1H), 5.82 (br, 1H), 4.80 (br, 1H), 3.92 (s, 3H), 4.40 (br, 2H), 2.39 (s, 3H), 2.10 (t, J = 25 Hz, 3H), 0.72 (d, J = 6.5 Hz, 3H); MS ESI: calcd for $C_{34}H_{27}F_8N_3O_5$ [M + H] 710.18, found 710.16.

3′-(2-(Dimethylamino)-4-(((4S,5R)-4-methyl-2-oxo-5-(3-(trifluoromethyl)phenyl)oxazolidin-3-yl)methyl)pyrimidin-5-yl)-4′-methoxy-2-methyl-[1,1′-biphenyl]-4-carboxylic Acid (27). ¹H NMR (500 MHz, CD₃OD) ppm δ 8.14 (s, 1H), 7.94 (s, 1H), 7.88 (d, J = 7.8Hz, 1H), 7.68 (d, J = 7.9Hz, 1H), 7.56−7.61 (m, 3H), 7.45−7.47 (d, J = 8.5 Hz, 1H), 7.36 (d, J = 8.0 Hz, 1H), 7.22−7.26 (m, 2H),5.75 (d, J = 8.6 Hz, 1H), 4.65 (br, 1H), 4.39 (br, 1H), 4.21 (br, 1H), 3.91 (s, 3H), 3.24 (s, 6H), 2.36 (s, 3H), 0.70 (d, J = 6.4 Hz, 3H); MS ESI: calcd for $C_{33}H_{31}F_3N_4O_5$ [M + H] 621.22, found 621.34.

3′-(2-(Dimethylamino)-4-(((4S,5R)-4-methyl-2-oxo-5-(3-(trifluoromethoxy)phenyl)oxazolidin-3-yl)methyl)pyrimidin-5-yl)-4′-methoxy-2-methyl-[1,1′-biphenyl]-4-carboxylic Acid (28). ¹H NMR (500 MHz, CD₃OD) ppm δ 8.12 (s, 1H), 7.93 (s, 1H), 7.88 (d, J = 7.8 Hz, 1H), 7.49 (m, 1H), 7.40 (d, J = 8.4 Hz, 1H), 7.35 (d, J = 7.9 Hz, 1H), 7.27 (m, 3H), 7.19 (m, 2H), 5.65 (br, 1H), 4.65 (br, 1H), 4.30 (br, 1H), 4.10 (br, 1H), 3.88 (s, 3H), 3.24 (s, 6H), 2.36 (s, 3H), 0.69 (s, 3H); MS ESI: calcd for $C_{33}H_{31}F_3N_4O_6$ [M + H] 637.22, found 637.22.

3′-(2-(Dimethylamino)-4-(((4S,5R)-4-methyl-2-oxo-5-(4-(trifluoromethoxy)phenyl)oxazolidin-3-yl)methyl)pyrimidin-5-yl)-4′-methoxy-2-methyl-[1,1′-biphenyl]-4-carboxylic Acid (29). ¹H NMR (500 MHz, CD₃OD) ppm δ 8.12 (1H, s), 7.93 (1H, s), 7.87 (1H, d, J = 8.6 Hz), 7.34−7.42 (5H, m), 7.29 (1H, d, J = 8.4 hz), 7.20 (1H, s), 7.19 (1H, d, J = 8.7 Hz), 5.64 (1H, d, J = 7.2 Hz), 4.74 (1H, br), 4.30 (1H, br), 4.09 (1H, br), 3.88 (3H, s), 3.24 (6H, s), 2.36 (3H, s), 0.68 (3H, d, J = 3.1 Hz); MS ESI: calcd for $C_{33}H_{31}F_3N_4O_6$ [M + H] 637.22, found 637.43.

3′-(4-(((4S,5R)-5-(3-Chlorophenyl)-4-methyl-2-oxooxazolidin-3-yl)methyl)-2-(dimethylamino)pyrimidin-5-yl)-4′-methoxy-2-meth-yl-[1,1′-biphenyl]-4-carboxylic Acid (30). ¹H NMR (500 MHz, CD₃OD) ppm δ 8.11 (1H, s), 7.93 (1H, s), 7.88 (1H, d, J = 7.9 Hz, 1H),

7.33−7.41 (m, 4H), 7.30 (1H, s), 7.20 (m, 3H), 5.60 (br, 1H), 4.61 (br, 1H), 4.29 (br, 1H), 4.10 (br, 1H), 3.88 (s, 3H), 3.31 (s, 6H), 2.36 (s, 3H), 0.68 (br, 3H); MS ESI: calcd for $C_{32}H_{31}ClN_4O_5$ [M + H] 587.20, found 587.34.

3′-(4-(((4S,5R)-5-(3-Chloro-5-(trifluoromethyl)phenyl)-4-methyl-2-oxooxazolidin-3-yl)methyl)-2-(dimethylamino)pyrimidin-5-yl)-4′-methoxy-2-methyl-[1,1′-biphenyl]-4-carboxylic Acid (31). MS ESI: calcd for $C_{33}H_{30}ClF_3N_4O_5$ [M + H] 655.19, found 655.16.

3′-(2-(Dimethylamino)-4-(((4S,5R)-5-(3-fluoro-5-(trifluoromethyl)phenyl)-4-methyl-2-oxooxazolidin-3-yl)methyl)-pyrimidin-5-yl)-4′-methoxy-2-methyl-[1,1′-biphenyl]-4-carboxylic Acid (32). ¹H NMR (500 MHz, CD₃OD) ppm δ 8.12 (s, 1H), 7.93 (s, 1H), 7.87 (d, J = 7.7 Hz, 1H), 7.42−7.48 (m, 2H), 7.35−7.41 (m, 3H), 7.18−7.20 (m, 2H), 5.73 (br, 1H), 4.66 (br, 1H), 4.33 (br, 1H), 4.08 (br, 1H), 3.90 (s, 3H), 3.24 (s, 6H), 2.36 (s, 3H), 0.69 (s, 3H); MS ESI: calcd for $C_{33}H_{30}F_4N_4O_5$ [M + H] 639.22, found 639.39.

3′-(4-(((4S,5R)-5-(3,5-Dichlorophenyl)-4-methyl-2-oxooxazoli-din-3-yl)methyl)-2-(dimethylamino)pyrimidin-5-yl)-4′-methoxy-2-methyl-[1,1′-biphenyl]-4-carboxylic Acid (33). ¹H NMR (500 MHz, CD₃OD) ppm δ 8.11 (s, 1H), 7.92 (s, 1H), 7.87 (d, J = 7.9 Hz, 1H), 7.44 (s, 1H), 7.40 (d, J = 8.5 Hz, 1H), 7.34 (d, J = 7.9 Hz, 1H), 7.25 (s, 2H), 7.17−7.19 (m, 2H), 5.59 (br, 1H), 4.61 (br, 1H), 4.29 (br, 1H), 4.10 (br, 1H), 3.88 (s, 3H), 3.28 (s, 6H), 2.35 (s, 3H), 0.71 (br, 3H); MS ESI: calcd for $C_{32}H_{30}Cl_2N_4O_5$ [M + H] 621.16, found 621.34.

3′-(4-(((4S,5R)-5-(3,5-Difluorophenyl)-4-methyl-2-oxooxazolidin-3-yl)methyl)-2-(dimethylamino)pyrimidin-5-yl)-4′-methoxy-2-methyl-[1,1′-biphenyl]-4-carboxylic Acid (34). ¹H NMR (500 MHz, CD₃OD) ppm δ 8.14 (s, 1H), 7.95 (s, 1H), 7.88 (d, J = 8.0 Hz, 1H), 7.46 (m, 1H), 7.36 (d, J = 7.9 Hz, 1H), 7.21−7.25 (m, 2H), 6.93−6.99 (m, 3H), 5.65 (d, J = 8.5 Hz, 1H), 4.65 (br, 1H), 4.35 (br, 1H), 4.20 (br, 1H), 3.91 (s, 3H), 3.24 (s, 6H), 2.36 (s, 3H), 0.74 (d, J = 6.4 Hz, 3H); MS ESI: calcd for $C_{32}H_{30}F_2N_4O_5$ [M + H] 589.22, found 589.22.

3′-(2-(Dimethylamino)-4-(((4S,5R)-4-methyl-2-oxo-5-(5-(trifluoromethyl)pyridin-3-yl)oxazolidin-3-yl)methyl)pyrimidin-5-yl)-4′-methoxy-2-methyl-[1,1′-biphenyl]-4-carboxylic Acid (35). ¹H NMR (500 MHz, CD₃OD) ppm δ 8.92 (s, 1H), 8.80 (s, 1H), 8.15 (s, 1H), 8.08 (s, 1H), 7.95 (s, 1H), 7.88 (d, J = 9.0 Hz, 1H), 7.46 (d, J = 8.5 Hz, 1H), 7.35 (d, J = 7.9 Hz, 1H), 7.24 (m, 2H), 5.76 (br, 1H), 4.66 (br, 1H), 4.40 (br, 1H), 4.10 (br, 1H), 3.89 (s, 3H), 3.28 (s, 6H), 2.37 (s, 3H), 0.75 (d, J = 6.3 Hz, 3H); MS ESI: calcd for $C_{32}H_{30}F_3N_5O_5$ [M + H] 622.22, found 622.39.

3′-(2-(Dimethylamino)-4-(((4S,5R)-4-methyl-2-oxo-5-(2-(trifluoromethyl)pyridin-4-yl)oxazolidin-3-yl)methyl)pyrimidin-5-yl)-4′-methoxy-2-methyl-[1,1′-biphenyl]-4-carboxylic Acid (36). ¹H NMR (500 MHz, CD₃OD) ppm δ 8.74 (d, J = 7.8Hz, 1H), 8.12 (s, 1H), 7.94 (s, 1H), 7.86 (d, J = 8.5Hz, 1H), 7.76 (s, 1H), 7.60 (d, J = 4.7 Hz, 1H), 7.40 (d, J = 8.4 Hz, 1H), 7.35 (d, J = 8.0 Hz, 1H), 7.24 (m, 2H), 5.86 (d, J = 8.1 Hz, 1H), 4.68 (br, 1H), 4.42 (br, 1H), 4.20 (br, 1H), 3.89 (s, 3H), 3.28 (s, 6H), 2.37 (s, 3H), 0.70 (br, 3H); MS ESI: calcd for $C_{32}H_{30}F_3N_5O_5$ [M + H] 622.22, found 622.32.

2,2,2-Trifluoroacetic acid--3′-(2-(dimethylamino)-4-(((4S,5S)-4-methyl-2-oxo-5-(6-(trifluoromethyl)pyridin-2-yl)oxazolidin-3-yl)-methyl)pyrimidin-5-yl)-4′-methoxy-2-methyl-[1,1′-biphenyl]-4-car-boxylic Acid (37). ¹H NMR (500 MHz, CD₃OD) ppm δ 8.13 (1H, s), 8.10 (1H, t, J = 7.9 Hz), 7.94 (1H, s), 7.88 (1H, d, J = 7.4 hz), 7.80 (1H, d, J = 7.8 Hz), 7.70 (1H, d, J = 8.0 Hz), 7.44 (1H, dd, J = 8.5, 2.1 Hz), 7.36 (1H, d, J = 7.9 Hz), 7.26 (1H, s), 7.22 (1H, d, J = 8.4 Hz), 5.69 (1H, d, J = 8.1 Hz), 4.78 (1H, d, J = 10.2 hz), 4.75 (1H, br), 4.46 (1H, br), 4.17 (1H, br), 3.90 (3H, s), 3.29 (6H, s), 2.37 (3H, s), 0.71 (3H, d, J = 6.1 Hz); MS ESI: calcd for $C_{32}H_{30}F_3N_5O_5$ [M + H] 622.22, found 622.32.

Preparation of **38** via first-generation (Scheme 1) and second-generation synthesis (Scheme 2b):

(2S)-tert-Butyl 2-((3,5-Bis(trifluoromethyl)phenyl)((tert-butyldimethylsilyl)oxy)methyl)pyrrolidine-1-carboxylate (40). To a solution of 1-bromo-3,5-bis(trifluoromethyl)benzene (1.85 g, 6.32 mmol) in 6 mL of THF was added *n*BuLi (2.4 mL, 6.1 mmol of hexane solution) dropwise via a syringe at −78 °C. After the resulting reaction mixture was stirred at −78 °C, 5 min, a solution of (*S*)-*tert*-butyl 2-formylpyrrolidine-1-carboxylate (1.05 g, 5.3 mmol) in 5 mL of THF was added via a syringe. The resulting reaction mixture was allowed to

warm up to ambient temperature slowly. TBSOTf was added. After stirring at ambient temperature for 30 min, it was diluted with 60 mL of EtOAc/hexane (1:4) and washed with 60 mL of water. Organics were separated and dried over sodium sulfate, filtered, and concentrated. Crude product was purified on Combiflash prepacked silica gel column eluted with gradient solvents from hexane to 1:9 EtOAc/hexane to give the desired product (1.2 g, 43% yield) of mixture of two diastereomers as a yellow liquid. The two diastereomers each show as a pair of rotamers. It is difficult to assign peaks of ^{1}H NMR spectra. ^{1}H NMR (500 MHz, CDCl$_3$) δ 7.92 (s), 7.82 (s), 7.80 (s), 7.77 (s), 5.3−5.6 (m, 1H), 3.8−4.2 (m, 1H), 1.2−3.6 (m, 6H), 1.54−1.55 (s, 9H), 0.95-0.96 (s, 9H), 0.04 (s, 6H).

(2S)-tert-Butyl 2-((3,5-Bis(trifluoromethyl)phenyl)((tert-butyldimethylsilyl)oxy)methyl)-5-oxopyrrolidine-1-carboxylate (41). To a 250 mL round-bottom flask were added **40** (0.60 g, 1.14 mmol), NaIO$_4$ (0.61 g, 2.84 mmol), RuCl$_3$·H$_2$O (13 mg, 0.057 mmol), 30 mL of EtOAc, and 30 mL of water. After flushing with N$_2$, the reaction mixture was stirred vigorously overnight. TLC indicated complete conversion. It was diluted with 30 mL of water/30 mL of hexane. Organics were separated, dried over sodium sulfate, filtered, and concentrated. Crude product was purified on Combiflash prepacked silica gel column eluted with hexane to 1:4 EtOAc/hexane to give the desired product (0.41 g, 67% yield) as a colorless sticky material. It solidified over time. NMR indicated a pair of diastereomers at 1:1 ratio. ^{1}H NMR (500 MHz, CDCl$_3$) δ 7.90 (s), 7.86 (s), 7.77 (s), 5.38 (s), 5.38 (d, J = 4.5 Hz), 4.5 (m), 4.3 (d, J = 9.5 Hz), 2.8 (m) 2.4 (m), 1.4−2.2 (m), 1.65 (s, 9H), 1.59 (s, 9H), 0.98 (s, 9H), 0.95 (s, 9H), 0.41 (6H).

tert-Butyl (5S)-5-((S)-(3,5-Bis(trifluoromethyl)phenyl)((tert-butyldimethylsilyl)oxy)methyl)-2-(2-chloro-5-(trifluoromethyl)-phenyl)-2-hydroxypyrrolidine-1-carboxylate (42). To a solution of 2-bromo-1-chloro-4-(trifluoromethyl)benzene (0.38 g, 1.37 mmol) in 5 mL of THF was added a solution of iPrMgCl (0.68 mL, 1.37 mmol) in THF at 0 °C. After stirring for 10 min, it was transferred to a flask contains a solution of **41** (0.57 g, 1.05 mmol) in 6 mL of THF at −78 °C. After stirring at −78 °C for 5 min, it was allowed to warm up to ambient temperature. It was quenched by addition of 20 mL of water and 20 mL of NH$_4$Cl. The mixture was extracted with 60 mL of E/H (1:3). Organics were dried over sodium sulfate, filtered, and concentrated. Crude product was purified on Combiflash prepacked silica gel column eluted with hexane to 1:9 E/H give desired product (0.54 g, 71%).

(3,5-Bis(trifluoromethyl)phenyl)((2S)-5-(2-chloro-5-(trifluoromethyl)phenyl)pyrrolidin-2-yl)methanol (44). To a solution of **42** (250 mg, 0.35 mmol) in 2 mL of DCM was added TFA (0.8 mL, 10.4 mmol). The resulting reaction mixture was stirred at ambient temperature for 30 min. Volatiles were removed. Residue was dissolved in 20 mL of EtOAc, washed with 30 mL of 5% KOH, then 10 mL of brine. Organics were dried over sodium sulfate, filtered, and concentrated. Residue was dissolved in 2 mL of THF and treated with TBAF (0.70 mL, 1 M in THF) at room temperature for 30 min. LC-Mass indicated complete conversion. MeOH (3 mL) was added. NaBH$_4$ (131 mg, 0.35 mmol) was added in portions at 0 °C. The resulting reaction mixture was stirred at 0 °C for 2 h and allowed to warm up to ambient temperature slowly. Volatiles were removed. Residue was diluted with 20 mL of EtOAc, washed with 15 mL of KOH, then 10 mL of brine. Organics were dried over sodium sulfate, filtered, and concentrated. Crude product was purified on Combifalsh prepacked silica gel column, eluted with hexane to 1:4 E/H. Fractions contain desired product (mixture of diastereomers) were combined to give 170 mg of viscous material. NMR indicated it contains a significant amount of TBAF. It was carried on to the next step without further purification.

(7aS)-1-(3,5-Bis(trifluoromethyl)phenyl)-5-(2-chloro-5-(trifluoromethyl)phenyl)tetrahydropyrrolo[1,2-c]oxazol-3(1H)-one (Diastereomers 45a−d). To a solution of **44** in 2 mL of DCM was added a solution of phosgene in toluene. The resulting reaction mixture was at ambient temperature for 30 min. It was diluted with 15 mL of EtOAc and washed with 15 mL of 10% KOH. Organics were dried over sodium sulfate, filtered, and concentrated. Residue was purified on

Combiflash prepacked silica gel column, eluted with hexane to 1:4 E/H. Four fractions were collected. The first fraction contains mainly the **45b**. The second fraction contains **45a** and **45b** (a:b ~ 3:1 ratio, 45 mg), this material was used for the next step directly without further separation. The third fraction contains mainly **45c**. The fourth fraction contains mainly **45d**. ^{1}H NMR (500 MHz, CDCl$_3$) for **45a**: δ 7.93 (s, 1H), 7.87 (s, 2H), 7.74 (s, 1H), 7.53 (s, 2H), 6.14 (d, J = 8.0 Hz, 1H), 5.37 (t, J = 8.1 Hz, 1H), 4.60 (m, 1H), 2.94 (m, 1H), 1.69 (m, 1H), 1.56 (m, 1H), 1.26 (m, 1H); ^{1}H NMR (500 MHz, CDCl$_3$) for **45b**: δ 8.50 (s, 1H), 7.94 (s, 2H), 7.83 (s, 1H), 7.52 (s, 2H), 6.03 (br, 1H), 5.6 (br, 1H), 4.2 (br, 1H), 2.88 (br, 1H), 2.4 (br, 1H), 2.3 (br, 1H), 2.0 (br, 1H); ^{1}H NMR (500 MHz, CDCl$_3$) for **45c**: δ 7.95 (s, 1H), 7.92 (s, 2H), 7.58 (m, 2H), 7.49 (s, 1H), 5.62 (d, J = 8.0 Hz, 1H), 5.24 (dd, J = 8.9 Hz, J = 2.4 Hz, 1H), 4.28 (m, 1H), 2.79 (m, 1H), 2.35 (m, 1H), 2.24 (m, 1H), 2.06 (m, 1H); ^{1}H NMR (500 MHz, CDCl$_3$) for **45d**: δ 7.97 (s, 1H), 7.93 (s, 2H), 7.55 (s, 1H), 7.5 (m, 2H), 5.54 (d, J = 4.1 Hz, 1H), 5.35 (t, J = 7.9 Hz, 1H), 4.16 (m, 1H), 3.07 (m, 1H), 2.40 (m, 1H), 2.00 (m, 1H), 1.85 (m, 1H).

(1R,5S,7aS)-1-(3,5-Bis(trifluoromethyl)phenyl)-5-(4′-fluoro-5′-isopropyl-2′-methoxy-4-(trifluoromethyl)-[1,1′-biphenyl]-2-yl)-tetrahydropyrrolo[1,2-c]oxazol-3(1H)-one (38a) and (1R,5R,7aS)-1-(3,5-bis(trifluoromethyl)phenyl)-5-(4′-fluoro-5′-isopropyl-2′-me-thoxy-4-(trifluoromethyl)-[1,1′-biphenyl]-2-yl)tetrahydropyrrolo-[1,2-c]oxazol-3(1H)-one (38b). To a vial contains **45a** and **45b** (45 mg, 87 μmol, 7a:7b ~ 3:1 ratio) were added (4-fluoro-5-isopropyl-2-methoxyphenyl)boronic acid (55 mg, 260 μmol), PdOAc$_2$ (2.0 mg, 8.7 μmol), DtBPF (4.1 mg, 8.7 μmol), K$_3$PO$_4$ (74, 350 μmol), THF (1 mL) and water (50 μL). The vial was flushed with N$_2$ and was sealed. The reaction mixture was heated at 70 °C overnight. The reaction mixture was diluted with dimethyl sulfoxide (DMSO) and water and acidified with TFA. It was purified on Gilson HPLC with a reversed-phase column, eluted with water/CH$_3$CN (modified with 0.05% TFA) gradient solvent. Four fractions were collected. The first fraction contains mainly unreacted **45b**. The second fraction contains **45a** (13 mg recovered). The third fraction contains mainly **38b** and small amount impurity from boronic acid fragment. It was repurified by prep-TLC eluted with 1:4 E/H to give 4 mg of clean **38b** as fluffy white solid after lyophilizing from tBuOH and water. From the fourth fraction, it afforded **38a** (11 mg) as fluffy white solid after lyophilizing from tBuOH and water. ^{1}H NMR (500 MHz, CDCl$_3$) for **38a** major rotamer (56%): δ 7.88 (s, 1H, overlap with **38a** minor rotamer), 7.82 (s, 2H), 7.75 (s, 1H), 7.6 (d, 1H, overlap with **38a** minor rotamer), 7.3 (d, 1H, overlap with **38a** minor rotamer), 6.92 (d, J$_{H-F}$ = 8.6 Hz, 1H), 6.71 (d, J$_{H-F}$ = 12 Hz, 1H), 6.07 (d, J = 7.9 Hz, 1H), 5.08 (t, J = 8.3 Hz, 1H), 4.47 (m, 1H), 3.84 (s, 3H), 3.2 (m, 1H), 1−2.1 (m, 4H), 1.24 (d, J = 7.0 Hz, 3H), 1.19 (d, J = 6.9 Hz, 3H); ^{1}H NMR (500 MHz, CDCl$_3$) for **38a** minor rotamer (44%): δ 7.88 (s, 1H, overlap with **38a** major rotamer), 7.81 (s, 2H), 7.72 (s, 1H), 7.6 (d, 1H, overlap with **8a** major rotamer), 7.3 (d, 1H, overlap with **38a** major rotamer), 7.18 (d, J$_{H-F}$ = 8.6 Hz, 1H), 6.66 (d, J$_{H-F}$ = 12 Hz, 1H), 6.04 (d, J = 8.0 Hz, 1H), 4.95 (t, J = 8.3 Hz, 1H), 4.55 (m, 1H), 3.68 (s, 3H), 3.2 (m, 1H, overlap with **8a** major rotamer), 1−2.1 (m, 4H), 1.31 (d, J = 6.9 Hz, 3H), 1.28 (d, J = 6.9 Hz, 3H); MS ESI calcd for C$_{31}$H$_{25}$F$_{10}$NO$_3$ [M + H]: 650.17, found 650.29; ^{1}H NMR (500 MHz, CDCl$_3$) for **38b** major rotamer (81%): δ 7.96 (s, 1H, overlap with **38b** minor rotamer), 7.83 (s, 2H), 7.57 (d, J = 8.2 Hz, 1H, overlap with **38b** minor rotamer), 7.35 (d, J = 8.8 Hz, 1H, overlap with **38b** minor rotamer), 7.33 (d, J = 7.9 Hz, 1H, overlap with **38b** minor rotamer), 7.16 (s, 1H), 6.66 (d, J$_{H-F}$ = 12.1 Hz, 1H), 5.84 (d, J = 9.0 Hz, 1H), 4.7 (m, 1H), 4.51 (dd, J = 9.4, 2.8 Hz, 1H), 3.70 (s, 3H), 3.23 (m, 1H), 2.45 (m, 1H), 2.2 (m, 1H), 1.8 (m, 1H), 1.2 (m, 1H), 1.28 (d, J = 6.9 Hz, 6H); ^{1}H NMR (500 MHz, CDCl$_3$) for **38b** minor rotamer (19%): δ 7.96 (s, 1H, overlap with **38b** major rotamer), 7.9 (s, 2H), 7.55 (d, 1H, overlap with **38b** major rotamer), 7.35 (d, 1H, overlap with **38b** major rotamer), 6.85 (d, J$_{H-F}$ = 8.5 Hz, 1H), 6.70 (d, J$_{H-F}$ = 12.0 Hz, 1H), 5.87 (d, J = 9.0 Hz, 1H), 4.7 (m, 1H), 4.6 (m, 1H), 3.78 (s, 3H), 1.2−2.5 (m, 5H), 1.25 (d, 6H, overlap with **38b** major rotamer). MS ESI calcd for C$_{31}$H$_{25}$F$_{10}$NO$_3$ [M + H]: 650.17, found 650.29.

(1S,5R,7aS)-1-(3,5-Bis(trifluoromethyl)phenyl)-5-(4′-fluoro-5′-isopropyl-2′-methoxy-4-(trifluoromethyl)-[1,1′-biphenyl]-2-yl)-

tetrahydropyrrolo[1,2-c]oxazol-3(1H)-one (38c). **38c** was synthesized from **45c** with a similar procedure for **38a**. ^{1}H NMR (500 MHz, CDCl$_3$) for **38c** major rotamer (74%): δ 7.93 (s, 1H, overlap with **38c** minor rotamer), 7.84 (s, 2H), 7.39 (d, *J* = 7.9 Hz, 1H) 7.35 (d, *J*$_{H-F}$ = 8.8 Hz, 1H), 6.69 (d, *J*$_{H-F}$ = 12 Hz, 1H), 5.56 (d, *J* = 8.5 Hz, 1H), 4.6 (dd, *J* = 9.0, 2.6 Hz, 1H), 4.15 (m, 1H), 3.74 (s, 3H), 3.24 (m, 1H), 2.55 (m, 1H), 2.45 (m, 1H), 2.25 (m, 2H), 1.29 (d, *J* = 6.9 Hz, 3H), 1.28 (d, *J* = 6.9 Hz, 3H). MS ESI calcd for C$_{31}$H$_{25}$F$_{10}$NO$_3$ [M + H]: 650.17, found 650.30.

(1S,5S,7aS)-1-(3,5-Bis(trifluoromethyl)phenyl)-5-(4′-fluoro-5′-isopropyl-2′-methoxy-4-(trifluoromethyl)-[1,1′-biphenyl]-2-yl)-tetrahydropyrrolo[1,2-c]oxazol-3(1H)-one (38d). **38d** was synthesized from **45d** with a similar procedure for **38a**. ^{1}H NMR (500 MHz, CDCl$_3$) for **38c** major rotamer (53%): δ 7.98 (s, 1H, overlap with **38d** minor rotamer), 7.92 (s, 2H), 7.56 (s, 2H, overlop with **38d** minor rotamer), 6.96 (d, *J*$_{H-F}$ = 9.6 Hz, 1H), 6.72 (d, *J*$_{H-F}$ = 12 Hz, 1H), 5.42 (s, 1H), 5.09 (t, *J* = 8.0, Hz, 1H), 4.03 (m, 1H), 3.85 (s, 3H), 3.24 (m, 1H, overlop with minor rotamer), 1.6–2.4 (m, 4H), 1.29 (6H, overlap with minor rotamer). ^{1}H NMR (500 MHz, CDCl$_3$) for **38c** minor rotamer (47%): δ 7.97 (s, 1H, overlap with **38d** major rotamer), 7.88 (s, 2H), 7.59 (d, *J* = 7.3 Hz, 1H, overlop with **38d** major rotamer), 7.32 (d, *J* = 7.5 Hz, 1H), 7.18 (d, *J*$_{H-F}$ = 8.7 Hz, 1H), 6.63 (d, *J*$_{H-F}$ = 12 Hz, 1H), 5.42 (s, 1H, overlap with major rotamer), 4.94 (t, *J* = 8.0, Hz, 1H), 3.94 (m, 1H), 3.72 (s, 3H), 3.24 (m, 1H, overlop with minor rotamer), 1.6–2.4 (m, 4H), 1.29 (6H, overlap with major rotamer). MS ESI calcd for C$_{31}$H$_{25}$F$_{10}$NO$_3$ [M + H]: 650.17, found 650.29.

(R,E)-N-(2-Bromo-5-(trifluoromethyl)benzylidene)-2-methylpropane-2-sulfinamide (54). To a THF solution (20 mL) of **53** (2.2 g, 8.7 mmol) and (*R*)-(+)-2-methyl-2-propanesulfinamide (1.16 g, 9.56 mmol) was added Ti(OEt)$_4$ (3.65 mL, 17.4 mmol) via a syringe dropwise. After addition is completed, the reaction mixture was stirred at 40 °C for 1 h. NMR indicated complete conversion. Brine (100 mL) was added, followed by 100 mL of EtOAc. The resulting mixture was stirred at room temperature for 15 min. It was filtered. Layers were separated from the filtrate. Organics were dried over sodium sulfate, filtered, and concentrated. Residue was purified on Combiflash prepacked silica gel column, eluted with 0–25% EtOAc in hexane to give the desire product (2.6 g, 84% yield) as a colorless crystalline solid. ^{1}H NMR (500 MHz, CDCl$_3$) for **54**: δ 9.01 (s, 1H), 8.29 (d, *J* = 1.8 Hz, 1H), 7.82 (d, *J* = 8.4 Hz, 1H), 7.61 (dd, *J* = 1.8, 8.3 Hz, 1H), 1.32 (s, 9H).

(R)-N-((S)-1-(2-Bromo-5-(trifluoromethyl)phenyl)pent-4-en-1-yl)-2-methylpropane-2-sulfinamide (55). To a 250 mL round-bottom flask cooled with a water bath was added **54** (2.6 g, 7.3 mmol) and 80 mL of DCM. Grignard reagent but-3-en-1-ylmagnesium bromide (17.5 mL, 0.5 M in THF) was added rapidly via a syringe. Right after addition, the reaction mixture was quenched by addition of 100 mL of NH$_4$Cl. Hexane (150 mL) was added. Layers were separated. Organics were dried over sodium sulfate, filtered, and concentrated. Crude product was purified on Combiflash prepacked silica gel column, eluted with hexane to 1:2 E/H to give 2 g desired product (66.5% yield). ^{1}H NMR (500 MHz, CDCl$_3$) for **55**: 7.70 (d, *J* = 8.3 Hz, 1H), 7.68 (d, *J* = 1.9 Hz, 1H), 7.40 (dd, *J* = 2.0, 8.3 Hz, 1H), 5.82 (m, 1H), 5.12 (dd, *J* = 1.6, 17.2 Hz, 1H), 5.06 (dd, *J* = 1.4, 10.2 Hz, 1H), 5.0 (m, 1H), 3.57 (d, *J* = 2.2 Hz, 1H), 2.2 (m, 1H), 2.15 (m, 1H), 2.0 (m, 1H), 1.9 (m, 1H), 1.22 (s, 9H).

(S)-Benzyl (1-(2-Bromo-5-(trifluoromethyl)phenyl)pent-4-en-1-yl)carbamate. To a solution of **55** (2.0 g, 4.85 mmol) in 1.5 mL of MeOH was added a solution of HCl in dioxane (8.5 mL, 4M). The reaction mixture was stirred at room temperature for 30 min. Volatiles were removed. Residue was diluted with 60 mL of E/H (1:3), washed with 50 mL of 5% KOH, and then 30 mL of brine. Organics were dried over sodium sulfate, filtered, and concentrated. Crude product was diluted with 10 mL of DCM. DIEA (2.7 nL, 15.6 mmol) was added, followed by addition of CBZ-Cl (1.33 mL, 7.8 mmol) dropwise via a syringe at 0 °C. After 30 min, LC-Mass indicated a still significant amount of sm. 0.5 mL of cBZ-Cl were added. The reaction mixture was stirred at 0 °C for another 15 min. The reaction mixture was diluted with 75 mL of E/H 1:3, washed sequentially with 100 mL of 5% KOH, 60 mL of sat. NH$_4$Cl and 30 mL of brine. Organics were dried over

sodium sulfate, filtered, and concentrated. Crude product was purified on Combiflash prepacked silica gel column, eluted with 0–10% EtOAc in hexane to give 1.65 g desired product as a white solid (72% yield). ^{1}H NMR (500 MHz, CDCl$_3$): 7.69 (d, *J* = 8.1 Hz, 1H), 7.53 (d, *J* = 1.7 Hz, 1H), 7.40 (m, 6H), 5.83 (m, 1H), 5.28 (br, 1H), 5.1 (m, 5H), 2.2 (m, 1H), 2.15 (m, 1H), 1.9 (m, 1H), 1.75 (m, 1H).

(S,E)-Benzyl (5-(3,5-Bis(trifluoromethyl)phenyl)-1-(2-bromo-5-(trifluoromethyl)phenyl)pent-4-en-1-yl)carbamate (56). To a 25 mL round-bottom flask equipped with a reflux condenser were added material from prior step (1.65 g, 3.65 mmol), 1,3-bis(trifluoromethyl)-5-vinylbenzene (1.8 g, 7.5 mmol), and 10 mL of dichloromethane. After flushing with N$_2$, Zhan catalyst (RC301 0.14 g, 0.19 mmol) was added under N$_2$. The reaction mixture was heated at 60 °C 30 for min. NMR indicated 80% conversion. More bis(trifluoromethyl)-5-vinylbenzene (0.6 g, 2.5 mmol) was added. The reaction mixture was heated at 60 °C for 25 min. NMR indicated ∼90% conversion. It was diluted with hexane and loaded on to Combiflash prepacked silica gel column, eluted with hexane to 15% EtOAc in hexane to give 2.2 g desired product as a white solid (90% yield). ^{1}H NMR (500 MHz, CDCl$_3$) for **56**: 7.73 (s, 3H), 7.56 (s, 1H), 7.40 (m, 7H), 6.47 (d, *J* = 15.9 Hz, 1H), 6.4 (m, 1H), 5.3 (br, 1H), 5.2 (br, 1H), 5.1 (br, 2H), 2.4 (m, 2H), 2.05 (br, 1H), 1.9 (br, 1H).

Benzyl ((S)-3-((2R,3R)-3-(3,5-Bis(trifluoromethyl)phenyl)oxiran-2-yl)-1-(2-bromo-5-(trifluoromethyl)phenyl)propyl)carbamate (57). To a 250 mL round-bottom flask were added **13** (2.2 g, 3.36 mmol), sodium tetraborate decahydrate (1.3 g, 3.36 mmol), 20 mL of 0.4 mM ethylenediaminetetraacetic acid disodium salt dihydrate solution, Bu$_4$NHSO$_4$ (0.11 g, 0.034 mmol), D-Epoxone (0.35 g, 1.35 mmol), 15 mL of CH$_3$CN, and 20 mL of EtOAc. Oxone (6.2 g, 10.1 mmol) in 25 mL of 0.4 mM ethylenediaminetetraacetic acid disodium salt dihydrate solution and 25 mL of K$_2$CO$_3$ (4.88 g, 35.3 mmol) in water were added simultaneously into the flask via syringe pump over 1.2 h at 0 °C. NMR indicated only 30% conversion. After aqueous workup, crude product mixture was subjected the same reaction condition two time. NMR indicated 75% conversion. The reaction mixture was diluted with 150 mL of E/H (1:1) and 100 mL of water. Organics were washed with 50 mL of brine, dried over sodium sulfate, filtered, and concentrated. Crude product was purified on Combiflash prepacked silica gel column, eluted with hexane to 1:7 E/H to give 1.5 g desired product as a white solid (67% yield). ^{1}H NMR (500 MHz, CDCl$_3$) for **57**: 7.84 (s, 1H), 7.73 (s, 2H), 7.4 (d, *J* = 8.0 Hz, 1H), 7.38 (br, 5H), 5.4 (br, 1H), 5.2 (br, 1H), 5.13 (s, 2H), 3.79 (s, 1H), 3.03 (br, 1H), 2.0 (br, sH), 1.75 (br, 1H).

(1R,5S,7aS)-1-(3,5-Bis(trifluoromethyl)phenyl)-5-(2-bromo-5-(trifluoromethyl)phenyl)tetrahydropyrrolo[1,2-c]oxazol-3(1H)-one (58). To a microwave tube were added **57** (1.1 g, 1.64 mmol), DBU (50 mg, 0.33 mmol), and DMF (12 mL). The tube was sealed and flushed with nitrogen gas. It was heated with microwave at 200 °C for 3 min. The reaction mixture was diluted with 100 mL of NH$_4$Cl and 100 mL of E/H (1:2). Organics were separated and washed with 50 mL of NH$_4$Cl, dried over sodium sulfate, filtered, and concentrated. Crude product was purified on Combiflash prepacked silica gel column, eluted with hexane to 1:4 E/H to give 0.63 g desired product as a white solid (68% yield). ^{1}H NMR (500 MHz, CDCl$_3$) for **58**: δ 7.93 (s, 1H), 7.88 (s, 2H), 7.72 (d, *J* = 8.4 Hz, 1H), 7.7 (d, *J* = 1.9 Hz, 1H), 7.44 (dd, *J* = 2.0, 8.2 Hz, 1H), 6.14 (d, *J* = 8.0 Hz, 1H), 5.34 (t, *J* = 8.0 Hz, 1H), 4.61 (m, 1H), 3.0 (m, 1H), 1.67 (m, 1H), 1.55 (m, 1H), 1.26 (m, 1H).

Preparation of Bicyclic Derivatives 46−52. *(1R,5S,7aS)-1-(3,5-Bis(trifluoromethyl)phenyl)-5-(4′-fluoro-5′-isopropyl-2′-methoxy-4-(trifluoromethyl)-[1,1′-biphenyl]-2-yl)tetrahydropyrrolo[1,2-c]-thiazol-3(1H)-one (46).* Step 1. A solution of (2S,5S)-*tert*-butyl 2-(3,5-bis(trifluoromethyl)benzoyl)-5-(2-chloro-5-(trifluoromethyl)phenyl)-pyrrolidine-1-carboxylate (500 mg, 0.848 mmol) in THF (30 mL) was cooled to −78 °C. K-Selectride (1.695 mL, 1.695 mmol) was added dropwise. The reaction was stirred at −78 °C for 1 h. The reaction was diluted with EtOAc, quenched with NH$_4$Cl solution, washed with brine, dried over Na$_2$SO$_4$, filtered, and concentrated. The residue was purified by column chromatography to obtain (2S,5S)-*tert*-butyl 2-((S)-(3,5-bis(trifluoromethyl)phenyl)(hydroxy)methyl)-5-(2-chloro-5-(trifluoromethyl)phenyl)pyrrolidine-1-carboxylate. ^{1}H NMR (500

MHz, CDCl$_3$): δ 7.87 (s, 2H); 7.85 (s, 1H); 7.45–7.50 (m, 2H); 7.22 (s, 1H); 5.44 (d, J = 3.5 Hz, 1H); 5.24 (d, J = 8.4 Hz, 1H); 5.06 (dd, J = 8.1, 3.5 Hz, 1H); 4.54 (t, J = 8.1 Hz, 1H); 2.04–2.07 (m, 3H, merged with solvent peak); 1.81–1.85 (m, 1H); 1.62–1.70 (m, 1H); 1.55–1.59 (m, 3H, merged with water peak); 1.19–1.20 (m, 9H).

Step 2. To a solution of (2*S*,5*S*)-*tert*-butyl 2-((*S*)-(3,5-bis-(trifluoromethyl)phenyl)(hydroxy)methyl)-5-(2-chloro-5-(trifluoromethyl)phenyl)pyrrolidine-1-carboxylate (100 mg, 0.169 mmol) in DCM (1.5 mL) was added Et$_3$N (0.031 mL, 0.220 mmol). The resulting solution was kept at 0 °C and methanesulfonyl chloride (0.014 mL, 0.186 mmol) was added. The reaction mixture was stirred for 30 min. It was diluted with DCM, washed sequentially with NH$_4$Cl and brine, dried over Na$_2$SO$_4$, filtered, and concentrated. The residue was purified by column chromatography to obtain (2*S*,5*S*)-*tert*-butyl 2-((*S*)-(3,5-bis(trifluoromethyl)phenyl)((methylsulfonyl)oxy)methyl)-5-(2-chloro-5-(trifluoromethyl)phenyl)pyrrolidine-1-carboxylate. ^{1}H NMR (500 MHz, CDCl$_3$): δ 7.96–7.97 (m, 1H); 7.82 (s, 2H); 7.45 (s, 2H); 7.20 (s, 1H); 6.42 (d, J = 4.9 Hz, 1H); 4.74–4.79 (m, 2H); 3.17 (s, 3H); 1.96–2.10 (m, 4H); 1.41–1.45 (m, 1H); 1.21 (s, 8H).

Step 3. To a solution of (2*S*,5*S*)-*tert*-butyl 2-((*S*)-(3,5-bis-(trifluoromethyl)phenyl)((methylsulfonyl)oxy)methyl)-5-(2-chloro-5-(trifluoromethyl)phenyl)pyrrolidine-1-carboxylate (1.5 g, 2.239 mmol) in DCM (3 mL) was added TFA (2.59 mL, 33.6 mmol). The reaction was stirred for 45 min. The volatiles were removed, and the residue was dissolved in EtOAc. The resulting mixture was washed with saturated NaHCO$_3$, then brine, dried over Na$_2$SO$_4$, filtered, and concentrated to afford (*S*)-(3,5-bis(trifluoromethyl)phenyl)((2*S*,5*S*)-5-(2-chloro-5-(trifluoromethyl)phenyl)pyrrolidin-2-yl)methyl methanesulfonate. It was used for the next step without further purification.

Step 4. To a solution of (*S*)-(3,5-bis(trifluoromethyl)phenyl)-((2*S*,5*S*)-5-(2-chloro-5-trifluoromethyl)phenyl)pyrrolidin-2-yl)methyl methanesulfonate (170 mg, 0.298 mmol) in DCM (3 mL) was added 2,6-di-*tert*-butyl-4-methylpyridine (123 mg, 0.597 mmol), followed by SS-isopropyl carbonochlorido(dithioperoxoate) (102 mg, 0.597 mmol) at 0 °C. The reaction was stirred for 30 min. To the resulting mixture was added MeOH (1.00 mL) followed by triphenylphosphine (156 mg, 0.597 mmol). The reaction mixture was stirred for 30 min. The volatiles were removed. The reaction was diluted with DCM, neutralized with satd. NaHCO$_3$, washed with brine, dried over Na$_2$SO$_4$, filtered, and concentrated. The residue was purified by column chromatography to afford (1*R*,5*S*,7a*S*)-1-(3,5-bis(trifluoromethyl)-phenyl)-5-(2-chloro-5-(trifluoromethyl)phenyl)tetrahydropyrrolo-[1,2-*c*]thiazol-3(1*H*)-one. ^{1}H NMR (500 MHz, CDCl$_3$): δ 7.95 (s, 2H); 7.93 (s, 1H); 7.56 (s, 1H); 7.52 (s, 2H); 5.35 (t, J = 7.9 Hz, 1H); 5.30 (d, J = 8.2 Hz, 1H); 4.86–4.91 (m, 1H); 2.75–2.81 (m, 1H); 1.78–1.86 (m, 1H); 1.54–1.62 (m, 2H); 1.33–1.41 (m, 1H). MS ESI/APCI calcd for C$_{21}$H$_{13}$ClF$_9$NOS [M + H]$^+$ 533.8, found 533.8.

Step 5. In a microwave vial was taken (1*R*,5*S*,7a*S*)-1-(3,5-bis(trifluoromethyl)phenyl)-5-(2-chloro-5-(trifluoromethyl)phenyl)-tetrahydropyrrolo[1,2-*c*]thiazol-3(1*H*)-one (20 mg, 0.037 mmol) in *N*,*N*-dimethylacetamide (0.5 mL). The mixture was degassed with nitrogen. Chloro(2-dicyclohexylphosphino-2′,4′,6′-triisopropyl-1,1′-biphenyl)[2-(2′-amino-1,1′-biphenyl)]palladium(II) (2.95 mg, 3.75 μmol), aqueous K$_3$PO$_4$ solution (0.037 mL, 0.075 mmol) were added, followed by (4-fluoro-5-isopropyl-2-methoxyphenyl)boronic acid (11.92 mg, 0.056 mmol). The resulting mixture was stirred at 85 °C for 1 h. After cooling, EtOAc was added. The resulting mixture was washed sequentially with NH$_4$Cl solution and brine, dried over Na$_2$SO$_4$, filtered, and concentrated. The crude product was purified by reversed-phase HPLC to yield the title compound **46**. ^{1}H NMR (500 MHz, CDCl$_3$, 1:1 mixture of atropisomers): δ 7.81–7.84 (m, 6 H, contains for two atropisomers protons); 7.53–7.56 (m, 4 H, contains for two atropisomers protons); 7.28 (s, 2H, contains for two atropisomers protons); 7.20 (d, J = 8.6 Hz, 1H); 6.88 (d, J = 8.6 Hz, 1H); 6.65 (dd, J = 23.7, 12.0 Hz, 2H, contains for two atropisomers protons); 5.22 (d, J = 8.3 Hz, 1H); 5.12–5.14 (m, 1H); 5.02 (t, J = 8.1 Hz, 1H); 4.84 (t, J = 8.1 Hz, 1H); 4.73–4.78 (m, 1H); 4.58–4.63 (m, 1H); 3.80 (s, 3H); 3.65 (d, J = 0.6 Hz, 3H); 3.14–3.24 (m, 2H); 1.17–1.29 (m, 12H). MS ESI/APCI calcd for C$_{31}$H$_{25}$F$_{10}$NO$_2$S [M + H]$^+$ 665.6, found 666.0. RTA (95% HS): 2350 nM.

(1*R*,5*S*,7a*S*)-1-[3,5-Bis(trifluoromethyl)phenyl]-5-[4′-fluoro-2′-methoxy-5′-(1-methylethyl)-4-(trifluoromethyl)biphenyl-2-yl]-hexahydro-3*H*-pyrrolizin-3-one (47). *Step 1.* To a solution of triethyl phosphonoacetate (3.8 mL, 16.9 mmol) in toluene (40.0 mL) was added sodium hydride (0.68 g, 16.9 mmol) at 0 °C. The resulting solution was stirred at room temperature for 0.5 h. The reaction was cooled back to 0 °C, *tert*-butyl (2*S*,5*S*)-2-(3,5-bis(trifluoromethyl)-benzoyl)-5-(2-chloro-5-(trifluoromethyl)phenyl)pyrrolidine-1-carboxylate (5.00 g, 8.47 mmol) in toluene (20.0 mL) was added slowly. The resulting solution was stirred at room temperature for 2.5 h. The reaction was quenched by the addition of saturated NH$_4$Cl solution (40.0 mL). It was diluted with ethyl acetate (50 mL), and the layers were separated. The organic layer was washed with water, dried over anhydrous Na$_2$SO$_4$, and concentrated to yield *tert*-butyl (2*S*,5*S*)-2-((*Z*)-1-(3,5-bis(trifluoromethyl)phenyl)-3-ethoxy-3-oxoprop-1-en-1-yl)-5-(2-chloro-5-(trifluoromethyl)phenyl)pyrrolidine-1-carboxylate as a solid that was carried forward to the next step without further purification. LC-MS APCI calcd for C$_{29}$H$_{27}$ClF$_9$NO$_4$ [M-Boc]$^+$ 559.9, found 560.0.

Step 2. To a nitrogen-purged solution of tert-butyl (2*S*,5*S*)-2-((*Z*)-1-(3,5-bis(trifluoromethyl)phenyl)-3-ethoxy-3-oxoprop-1-en-1-yl)-5-(2-chloro-5-(trifluoromethyl)phenyl)pyrrolidine-1-carboxylate (2.6 g, 3.93 mmol) in ethyl acetate (30.0 mL) was added platinum(IV) oxide (600 mg) and the resulting mixture was stirred at room temperature under H$_2$ for 16 h. The reaction mixture was filtered through a bed of diatomaceous earth and the filtrate was concentrated to yield *tert*-butyl (2*S*,5*S*)-2-((*R*)-1-(3,5-bis(trifluoromethyl)phenyl)-3-ethoxy-3-oxopropyl)-5-(2-chloro-5-(trifluoromethyl)phenyl)-pyrrolidine-1-carboxylate as a solid that was carried forward to the next step without further purification. LC-MS APCI calcd for C$_{29}$H$_{29}$ClF$_9$NO$_4$ [M + H − Boc]$^+$ 562.2, found 562.2.

Step 3. To a solution of *tert*-butyl (2*S*,5*S*)-2-((*R*)-1-(3,5-bis-(trifluoromethyl)phenyl)-3-ethoxy-3-oxopropyl)-5-(2-chloro-5-(trifluoromethyl)phenyl)pyrrolidine-1-carboxylate (2.3 g, 3.47 mmol) in dichloromethane (10.0 mL) was added trifluoroacetic acid (20.0 mL). The resulting solution was stirred at room temperature for 16 h. The reaction solution was concentrated. The residue was partitioned between ethyl acetate (100.0 mL) and aqueous 10% NaHCO$_3$ solution (50.0 mL). The organic layer was washed with water, dried over anhydrous Na$_2$SO$_4$, and concentrated to yield ethyl (*R*)-3-(3,5-bis(trifluoromethyl)phenyl)-3-((2*S*,5*S*)-5-(2-chloro-5-(trifluoromethyl)phenyl)pyrrolidin-2-yl)propanoate. The crude product was taken up in toluene (25.0 mL) in a 100 mL seal tube. Triethylamine (1.93 mL, 14.9 mmol) was added, and the reaction solution was heated at 100 °C for 16 h. The reaction solution was concentrated. The residue was diluted with ethyl acetate (75.0 mL), washed with water, dried over anhydrous Na$_2$SO$_4$, and concentrated. The crude product was purified by flash column chromatography to yield (1*R*,5*S*,7a*S*)-1-(3,5-bis(trifluoromethyl)phenyl)-5-(2-chloro-5-(trifluoromethyl)phenyl)hexahydro-3*H*-pyrrolizin-3-one as a solid. LC-MS APCI calcd for C$_{22}$H$_{15}$ClF$_9$NO [M + H]$^+$ 515.6, found 516.0. ^{1}H NMR (300 MHz, DMSO-*d$_6$*): δ 8.02 (s, 3H), 7.73–7.65 (m, 3H), 5.04 (t, J = 8.07 Hz, 1H), 4.63–4.55 (m, 1H), 4.30 (q, J = 7.77 Hz, 1H), 3.19–3.10 (m, 1H), 2.85 (q, J = 6.87 Hz, 1H), 2.63–2.56 (m, 1H), 1.60–1.54 (m, 1H), 1.37–1.33 (m, 1H), 1.15–1.00 (m, 1H).

Step 4. In a microwave vial was taken (1*R*,5*S*,7a*S*)-1-(3,5-bis(trifluoromethyl)phenyl)-5-(2-chloro-5-(trifluoromethyl)phenyl)-hexahydro-3*H*-pyrrolizin-3-one (20 mg, 0.037 mmol) in *N*,*N*-dimethylacetamide (0.5 mL). The mixture was degassed with nitrogen. Chloro(2-dicyclohexylphosphino-2′,4′,6′-triisopropyl-1,1′-biphenyl)-[2-(2′-amino-1,1′-biphenyl)]palladium(II) (2.95 mg, 3.75 μmol), aqueous K$_3$PO$_4$ solution (0.037 mL, 0.075 mmol) were added, followed by (4-fluoro-5-isopropyl-2-methoxyphenyl)boronic acid (11.92 mg, 0.056 mmol). The resulting mixture was stirred at 85 °C for 1 h. After cooling, EtOAc was added. The resulting mixture was washed sequentially with NH$_4$Cl solution and brine, dried over Na$_2$SO$_4$, filtered, and concentrated. The crude product was purified by reversed-phase HPLC to yield the title compound **47**. Calcd 648.2, found 649.2.

Preparation of Compounds 48a−b and 49. **((1*R*,5*S*,7a*S*)-1-(3,5-Bis(trifluoromethyl)phenyl)-5-(2-chloro-5-(trifluoromethyl)-**

phenyl)tetrahydro-1H-pyrrolo[1,2-c]imidazol-3(2H)-one (Intermediate 8-1). Step 1. To a 500 mL three-neck RBF equipped with a magnetic stirring bar were added, under N_2 atmosphere, 3-bromo-4-chloro-benzotrifluoride (16.5 mL, 110 mmol) and dry THF (150 mL). The resulting solution was cooled to 0 °C. To this solution was added *i*-PrMgBr (110 mL, 110 mmol) and the reaction was warmed to rt and stirred for 1 h. To another 500 mL RBF containing a solution of CuBr·Me₂S (18.8 g, 91.5 mmol) in THF (100 mL) was added BF₃·OEt₂ (14 mL, 110 mmol) dropwise at −40 °C. The resulting solution was stirred at that temperature for 45 min. Then, the Grignard reagent prepared previously was added dropwise to this solution while maintaining the internal temperature at −32 to −38 °C. After completion of addition, the reaction mixture was stirred at that temperature for 1 h. The reaction mixture was cooled to −78 °C, and a solution of (2*S*)-1-*t*-butyl 2-ethyl 5-methoxypyrrolidine-1,2-dicarboxylate (25.0 g, 91.5 mmol) in THF (50 mL) was added dropwise. The resulting reaction mixture was allowed to warm up to rt and was stirred for 14 h. The reaction mixture was cooled to 0 °C, and saturated aqueous NH₄Cl solution (100 mL) was added followed by aqueous NH₄OH solution (100 mL) and water (300 mL). The layers were separated. The aqueous layer was extracted with EtOAc (3 × 200 mL). The combined organics were dried over anhydrous Na₂SO₄ and concentrated. The crude product was purified by column chromatography eluting with 5% EtOAc in petroleum ether to yield (2*S*,5*S*)-1-*tert*-butyl 2-ethyl 5-(2-chloro-5-(trifluoromethyl)-phenyl)pyrrolidine-1,2-dicarboxylate (34.0 g, 79.8 mmol) as a colorless liquid. ¹H NMR (400 MHz, CDCl₃) δ 7.32−7.47 (m, 3 H), 5.39−5.50 (m, 1H), 4.58−4.70 (m, 1H), 4.22−4.28 (m, 2H), 2.55 (m, 1H), 2.18 (m, 1H), 2.05 (m, 1H), 1.83 (m, 1H), 1.16−1.43 (m, 12H); LC-MS ESI calcd for C₁₉H₂₃ClF₃NO₄ [M-Boc]⁺ 321.84, found 322.2.

Step 2. To a 250 mL RBF containing a solution of (2*S*,5*S*)-1-*tert*-butyl 2-ethyl 5-(2-chloro-5-(trifluoromethyl)phenyl)pyrrolidine-1,2-dicarboxylate (4.00 g, 9.48 mmol) and 1-bromo-3,5-bis-(trifluoromethyl)benzene (2.5 mL, 14.22 mmol) in diethyl ether (40 mL) was added *n*-BuLi (1.6 M in hexanes, 8.9 mL, 14.2 mmol) dropwise at −78 °C. The resulting solution was stirred at that temperature for 2 h and was allowed to warm to rt and stirred for another 3 h. The reaction was quenched by addition of saturated NH₄Cl solution (20 mL). It was diluted with diethyl ether (100 mL) and the layers were separated. The organic layer was rinsed with water (3 × 200 mL), dried over brine and anhydrous Na₂SO₄, and concentrated. The crude product was purified by column chromatography eluting with 5% EtOAc in petroleum ether to yield (2*S*,5*S*)-*tert*-butyl 2-(3,5-bis(trifluoromethyl)benzoyl)-5-(2-chloro-5-(trifluoromethyl)phenyl)pyrrolidine-1-carboxylate (3.80 g, 6.44 mmol) as a colorless, gummy solid. ¹H NMR (400 MHz, CDCl₃) δ 8.49 (d, 2H, *J* = 12 Hz), 8.13 (d, 1H, *J* = 15 Hz), 7.86−7.91 (m, 1H), 7.48−7.55 (m, 2H), 5.55−5.73 (m, 2H), 2.37−2.59 (m, 2H), 1.90−1.96 (m, 2H), 1.17 (s, 9H); LC-MS ESI calcd for C₂₅H₂₁ClF₉NO₃ [M-Boc]⁺ 489.88, found 490.0.

Step 3. To a solution of (2*S*,5*S*)-*tert*-butyl 2-(3,5-bis-(trifluoromethyl)benzoyl)-5-(2-chloro-5-(trifluoromethyl)phenyl)-pyrrolidine-1-carboxylate (2.00 g, 3.39 mmol) in MeOH (20 mL) were added NH₄OAc (2.61 g, 33.9 mmol) and NaCNBH₃ (639 mg, 10.2 mmol). The resulting reaction mixture was heated in a 100 mL pressure tube at 100 °C for 16 h. After cooling to rt, silica gel was added to the reaction mixture to make a slurry. It was purified by column chromatography to yield (2*S*,5*S*)-*tert*-butyl 2-((*R*)-amino(3,5-bis-(trifluoromethyl)phenyl)methyl)-5-(2-chloro-5-(trifluoromethyl)-phenyl)pyrrolidine-1-carboxylate (620 mg, 1.05 mmol). LC-MS ESI calcd for C₂₅H₂₄ClF₉N₂O₂ [M + H]⁺ 590.1, 592.1, found 491.0, 493.0.

Step 4. To a solution (2*S*,5*S*)-*tert*-butyl 2-((*R*)-amino(3,5-(trifluoromethyl)phenyl)methyl)-5-(2-chloro-5-(trifluoromethyl)-phenyl)pyrrolidine-1-carboxylate (620 mg, 1.05 mmol) in CH₂Cl₂ (5 mL) was added a solution of HCl in dioxane (10 mL), and the reaction was stirred at rt for 4 h. The reaction solution was concentrated, the residue was partitioned between CH₂Cl₂ and 10% NaHCO₃ aqueous solution. The aqueous layer was extracted with CH₂Cl₂, dried over anhydrous Na₂SO₄, and concentrated to yield (*R*)-(3,5-(trifluoromethyl)phenyl)((2*S*,5*S*)-5-(2-chloro-5-(trifluoromethyl)-phenyl)pyrrolidin-2-yl)methanamine (525 mg, 1.05 mmol). It was

carried forward to the next step without further purification. LC-MS ESI calcd for C₂₀H₁₆ClF₉N₂ [M + H]⁺ 491.1, 493.1, found 491.0, 493.0.

Step 5. To a solution of (*R*)-(3,5-bis(trifluoromethyl)phenyl)-((2*S*,5*S*)-5-(2-chloro-5-(trifluoromethyl)phenyl)pyrrolidin-2-yl)-methanamine (525 mg, 1.07 mmol) in CH₂Cl₂ (10 mL) were added Et₃N (0.45 mL, 3.21 mmol) and triphosgene (476 mg, 1.60 mmol) at 0 °C. The resulting reaction mixture was allowed to warm up to rt and stirred for 3 h. It was then diluted with CH₂Cl₂, rinsed with 1.5 N HCl aqueous solution and water, dried over anhydrous Na₂SO₄, and concentrated. The crude product was purified by column chromatography eluted with 10% EtOAc in petroleum ether to yield **Intermediate 8-1** (180 mg, 0.35 mmol). ¹H NMR (400 MHz, CDCl₃) δ 7.89 (m, 3 H), 7.80 (s, 1H), 7.48 (d, 2H, *J* = 2 Hz), 5.51 (s, 1H), 5.43−5.45 (d, 1H, *J* = 9 Hz), 5.27−5.31 (t, 1H, *J* = 8 Hz), 4.41−4.47 (m, 1H), 2.83−2.91 (m, 1H), 1.51−1.59 (m, 1H), 1.41 (m, 2H); LC-MS ESI calcd for C₂₁H₁₄ClF₉N₂O [M + H]⁺ 517.1, 519.1, found 516.8, 518.8.

(1R,5S,7aS)-1-(3,5-Bis(trifluoromethyl)phenyl)-5-(2-chloro-5-(trifluoromethyl)phenyl)-2-methyltetrahydro-1H-pyrrolo[1,2-c]-imidazol-3(2H)-one (Intermediate 8-2). To a solution of (1*R*,5*S*,7a*S*)-1-(3,5-bis(trifluoromethyl)phenyl)-5-(2-chloro-5-(trifluoromethyl)phenyl)tetrahydro-1*H*-pyrrolo[1,2-*c*]imidazol-3(2*H*)-one (120 mg, 0.23 mmol) in DMF (5 mL), stirring at 0 °C was added NaH (11 mg, 0.28 mmol), and the reaction was stirred for 30 min, after which MeI (0.02 mL, 0.35 mmol) was added and the solution was stirred at rt for 3 h. Ice was added to the reaction mixture, the layers separated and the aqueous fraction was extracted was with EtOAc. The combined organic fractions were dried over anhydrous Na₂SO₄ and concentrated to yield (1*R*,5*S*,7a*S*)-1-(3,5-bis(trifluoromethyl)phenyl)-5-(2-chloro-5-(trifluoromethyl)phenyl)-2-methyltetrahydro-1*H*-pyrrolo[1,2-*c*]imidazol-3(2*H*)-one (120 mg, 0.23 mmol). ¹H NMR (400 MHz, CDCl₃): δ 7.92 (s, 1H), 7.80 (s, 1H), 7.77 (s, 2H), 7.49−7.48 (m, 2H), 5.29 (t, *J* = 8.28 Hz, 1H), 5.07 (d, *J* = 8.80 Hz, 1H), 4.31−3.29 (m, 1H), 2.85 (s, 3H), 2.84−2.79 (m, 1H), 1.61−1.52 (m, 1H), 1.32−1.25 (m, 2H). LC-MS ESI calcd for C₂₂H₁₆ClF₉N₂O [M + H]⁺ 531.09, found, 531.0.

(3R,3aS,6S)-3-(3,5-Bis(trifluoromethyl)phenyl)-6-(2-chloro-5-(trifluoromethyl)phenyl)hexahydropyrrolo[1,2-b][1,2,5]thiadiazole 1,1-Dioxide (Intermediate 8-3). To a solution of (*R*)-(3,5-bis-(trifluoromethyl)phenyl)((2*S*,5*S*)-5-(2-chloro-5-(trifluoromethyl)-phenyl)pyrrolidin-2-yl)methanamine (300 mg, 0.61 mmol) in pyridine (5.0 mL) was added sulfuric diamide (176 mg, 1.81 mmol) at room temperature. The reaction mixture was heated at 105 °C for 16 h. The reaction mixture was concentrated. The crude product was purified by flash column chromatography using 10% ethyl acetate in hexanes to yield (3*R*,3a*S*,6*S*)-3-(3,5-bis(trifluoromethyl)phenyl)-6-(2-chloro-5-(trifluoromethyl)phenyl)hexahydropyrrolo[1,2-*b*][1,2,5]thiadiazole 1,1-dioxide (130 mg, 0.23 mmol) as a white solid. ¹H NMR (300 MHz, CDCl₃): δ 7.93 (d, *J* = 3.54 Hz, 2H), 7.88 (s, 2H), 7.50 (d, *J* = 1.20 Hz, 2H), 5.44−5.36 (m, 2H), 4.75 (d, *J* = 4.05 Hz, 1H), 4.68−4.61 (m, 1H), 2.63−2.59 (m, 1H), 1.64 (t, *J* = 11.91 Hz, 2H), 1.58−1.49 (m, 1H). **LC-MS** ESI calcd for C₂₀H₁₄ClF₉N₂O₂S [M − H]⁺ 551.8, found 551.84.

4-(5-(2-((1R,5S,7aS)-1-(3,5-Bis(trifluoromethyl)phenyl)-3-oxohex-ahydro-1H-pyrrolo[1,2-c]imidazol-5-yl)-4-(trifluoromethyl)phenyl)-6-methoxypyridin-3-yl)-3-methylbenzoic Acid (Exemplar Compound Related to 48a, 48b, 49). Step 1. To a 2−5 mL microwave reaction vial was charged **Intermediate 8-1** (20 mg, 0.039 mmol) along with methyl 4-(6-methoxy-5-(4,4,5,5-tetramethyl-1,3,2-dioxaborolan-2-yl)pyridin-3-yl)-3-methylbenzoate (19.46 mg, 0.043 mmol), potassium phosphate (18.07 mg, 0.085 mmol) and XPhos PreCat (1.430 mg, 1.935 μmol). The vial was sealed and degassed and refilled with nitrogen. Solvent THF (1 mL) and Water (0.1 mL) were then added and the vial was degassed again. The mixture was then exposed to microwave irradiation at 100 °C for 30 min. The mixture was then diluted with ethyl acetate (5 mL), filtered through a syringe filter, and was washed with ethyl acetate (2 × 1 mL). The filtrate was concentrated, and the residue was purified by MPLC (4 g silica gel, 0 to 25% ethyl acetate in hexanes, 40CV) to afford product methyl 4-(5-(2-((1*R*,5*S*,7a*S*)-1-(3,5-bis(trifluoromethyl)phenyl)-3-oxohexahydro-1*H*-pyrrolo[1,2-*c*]imidazol-5-yl)-4-(trifluoromethyl)phenyl)-6-me-

thoxypyridin-3-yl)-3-methylbenzoate as a white solid. LC-MS (ESI): $[M + H]^+$ for $C_{36}H_{28}F_9N_3O_4$: calcd 738.2 found 738.2.

Step 2. A 20 mL sample vial was charged with methyl 4-(5-(2-((1R,5S,7aS)-1-(3,5-bis(trifluoromethyl)phenyl)-3-oxohexahydro-1H-pyrrolo[1,2-c]imidazol-5-yl)-4-(trifluoromethyl)phenyl)-6-methoxypyridin-3-yl)-3-methylbenzoate (28 mg, 0.038 mmol) along with THF (0.5 mL), MeOH (0.500 mL), and water (0.1 mL), followed by addition of lithium hydroxide monohydrate (12 mg, 0.286 mmol). The mixture was then stirred at room temperature for 15 h overnight. The mixture was neutralized with HCl (1 N, 0.286 mL) and concentrated. The product was purified by reversed-phase HPLC using a column supplied by YMC 40-80% acetonitrile in water with 0.5% TFA to afford a white solid product 4-(5-(2-((1R,5S,7aS)-1-(3,5-bis(trifluoromethyl)phenyl)-3-oxohexahydro-1H-pyrrolo[1,2-c]imidazol-5-yl)-4-(trifluoromethyl)phenyl)-6-methoxypyridin-3-yl)-3-methylbenzoic acid. LC-MS (ESI): $[M + H]^+$ for $C_{35}H_{24}F_9N_3O_4$: calcd 724.2 found 724.1. RTA (95% HS): 335 nM. Exact mass of **48a**, **48b**, and **49** prepared by this scheme is provided in the SI.

(Z)-4-(3,5-Bis(trifluoromethyl)phenyl)but-3-en-1-yl trifluoromethanesulfonate (Intermediate 9-1). Step 1. To a 250 mL RBF were added 3-butyn-1-ol (500 mg, 7.13 mmol), 3,5-bis(trifluoromethyl)-bromobenzene (2.3 g, 7.9 mmol), Cs_2CO_3 (7.0 g, 21.4 mmol), $PdOAc_2$ (160 mg, 0.71 mmol), 2-dicyclohexylphosphino-2′-(N,N-dimethylamino)biphenyl (561 mg, 1.43 mmol), and acetonitrile (25 mL). The palladium catalyst and ligand are represented as "Pd" in Scheme A1. The mixture was stirred at 80 °C for 2 h. It was cooled down to room temperature, diluted with EtOAc (100 mL), and washed with water and 10% HCl. The organic layer was concentrated and purified by normal-phase column chromatography to yield 4-(3,5-bis(trifluoromethyl)phenyl)but-3-yn-1-ol as a yellow solid.). ^{1}H NMR (500 MHz, $CDCl_3$) δ 7.87 (s, 2H), 7.8 (s, 1H), 3.89 (m, 2H), 2.76 (m, 2H).

Step 2. To a 250 mL RBF were added 4-(3,5-bis(trifluoromethyl)-phenyl) but-3-yn-1-ol (4.9 g, 17.4 mmol) and Lindlar catalyst (0.18 g, 0.86 mmol), followed by EtOH (20 mL). The reaction mixture was stirred under an H_2 atmosphere from a balloon at room temperature overnight. NMR showed when the reaction was complete. The reaction mixture was filtered through a pad of Celite. The filtrate was concentrated, and the residue was purified by normal-phase column chromatography to yield (Z)-4-(3,5-bis(trifluoromethyl)phenyl)but-3-en-1-ol as a yellow oil. ^{1}H NMR (500 MHz, $CDCl_3$) δ 7.78 (m, 3H), 6.64 (d, J = 11.6 Hz, 1H), 5.70 (m, 1H), 3.82 (m, 2H), 2.60 (m, 2H).

Step 3. To a 100 mL RBF was added (Z)-4-(3,5-(trifluoromethyl)phenyl) but-3-en-1-ol (4.3 g, 15.1 mmol, dissolved in 50 mL of DCM). Tf_2O (3.1 mL, 18.2 mmol) was added at 0 °C, followed by pyridine (1.22 mL, 15.1 mmol). TLC and NMR showed when the reaction was complete. Volatiles were removed. The residue was dissolved in EtOAc, and the product was washed sequentially with 1 N HCl, then saturated $NaHCO_3$. The organic layer was dried over Na_2SO_4 and concentrated to give (Z)-4-(3,5-bis(trifluoromethyl)-phenyl)but-3-en-1-yl trifluoromethanesulfonate as a brown oil. It was used directly in the next step. ^{1}H NMR (500 MHz, $CDCl_3$) δ 7.83 (s, 1H), 7.70 (s, 2H), 6.78 (d, J = 11.5 Hz, 1H), 5.89 (m, 1H), 4.63 (m, 2H), 2.80 (m, 2H).

3-(3,5-Bis(trifluoromethyl)phenyl)-6-(2-chloro-5-(trifluoromethyl)phenyl)-3a,4,5,6-tetrahydro-3H-cyclopenta[c]-isoxazole (Intermediate 9-2). Step 1. To a 100 mL RBF were added nBuLi (5.8 mL, 9.3 mmol) and dry THF. Diisopropylamine (1.39 mL, 9.8 mmol) was added at 0 °C under N_2. After stirring for 10 min, the mixture was cooled to −78 °C. A THF solution of 2-(2-chloro-5-(trifluoromethyl)phenyl)-N-methoxy-N-methylacetamide (2.5 g, 8.9 mmol) was added. After the reaction mixture was stirred at −78 °C for 20 min, (Z)-4-(3,5-bis(trifluoromethyl)phenyl)but-3-en-1-yl trifluoromethanesulfonate (3.33 g, 7.99 mmol) was added. The reaction mixture was allowed to warm to room temperature and was stirred at room temperature for 1 h. The reaction mixture was diluted with EtOAc, washed with saturated NH_4Cl, and concentrated. The residue was purified by normal-phase column chromatography to yield (Z)-6-(3,5-(trifluoromethyl)phenyl)-2-(2-chloro-5-(trifluoromethyl)-phenyl)-N-methoxy-N-methylhex-5-enamide as a yellow oil. ^{1}H NMR

(500 MHz, $CDCl_3$) δ 7.75 (s, 1H), 7.69 (s, 1H), 7.67 (s, 2H), 7.50 (d, J = 8.3 Hz, 1H), 7.44 (d, J = 8.3 Hz, 1H), 6.50 (d, J = 11.4 Hz, 1H), 5.88 (m, 1H), 3.50 (s, 3H), 3.15 (s, 3H), 2.40 (m, 1H), 2.30 (m, 2H), 1.85 (m, 1H). $[M + H]^+$ 548, found 547.96.

Step 2. To a 100 mL RBF was added (Z)-6-(3,5-bis-(trifluoromethyl)phenyl)-2-(2-chloro-5-(trifluoromethyl)phenyl)-N-methoxy-N-methylhex-5-enamide (1.7 g, 3.10 mmol) in THF. DIBAL (3.72 mL, 3.72 mmol) was added at 0 °C. The mixture was stirred at room temperature until NMR showed that there was no starting material left. It was quenched by addition of 1 N HCl, extracted with EtOAc, concentrated, and purified by normal-phase column chromatography to yield (Z)-6-(3,5-bis(trifluoromethyl)phenyl)-2-(2-chloro-5-(trifluoromethyl)phenyl)hex-5-enal as a colorless oil. ^{1}H NMR (500 MHz, $CDCl_3$) δ 9.79 (s, 1H), 7.8 (s, 1H), 7.76 (s, 1H), 7.60 (s, 2H), 7.58 (d, J = 8.3 Hz, 1H), 7.47 (d, J = 8.3 Hz, 1H), 6.55 (d, J = 11.7 Hz, 1H), 5.82 (m, 1H), 4.18 (m, 1H), 2.58 (m, 1H), 2.38 (m, 2H), 1.95 (m, 1H).

Step 3. To a 100 mL RBF were added (Z)-6-(3,5-bis-(trifluoromethyl)phenyl)-2-(2-chloro-5-(trifluoromethyl)phenyl)hex-5-enal (600 mg, 1.23 mmol), hydroxylamine hydrochloride (341 mg, 4.91 mmol), pyridine (0.60 mL, 7.4 mmol), and DCM. The reaction mixture was stirred at room temperature for 15 min. NMR and LCMS showed a clean product. Volatiles were removed. The residue was purified by normal-phase column chromatography to yield (1E,5Z)-6-(3,5-bis(trifluoromethyl)phenyl)-2-(2-chloro-5-(trifluoromethyl)-phenyl)hex-5-enal oxime as a white solid. $[M + H]^+$ calcd: 504, found 503.9.

Step 4. To a 20 mL vial were added (1E,5Z)-6-(3,5-bis-(trifluoromethyl)phenyl)-2-(2-chloro-5-(trifluoromethyl)phenyl)hex-5-enal oxime (35 mg, 0.069 mmol) and NCS (11.1 mg, 0.083 mmol, dissolved in DMF). The reaction mixture was stirred at room temperature. NMR indicated that the starting material was consumed. TEA (0.25 mL, 1.78 mmol) in DCM was added dropwise. The resulting reaction mixture was stirred at room temperature for 10 min. LCMS showed the desired clean product. Volatiles were removed. Residue was purified by prep-TLC to yield **Intermediate 9-2** as a racemic mixture. ^{1}H NMR (500 MHz, $CDCl_3$) δ 7.88 (s, 1H), 7.78 (s, 2H), 7.52 (m, 3H), 5.98 (d, J = 9.9 Hz, 1H), 4.54 (m, 1H), 4.26 (m, 1H), 2.90 (m, 1H), 2.14 (m, 1H), 1.93 (m, 1H), 1.00 (m, 1H). $[M + H]^+$ calcd: 501, found 501.8.

4-(5-(2-((3S,3aR,6S)-3-(3,5-Bis(trifluoromethyl)phenyl)-3a,4,5,6-tetrahydro-3H-cyclopenta[c]isoxazol-6-yl)-4-(trifluoromethyl)-phenyl)-6-methoxypyridin-3-yl)-3-methylbenzoic acid (51a), and 4-(5-(2-((3R,3aS,6R)-3-(3,5-bis(trifluoromethyl)phenyl)-3a,4,5,6-tetrahydro-3H-cyclopenta[c]isoxazol-6-yl)-4-(trifluoromethyl)phenyl)-6-methoxypyridin-3-yl)-3-methylbenzoic Acid (51b) (Exemplar Compounds Related to 51). Step 1. To a 5 mL RBF were added 3-(3,5-bis(trifluoromethyl)phenyl)-6-(2-chloro-5-(trifluoromethyl)phenyl)-3a,4,5,6-tetrahydro-3H-cyclopenta[c]isoxazole (**Intermediate 10-1**) (50 mg, 0.1 mmol), tert-butyl 4-(6-methoxy-5-(4,4,5,5-tetramethyl-1,3,2-dioxaborolan-2-yl)pyridin-3-yl)-3-methylbenzoate (51 mg, 0.12 mmol), potassium phosphate (42.3 mg, 0.199 mmol), XPhos precatalyst (7.84 mg, 9.96 μmol), 1,4-dioxane (2 mL) and water (0.2 mL). The mixture was stirred at 90 °C for 2 h. After cooling down, volatiles were removed. The residue was purified by silica gel column chromatography to yield the target compound as a racemic mixture. $[M − H]^+$ 763.2, found 763.3.

Step 2. To a 10 mL scintillation vial were added tert-butyl 4-(5-(2-(3-(3,5-bis(trifluoromethyl)phenyl)-3a,4,5,6-tetrahydro-3H-cyclopenta[c]isoxazol-6-yl)-4-(trifluoromethyl)phenyl)-6-methoxypyridin-3-yl)-3-methylbenzoate (20 mg, 0.026 mmol) and DCM (0.5 mL), followed by TFA (0.81 mL, 10.5 mmol). After the reaction mixture was stirred at room temperature for 10 min, LCMS showed all of the starting material has converted. Volatiles were removed. Residue was purified by reversed-phase HPLC to yield 4-(5-(2-((3S,3aR,6S)-3-(3,5-bis(trifluoromethyl)phenyl)-3a,4,5,6-tetrahydro-3H-cyclopenta-[c]isoxazol-6-yl)-4-(trifluoromethyl)phenyl)-6-methoxypyridin-3-yl)-3-methylbenzoic as a racemic mixture. The racemic mixture was separated by chiral SFC on Chiral Cel IA (4.6 mm × 250 mm) with 30% 2:1 MeOH:MeCN/CO_2 (2.1 mL/min, 100 bar, 35 °C) as the eluent to

give a pair of enantiomers with retention time of 2.16 (**51a**) and 2.85 min (**51b**), respectively. ^{1}H NMR (500 MHz, CDCl$_3$): δ 8.27 (d, J = 2.3 Hz, 1H), 8.08 (s, 1H), 8.05 (d, J = 2.3 Hz, 1H), 7.83 (s, 1H), 7.74 (s, 1H), 7.69 (s, 1H), 7.61(s, 2H), 7.57(s, 1H), 7.40 (d, J = 2.1 Hz, 1H), 7.38(d, J = 2.1 Hz, 1H), 5.92 (d, J = 10.6 Hz, 1H), 4.45 (m, 1H), 4.35 (m, 1H), 4.03 (s, 3H) 3.95. IC$_{50}$ RTA (95% HS): **51a**: 70 nM; **51b**: 10,000 nM.

Preparation of Bicyclic Derivatives 38, 73−107 via Third-Generation Synthesis (Scheme 2c). *(4S,5R)-5-[3,5-Bis-(trifluoromethyl)phenyl]-4-ethenyl-1,3-oxazolidin-2-one (**60**). Step 1.* To *N*-Boc-allylamine (50.0 g, 0.318mol) in anhydrous THF (800 mL) at −78 °C was added *sec*-butyllithium (1.30 M in cyclohexane, 538.0 mL, 0.7 mol) dropwise under a stream of N$_2$ gas. The resulting yellow solution was stirred at −78 °C for an additional 2 h, after which time ZnCl$_2$ (1.1 M in Et$_2$O, 349.8 mL, 0.35 mol) was added. The solution was stirred for 1 h before 3,5-bis-trifluoromethylbenzaldehyde (169.3 g, 0.700 mol) was added to the clear solution. The mixture was stirred at −78 °C for 1 h before quenching with acetic acid (227 mL). The reaction was poured into ice water (2 L), and the organic layer was washed with aqueous saturated NaHCO$_3$ (2 L × 2) and brine (1 L), dried (MgSO$_4$), and concentrated. The crude material was recrystallized from petroleum ether (300 mL) to yield *tert*-butyl {1-[3,5-bis(trifluoromethyl)phenyl]-1-hydroxybut-3-en-2-yl}carbamate (57 g) as a white powder. In total, this process yielded 2.8 kg of material. MS ESI calcd for C$_{17}$H$_{20}$F$_6$NO$_3$ [M + H]$^+$ 400.1, found 400.0.

Step 2. At 0 °C under N$_2$, NaH (20 g, 0.500 mol) was added slowly to the mixture of *tert*-butyl {1-[3,5-bis(trifluoromethyl)phenyl]-1-hydroxybut-3-en-2-yl}carbamate (100 g, 0.250 mol) in anhydrous THF (1.5 L) while stirring. After the addition, the mixture was stirred at 0 °C for 1 h, then at 80 °C for 2−6 h. (Caution: The mixture was stirred and heated at 80 °C for 0.5−1 h of bubbling). The resulting mixture was cooled to 0 °C and MeOH (0.1 L) and ice water (0.2 L) was added carefully to quench the reaction. The mixture was concentrated and then diluted with ethyl acetate (2 L), washed with water (0.5 L × 3), brine (0.5 L), dried, and concentrated to give a black oil. Flash chromatography on silica gel yielded the crude product which was recrystallized from ethyl acetate, dichloromethane, and petroleum ether to provide *cis*-5-[3,5-bis(trifluoromethyl)phenyl]-4-ethenyl-1,3-oxazolidin-2-one (25 g) as a white solid. The resultant solid was separated by chiral SFC (column, OJ 250 mm × 50 mm, 10 μm; mobile phase A: supercritical CO$_2$, B: IPA, A:B = 85:15 at 230 mL/min; column temp: 38 °C; nozzle pressure, 100 bar; nozzle temperature, 60 °C; evaporator temperature, 20 °C; trimmer temperature, 25 °C; wavelength, 220 nm). ^{1}H NMR (400 MHz, DMSO-d_6) δ 8.30 (s, 1H), 8.10 (s, 1H), 7.93 (s, 2H), 6.05−6.03 (d, 1H), 5.27−5.11 (m, 2H), 4.99−4.97 (d, 1H), 4.76−4.73 (t, 1H).

*(1R,5S,7aS)-1-[3,5-Bis(trifluoromethyl)phenyl]-5-[2-bromo-5-(trifluoromethyl)phenyl]tetrahydro-1H-pyrrolo[1,2-c][1,3]oxazol-3-one (**Intermediate 10-1**). Step 1.* To 2-bromo-5-trifluoromethylbenzaldehyde (20 g, 99 mmol) in THF (50 mL) was added vinyl magnesium bromide (1.0 M, 128 mL, 128 mmol) via a syringe addition at 0 °C. The reaction mixture was allowed to warm to room temperature and was stirred for 30 min. The reaction was quenched with the careful, dropwise addition of ethyl chloroformate (10.7 g, 99 mmol). After stirring for 30 min, the reaction was diluted with hexane (100 mL) and was partitioned with aqueous saturated NH$_4$Cl. The organic was further washed with HCl (1.0 M in water, 50 mL), then brine (30 mL) before drying over sodium sulfate, filtering and concentrating to dryness. The crude material was purified by column chromatography to yield 1-(2-bromo-5-fluorophenyl)prop-2-en-1-yl ethyl carbonate (14.5 g, 47.8 mmol). ^{1}H NMR (500 MHz, CDCl$_3$) δ 7.56 (m, 1H), 7.24 (m, 1H), 6.97 (m, 1H), 6.43 (d, J = 5.5 Hz, 1H), 6.01 (m, 1H), 5.35−5.42 (m, 2H), 4.28 (m, 2H), 1.38 (m, 3H).

Step 2. To a 500 mL RBF were added 1-(2-bromo-5-fluorophenyl)-prop-2-en-1-yl ethyl carbonate (10.4 g, 29.5 mmol), (4S,5R)-5-[3,5-bis(trifluoromethyl)phenyl]-4-ethenyl-1,3-oxazolidin-2-one (4 g, 12.3 mmol), DCM (20 mL), and the Helmchen dibenzo[a,e]-cyclooctatetraene (dbcot) iridium phosphoramidite catalyst complex (407 mg, 0.369 mmol). The reaction was stirred at 33 °C for 2 days open to air. The reaction was filtered over Celite and purified by column

chromatography to yield (4S,5R)-5-[3,5-bis(trifluoromethyl)phenyl]-3-{(1S)-1-[2-bromo-5-(trifluoromethyl)phenyl]prop-2-en-1-yl}-4-ethenyl-1,3-oxazolidin-2-one (4.5 g, 7.65 mmol). ^{1}H NMR (500 MHz, CDCl$_3$) δ 7.86 (m, 2H), 7.68 (s, 2H), 7.64 (s, 1H), 7.54 (d, J = 6.5 Hz, 1H), 6.22 (m, 1H), 5.75 (m, 2H), 5.43 (m, 2H), 5.20(m, 1H), 5.03 (d, J = 5.0 Hz, 1H), 4.8 (d, J = 8.5 Hz, 1H), 4.1 (m, 1H).

Step 3. To a 100 mL RBF equipped with a reflux condenser was added (4S,5R)-5-[3,5-bis(trifluoromethyl)phenyl]-3-{(1S)-1-[2-bromo-5-(trifluoromethyl)phenyl]prop-2-en-1-yl}-4-ethenyl-1,3-oxazolidin-2-one (4.5 g, 7.65 mmol) and toluene (20 mL). The system was flushed with nitrogen and 1,3-bis(2,4,6-trimethylphenyl)-4,5-dihydroimidazol-2-ylidene[2-(*i*-propoxy)-5-(*N,N*-dimethylaminosulfonyl)-phenyl]methyleneruthenium(II) dichloride (274 mg, 0.374 mmol) (Zhan catalyst-1B) was added. The reaction mixture was heated at 60 °C for 2 h. The solvent was removed under reduced pressure and the resultant oil was purified by column chromatography to yield (1R,5S,7aS)-1-[3,5-bis(trifluoromethyl)phenyl]-5-[2-bromo-5-(trifluoromethyl)phenyl]-5,7a-dihydro-1H-pyrrolo[1,2-c][1,3]oxazol-3-one (**Intermediate 10-1**) 4.0 g, 7.14 mmol). ^{1}H NMR (500 MHz, CDCl$_3$) δ 7.95 (s, 1H), 7.79 (s, 2H), 7.76 (d, J = 8.3 Hz, 1H), 7.60 (s, 1H), 7.47 (d, J = 8.2 Hz, 1H), 6.34 (d, J = 2.5 Hz, 1H), 6.17 (s, H), 6.12 (d, J = 8.8 Hz, 1H), 5.46(d, J = 8.7 Hz, 1H), 5.29 (d, J = 4.8 Hz, 1H).

Step 4. To (1R,5S,7aS)-1-[3,5-bis(trifluoromethyl)phenyl]-5-[2-bromo-5-(trifluoromethyl)phenyl]-5,7a-dihydro-1H-pyrrolo[1,2-c]-[1,3]oxazol-3-one (3.0 g, 5.36 mmol) in ethanol (10 mL) was added Wilkinson's catalyst (Rh(PPh$_3$)$_3$Cl) (495 mg, 0.536 mmol). The mixture was placed on a Parr shaker under an atmosphere of hydrogen gas at 40 psi overnight. Upon completion, the solvent was removed under reduced pressure and the resultant oil was purified by column chromatography to yield (1R,5S,7aS)-1-[3,5-bis(trifluoromethyl)-phenyl]-5-[2-bromo-5-(trifluoromethyl)phenyl]tetrahydro-1H-pyrrolo[1,2-c][1,3]oxazol-3-one (**Intermediate 10-2**), (3.0 g, 5.34 mmol). ^{1}H NMR (500 MHz, CDCl$_3$) δ 7.93 (s, 1H), 7.87 (s, 2H), 7.73 (m, 2H), 7.44 (d, J = 2 Hz, 1H), 6.14 (d, J = 7.9 Hz, 1H), 6.12 (d, J = 8.8 Hz, 1H), 5.35 (m, 1H), 4.63 (m, 1H), 3.03 (m, 1H), 1.69 (m, 1H), 1.25 (m, 2H).

Step 5. To a 40 mL vial in a glovebox were added (1R,5S,7aS)-1-[3,5-bis(trifluoromethyl)phenyl]-5-[2-bromo-5-(trifluoromethyl)phenyl]-tetrahydro-1H-pyrrolo[1,2-c][1,3]oxazol-3-one (intermediate B2, 2.0 g, 3.56 mmol), bis(pinacolato)diboron (1.84 g, 7.11 mmol), potassium acetate (0.87 g, 8.9 mmol), 1,1′-bis(di-*tert*-butylphosphino)ferrocene palladium dichloride (0.122 g, 0.178 mmol), and 20 mL of dimethylacetamide. The vial was sealed and heated at 80 °C for 20 H. The reaction mixture was diluted with methyl *t*-butyl ether and washed with 15% NaCl aqueous solution. Organics were treated with metal scavenger resin and concentrated. Crude product was purified by column chromatography to yield (1R,5S,7aS)-1-(3,5-bis-(trifluoromethyl)phenyl)-5-(2-(4,4,5,5-tetramethyl-1,3,2-dioxaboro-lan-2-yl)-5-(trifluoromethyl)phenyl)tetrahydropyrrolo[1,2-c]oxazol-3(1H)-one (**Intermediate 10-3**, 1.65 g, 2.71 mmol). MS ESI calcd for C$_{27}$H$_{25}$BF$_9$NO$_4$ [M + H]$^+$ 610.2, found 610.2.

The following intermediates in were prepared using the procedures outlined in the syntheses of **Intermediates 10-X** utilizing commercially available or known aldehydes.

2-Bromo-3-methyl-5-(trifluoromethyl)benzaldehyde. To a 100 mL round-bottom flask were added 2,2,6,6-tetramethylpiperidine (2.8 mL, 16.6 mmol), and 50 mL of THF. BuLi (9.5 mL, 15.2 mmol, 1.6 M hexane solution) was added via a syringe at 0 °C. After stirring at 0 °C for 15 min, the ice bath was replaced with dry ice/ether bath. To another 25 mL round-bottom flask was added 1-bromo-2-methyl-4-(trifluoromethyl)benzene (3.3 g, 13.8 mmol) and THF. After cooling with dry ice/acetone bath, this solution was cannular transferred to the first flask rapidly. Upon completion of transferring, DMF (2.1 mL, 27.6 mmol) was added immediately and the resulting reaction mixture was stirred at that temperature for 10 more minutes before it was allowed to warm to −20 °C slowly. The reaction was quenched at −20 °C with addition of 50 mL of 1 N HCl. This mixture was diluted with 100 mL of water and extracted with 100 mL of EtOAc/hexane 1:9. The organics were washed with 30 mL of NaHCO$_3$ aqueous solution, dried over sodium sulfate, filtered, and concentrated. Crude product was purified

by chromatography to give 1.8 g 2-bromo-3-methyl-5-(trifluoromethyl)benzaldehyde. ^{1}H NMR (500 MHz, CDCl$_3$) δ 10.50 (s, 1H), 8.03 (d, J = 1.4 Hz, 1H), 7.75 (d, J = 1.5 Hz, 1H), 2.60 (s, 3H).

5-Bromo-2-(trifluoromethyl)pyridine-4-carbaldehyde. Step 1. To 5-bromo-2-(trifluoromethyl)isonicotinic acid (20 g, 74.1 mmol), N,O-dimethylhydroxylamine hydrochloride (10.84 g, 111 mmol), and N,N-diisopropylethylamine (DIPEA) (38.8 mL, 222 mmol) in DMF (100 mL) was added 2,4,6-tripropyl-1,3,5,2,4,6-trioxatriphosphinane 2,4,6-trioxide (53.4 mL, 89 mmol) at 0 °C by a dropping funnel over a period of 10 min. The reaction was stirred for 2 h. The reaction was concentrated to half the amount and was diluted with EtOAc. The organic was partitioned with satd. NH$_4$Cl and then with brine. The organic was dried over Na$_2$SO$_4$, filtered, and concentrated in vacuo. 5-Bromo-N-methoxy-N-methyl-2-(trifluoromethyl)pyridine-4-carboxamide (21 g, 67.1 mmol) was carried forward as a crude oil. ^{1}H NMR (500 MHz, CDCl$_3$) δ 8.90 (s, 1H), 7.63 (s, 1H), 3.44 (s, 3H), 3.55 (s, 3H).

Step 2. To 5-bromo-N-methoxy-N-methyl-2-(trifluoromethyl)-pyridine-4-carboxamide (21 g, 67.1 mmol) in THF (200 mL) was added DIBAL-H in toluene (1 M, 73.8 mL, 73.8 mmol) through a syringe at −78 °C. The reaction was stirred for 40 min while it was warmed to −10 °C. The reaction was diluted with EtOAc (100 mL) and was quenched with 1 N HCl solution (150 mL). The reaction mixture was filtered on a Celite and silica gel bed. The layers were separated, and the organic layer was partitioned with saturated. NaHCO$_3$ and then brine. The organic layer was dried over Na$_2$SO$_4$, filtered, and concentrated in vacuo. The crude reaction was purified by column chromatography to yield 5-bromo-2-(trifluoromethyl)pyridine-4-carbaldehyde (13.1 g, 51.6 mmol). ^{1}H NMR (500 MHz, CDCl$_3$) δ 10.2 (s, 1H), 9.04 (s, 1H), 8.84 (s, 1H).

1-Ethenyl-3-methyl-5-(trifluoromethyl)benzene (Intermediate 12). To 1-bromo-3-methyl-5-(trifluoromethyl)benzene (500 mg, 2.51 mmol) were added THF (5 mL), aqueous tribasic potassium phosphate (2.0 M, 4.18 mL, 8.37 mmol), 2-ethenyl-4,4,5,5-tetramethyl-1,3,2-dioxaborolane (387 mg, 2.51 mmol), palladium(II) acetate (47 mg, 0.209 mmol), and 1,1′-bis(di-t-butylphosphino)ferrocene (99 mg, 0.209 mmol). The system was flushed with nitrogen gas and was heated at 80 °C for 1 h. The reaction was filtered and then diluted with ethyl acetate and water. The organic layer was dried over sodium sulfate, filtered, and concentrated. The crude product was purified by preparative TLC to yield 1-ethenyl-3-methyl-5-(trifluoromethyl)-benzene (300 mg, 1.61 mmol). ^{1}H NMR (500 MHz, CDCl$_3$) δ 7.47 (s, 1H), 7.40 (s, 1H), 7.34 (s, 1H), 6.76 (m, 1H), 5.85 (d, J = 17.6 Hz, 1H), 2.43 (s, 1H).

(1R,5S,7aS)-5-[2-Bromo-5-(trifluoromethyl)phenyl]-1-[3-methyl-5-(trifluoromethyl)phenyl]tetrahydro-1H-pyrrolo[1,2-c][1,3]oxazol-3-one (Intermediate 13-1). Step 1. To a 250 mL RBF were added (R)-(+)-2-methyl-2-propanesulfinamide (3.16 g, 26.1 mmol), 2-bromo-5-trifluorobenzaldehyde (6.0 g, 23.7 mmol), and THF (20 mL). Titanium(IV) ethoxide (10.8 g, 47.4 mmol) was added dropwise via a syringe before heating the reaction at 40 °C for 1 h. The reaction was cooled to room temperature and water (100 mL) and ethyl acetate (100 mL) were added. The organic was stirred with brine for 15 min and was filtered to remove solids. The organic was dried over sodium sulfate, filtered, and concentrated before purifying by column chromatography to yield N-{(E)-[2-bromo-5-(trifluoromethyl)phenyl]methylidene}-2-methylpropane-2-sulfinamide (8.0 g, 22.5 mmol) as a colorless crystalline solid. ^{1}H NMR (500 MHz, CDCl$_3$) δ 7.72 (m, 2H), 7.44 (m, 3H), 6.06 (d, J = 8.1 Hz, 1H), 5.33 (t, J = 8 Hz, 1H), 4.57 (m, 1H), 2.99 (m, 1H), 2.48 (s, 3H), 1.68 (m, 1H), 1.59 (m, 1H), 1.38 (m, 1H).

Step 2. To a 100 mL three-neck RBF equipped with stir bar and condenser was added Mg (excess), catalytic iodine, THF (20 mL), followed by 4-bromobut-1-ene (4.55 g, 33.7 mmol) in small increments. The mixture was heated to 40 °C for 1 h. The reaction was cooled to room temperature and the freshly made Grignard reagent was added via syringe into a 250 mL RBF with N-{(E)-[2-bromo-5-(trifluoromethyl)phenyl]methylidene}-2-methylpropane-2-sulfinamide (8.0 g, 22.5 mmol) in THF (100 mL). Upon completion, the reaction was quenched with saturated aqueous NH$_4$Cl and partitioned

with ethyl acetate. The organic was dried over sodium sulfate, filtered, concentrated and purified by column chromatography to yield N-{(1S)-1-[2-bromo-5-(trifluoromethyl)phenyl]pent-4-en-1-yl}-2-methylpropane-2-sulfinamide (6.0 g, 14.6 mmol). ^{1}H NMR (500 MHz, CDCl$_3$) δ 7.72 (m, 2H), 7.42 (d, J = 8.2 Hz, 1H), 5.87 (m, 1H), 5.13 (m, 2H), 5.02 (m, 1H), 2.24 (m, 1H), 2.18 (m, 1H), 2.08 (m, 1H), 1.98 (m, 1H), 1.27 (s, 9H).

Step 3. To N-{(1S)-1-[2-bromo-5-(trifluoromethyl)phenyl]pent-4-en-1-yl}-2-methylpropane-2-sulfinamide (6.0 g, 14.6 mmol) in methanol (80 mL) was added HCl (4 N in dioxanes, 25.5 mL, 102 mmol). The reaction was stirred overnight at room temperature and the solvent was removed in vacuo. The resulting oil was partitioned with ethyl acetate and was washed with 10% aqueous potassium hydroxide. The organic was dried over sodium sulfate and concentrated. (1S)-1-[2-Bromo-5-(trifluoromethyl)phenyl]pent-4-en-1-amine (4.4 g, 14.3 mmol) was carried forward without further purification. MS ESI calcd for C$_{12}$H$_{14}$BrF$_3$N [M + H]$^+$ 308.0 and 310.0, found 308.0 and 310.0.

Step 4. To DIPEA (7.48 mL, 42.8 mmol) and (1S)-1-[2-bromo-5-(trifluoromethyl)phenyl]pent-4-en-1-amine (4.4 g, 14.3 mmol) in DCM (20 mL) was added benzyl chloroformate at 0 °C. The reaction was stirred at room temperature for 2 h and was quenched with water. The organic was washed with 10% aqueous KOH and the aqueous was back-extracted with ethyl acetate. The combined organics were dried over sodium sulfate, filtered, concentrated, and then purified by column chromatography to yield benzyl {(1S)-1-[2-bromo-5-(trifluoromethyl)phenyl]pent-4-en-1-yl}carbamate (5.8 g, 13.1 mmol). ^{1}H NMR (500 MHz, CDCl$_3$) δ 7.72 (m, 1H), 7.58 (s, 1H), 7.39 (b, 5H), 7.1 (m, 1H), 5.83 (m, 1H), 5.3 (b, 1H), 5.15 (m, 3H), 2.22 (m, 1H), 2.18 (m, 1H), 1.95 (m, 1H), 1.78 (m, 1H).

Step 5. To a 100 mL RBF equipped with a reflux condenser was added benzyl {(1S)-1-[2-bromo-5-(trifluoromethyl)phenyl]pent-4-en-1-yl}carbamate (0.5 g, 1.13 mmol), 1-ethenyl-3-methyl-5-(trifluoromethyl)benzene (421 mg, 2.26 mmol) and dichloromethane (10 mL). The system was flushed with nitrogen and 1,3-bis(2,4,6-trimethylphenyl)-4,5-dihydroimidazol-2-ylidene[2-(i-propoxy)-5-(N,N-dimethylaminosulfonyl)phenyl]methyleneruthenium(II) dichloride (41 mg, 0.57 mmol) (Zhan catalyst-1B) was added before heating at 60 °C for 20 min. The reaction was cooled to room temperature and was directly purified by column chromatography to yield benzyl {(1R,4E)-1-[2-bromo-5-(trifluoromethyl)phenyl]-5-[3-methyl-5-(trifluoromethyl)phenyl]pent-4-en-1-yl}carbamate (500 mg, 0.833 mmol). ^{1}H NMR (500 MHz, CDCl$_3$) δ 7.72 (m, 1H), 7.58 (s, 1H), 7.39 (b, 5H), 6.4 (d, J = 8.2 Hz, 1H), 6.25 (m, 1H), 5.35 (m, 1H), 5.20 (m, 1H), 5.10 (s, 2H), 2.40 (s, 3H), 2.19 (m, 1H), 2.05 (m, 1H), 1.95 (m, 1H), 1.78 (m, 1H).

Step 6. To a 250 mL RBF were added tetrabutylammonium hydrogen sulfate (28 mg, 0.083 mmol), D-Epoxone (215 mg, 0.833 mmol), benzyl {(1R,4E)-1-[2-bromo-5-(trifluoromethyl)phenyl]-5-[3-methyl-5-(trifluoromethyl)phenyl]pent-4-en-1-yl}carbamate (500 mg, 0.833 mmol) followed by MeCN (7 mL) and EtOAc (6 mL). Sodium tetraborate decahydrate (318 mg, 0.833 mmol) in an aqueous ethylenediaminetetraacetic acid disodium salt dihydrate solution (0.4 mM, 7 mL) was added to the reaction at 0 °C. A solution of potassium carbonate (1.51 g, 8.33 mmol) in water (7 mL) and a solution of OXONE (1.54 g, 2.50 mmol) in an aqueous ethylenediaminetetraacetic acid disodium salt dihydrate (0.4 mM, 7 mL) were simultaneously added to the reaction at 0 °C over the course of 2 h. An additional solution of D-Epoxone (107 mg, 0.417 mmol) in MeCN (3 mL) was added via syringe pump over 1.5 h. The reaction was diluted with water (100 mL) and was extracted with ethyl acetate (2 × 100 mL). The organic was concentrated and purified by column chromatography to yield benzyl [(1S)-1-[2-bromo-5-(trifluoromethyl)phenyl]-3-{(2R,3R)-3-[3-methyl-5-(trifluoromethyl)phenyl]oxiran-2-yl}propyl]-carbamate (300 mg, 0.487 mmol). ^{1}H NMR (500 MHz, CDCl$_3$) δ 7.73 (m, 1H), 7.56 (s, 1H), 7.38−7.42 (b, 5H), 5.47 (m, 1H), 5.21(m, 1H), 5.12 (s, 2H), 3.67 (s, 1H), 3.02(s, 1H), 2.42 (s, 3H), 2.10 (m, 1H), 1.99 (m, 2H), 1.76 (m, 1H).

Step 7. To benzyl [(1S)-1-[2-bromo-5-(trifluoromethyl)phenyl]-3-{(2R,3R)-3-[3-methyl-5-(trifluoromethyl)phenyl]oxiran-2-yl}propyl]-

AF

carbamate (100 mg, 0.162 mmol) in DMF (2 mL) was added LiHMDS (1.0 M, 0.324 mL, 0.324 mmol) at 0 °C. The mixture was stirred at room temperature overnight and the solvent was removed under reduced pressure. The resultant residue was purified by preparative TLC to yield (1*R*,5*S*,7a*S*)-5-[2-bromo-5-(trifluoromethyl)phenyl]-1-[3-methyl-5-(trifluoromethyl)phenyl]tetrahydro-1*H*-pyrrolo[1,2-*c*]-[1,3]oxazol-3-one (75 mg, 0.148 mmol). ^{1}H NMR (500 MHz, CDCl$_3$) δ 7.72 (m, 2H), 7.46 (s, 1H), 7.44 (d, *J* = 8.8 Hz, 3H), 6.06 (d, *J* = 8.1 Hz, 1H), 5.33 (t, *J* = 8.0 Hz, 1H), 4.57 (m, 1H), 2.99 (m, 1H), 2.48 (s, 3H), 1.68 (m, 1H), 1.57 (m, 1H), 1.38 (m, 1H).

(1R,5S,8aS)-1-[3,5-Bis(trifluoromethyl)phenyl]-5-[2-bromo-5-(trifluoromethyl)phenyl]hexahydro[1,3]oxazolo[3,4-a]pyridin-3-one (Intermediate 13-2). Step 1. To a 100 mL three-neck RBF equipped with stir bar and condenser were added Mg (excess), catalytic iodine, and THF (20 mL), followed by 5-bromopent-1-ene (1.93 g, 12.9 mmol) in small increments. The mixture was heated to 40 °C for 1 h. The reaction was cooled to room temperature and the freshly made Grignard reagent was added via syringe into a 250 mL RBF with *N*-{(*E*)-[2-bromo-5-(trifluoromethyl)phenyl]methylidene}-2-methyl-propane-2-sulfinamide (2.3 g, 6.5 mmol) in THF (20 mL). Upon completion, the reaction was quenched with saturated aqueous NH$_4$Cl and partitioned with ethyl acetate. The organic was dried over sodium sulfate, filtered, concentrated and purified by column chromatography to yield *N*-{(1*S*)-1-[2-bromo-5-(trifluoromethyl)phenyl]hex-5-en-1-yl}-2-methylpropane-2-sulfinamide (1.5 g, 3.5 mmol). ^{1}H NMR (500 MHz, CDCl$_3$) δ 7.71 (d, *J* = 8.4 Hz, 1H), 7.63 (s, 1H), 7.41 (d, *J* = 6.4 Hz, 1H), 5.77 (m, 1H), 5.03 (m, 2H), 4.87 (m, 1H), 3.65 (m, 1H), 2.11 (m, 2H), 1.86 (m, 1H), 1.82 (m, 1H), 1.55 (m, 1H), 1.40 (m, 1H), 1.22 (s, 9H).

Step 2. To *N*-{(1*S*)-1-[2-bromo-5-(trifluoromethyl)phenyl]hex-5-en-1-yl}-2-methylpropane-2-sulfinamide (1.5 g, 3.5 mmol) was added HCl (4 N in dioxanes, 6.16 mL, 24.6 mmol). The reaction was stirred overnight at room temperature and the solvent was removed in vacuo. The resultant oil was partitioned with ethyl acetate and was washed with 10% aqueous potassium hydroxide. The organic was dried over sodium sulfate and concentrated. (1*S*)-1-[2-Bromo-5-(trifluoromethyl)phenyl]hex-5-en-1-amine (1.11 g, 3.45 mmol) was carried forward without further purification. MS ESI calcd for C$_{13}$H$_{16}$BrF$_3$N [M + H]$^+$ 322.0 and 324.0, found 322.2 and 324.2.

Step 3. To DIPEA (1.81 mL, 10.3 mmol) and (1*S*)-1-[2-bromo-5-(trifluoromethyl)phenyl]hex-5-en-1-amine (1.11 g, 3.45 mmol) in DCM (20 mL) was added benzyl chloroformate at 0 °C. The reaction was stirred at room temperature for 2 h and was quenched with water. The organic was washed with 10% aqueous KOH and the aqueous layer was back-extracted with ethyl acetate. The combined organics were dried over sodium sulfate, filtered, concentrated, and then purified by column chromatography to benzyl {(1*S*)-1-[2-bromo-5-(trifluoromethyl)phenyl]hex-5-en-1-yl}carbamate (1.5 g, 3.29 mmol). ^{1}H NMR (500 MHz, CDCl$_3$) δ 7.71 (m, 1H), 7.69 (s, 1H), 7.39−7.29 (b, 6H), 5.81 (m, 1H), 5.28 (m, 1H), 5.14 (s, 2H), 5.08 (m, 2H), 2.16 (m, 2H), 1.84 (m, 1H), 1.68 (m 1H), 1.59 (m, 1H), 1.51 (m, 1H).

Step 4. To a 100 mL RBF equipped with a reflux condenser was added benzyl {(1*S*)-1-[2-bromo-5-(trifluoromethyl)phenyl]hex-5-en-1-yl}carbamate (1.5 g, 3.29 mmol), 1-ethenyl-3,5-bis(trifluoromethyl)-benzene (1.58 g, 6.57 mmol) and dichloromethane (10 mL). The system was flushed with nitrogen and 1,3-bis(2,4,6-trimethylphenyl)-4,5-dihydroimidazol-2-ylidene[2-(*i*-propoxy)-5-(*N*,*N*-dimethylaminosulfonyl)phenyl]methyleneruthenium(II) dichloride (41 mg, 0.57 mmol) was added before heating at 60 °C for 20 min. The reaction was cooled to room temperature and was directly purified by column chromatography to yield benzyl {(1*R*,5*E*)-6-[3,5-bis(trifluoromethyl)phenyl]-1-[2-bromo-5-(trifluoromethyl)phenyl]hex-5-en-1-yl}carbamate (2.0 g, 2.99 mmol). ^{1}H NMR (500 MHz, CDCl$_3$) δ 7.81 (s, 1H), 7.67 (d, *J* = 8.3 Hz, 1H), 7.37 (d, *J* = 8.1 Hz, 1H), 5.82 (m, 1H), 5.05 (m, 2H), 4.41 (m, 1H), 3.82 (s, 1H), 2.13 (m, 2H), 1.76 (m, 1H), 1.42 (m, 1H).

Step 5. To a 250 mL RBF were added tetrabutylammoniuym hydrogen sulfate (97 mg, 0.284 mmol), D-Epoxone (370 mg, 1.43 mmol), and benzyl {(1*R*,5*E*)-6-[3,5-bis(trifluoromethyl)phenyl]-1-[2-bromo-5-(trifluoromethyl)phenyl]hex-5-en-1-yl}carbamate (1.9 g,

2.84 mmol), followed by MeCN (15 mL) and EtOAc (20 mL). Sodium tetraborate decahydrate (1.08 g, 2.84 mmol) in an aqueous ethylenediaminetetraacetic acid disodium salt dihydrate solution (0.4 mM, 7 mL) was added to the reaction at 0 °C. A solution of potassium carbonate (3.93 g, 28.4 mmol) in water (25 mL) and a solution of OXONE (5.24 g, 8.53 mmol) in an aqueous ethylenediaminetetraacetic acid disodium salt dihydrate (0.4 mM, 25 mL) were simultaneously added to the reaction at 0 °C over the course of 2 h. An additional solution of D-Epoxone (370 mg, 1.43 mmol) in MeCN (3 mL) was added via syringe pump over 1.5 h. The reaction was diluted with water (100 mL) and was extracted with ethyl acetate (2 × 100 mL). The organic was concentrated to yield a white solid that was resubjected to the reaction procedure. Benzyl {(1*S*)-4-{(2*S*,3*S*)-3-[3,5-bis-(trifluoromethyl)phenyl]oxiran-2-yl}-1-[2-bromo-5-(trifluoromethyl)-phenyl]butyl}carbamate (1.5 g, 2.19 mmol) was isolated by column chromatography. ^{1}H NMR (500 MHz, CDCl$_3$) δ 7.81 (s, 1H), 7.75 (s, 2H), 7.59 (s, 1H), 7.42 (m, 2H), 5.3 (m, 1H), 5.19 (m, 1H), 5.15 (m, 2H), 3.78 (m, 1H), 2.98 (m, 1H), 1.95 (m, 2H), 1.82−1.65 (br s, 2H).

Step 6. To benzyl {(1*S*)-4-{(2*S*,3*S*)-3-[3,5-bis(trifluoromethyl)-phenyl]oxiran-2-yl}-1-[2-bromo-5-(trifluoromethyl)phenyl]butyl}-carbamate (500 mg, 0.731 mmol) in DMF (2 mL) was added DBU (111 mg, 0.731 mmol). The system was heated to 125 °C for 6 h. The solvent was removed in vacuo. The reaction was diluted with ethyl acetate and water. The organic was dried over sodium sulfate, filtered, and concentrated. The resultant oil was purified by column chromatography to yield (*R*)-[3,5-bis(trifluoromethyl)phenyl]-{(2*S*,6*S*)-6-[2-bromo-5-(trifluoromethyl)phenyl]piperidin-2-yl}-methanol (280 mg, 0.509 mmol). ^{1}H NMR (500 MHz, CDCl$_3$) δ 7.9 (s, 2H), 7.81 (d, *J* = 5.4 Hz, 2H), 7.64 (d, *J* = 8.3 Hz, 1H), 7.35 (d, *J* = 8.3 Hz, 1H), 5.14 (d, *J* = 8.2 Hz, 1H), 4.51 (m, 1H), 3.16 (m, 1H), 2.06 (m, 1H), 1.95 (m, 1H), 1.80 (m, 2H), 1.62 (m, 1H), 1.29 (m, 1H).

Step 7. To (*R*)-[3,5-bis(trifluoromethyl)phenyl]{(2*S*,6*S*)-6-[2-bromo-5-(trifluoromethyl)phenyl]piperidin-2-yl}methanol (280 mg, 0.509 mmol) in DCM (5 mL) were added DIPEA (0.9 mL, 0.509 mmol) and phosgene (252 mg, 0.509 mmol). The reaction mixture was stirred at room temperature for 30 min before the solvent was removed and the reaction was diluted with ethyl acetate (15 mL) and aqueous KOH (15 mL). The organic was dried over sodium sulfate, filtered, and concentrated before purification by preparative TLC to yield (1*R*,5*S*,8a*S*)-5-[2-bromo-5-(trifluoromethyl)phenyl]-1-[3-methyl-5-(trifluoromethyl)phenyl]hexahydro[1,3]oxazolo[3,4-*a*]pyridin-3-one (200 mg, 0.347 mmol). MS ESI calcd for C$_{22}$H$_{16}$BrF$_9$NO$_2$ [M + H]$^+$ 576.0 and 578.0, found 576.1 and 578.1.

(1R,5S,7aS)-1-[3,5-Bis(trifluoromethyl)phenyl]-5-[5-bromo-2-(dimethylamino)pyridin-4-yl]tetrahydro-1H-pyrrolo[1,2-c][1,3]-oxazol-3-one (Intermediate 14-1). To **Intermediate 11-2** (130 mg, 0.245 mmol) in THF (0.5 mL) was added dimethylamine (2.0 M, 3.7 mL, 7.4 mmol). The system was sealed and heated to 150 °C by microwave irradiation for 1 h. The reaction was then directly purified by HPLC to yield (1*R*,5*S*,7a*S*)-1-[3,5-bis(trifluoromethyl)phenyl]-5-[5-bromo-2-(dimethylamino)pyridin-4-yl]tetrahydro-1*H*-pyrrolo[1,2-*c*]-[1,3]oxazol-3-one (80 mg, 0.149 mmol). MS ESI calcd for C$_{21}$H$_{19}$BrF$_6$N$_3$O$_2$ [M + H]$^+$ 538.0 and 540.0, found 538.0 and 540.0.

Methyl 5-[4-Methoxy-3-(4,4,5,5-tetramethyl-1,3,2-dioxaborolan-2-yl)phenyl]-4-methylpyridine-2-carboxylate (Intermediate 15). Step 1. To a solution of 5-bromo-4-methylpyridine-2-carboxylic acid methyl ester (2.207 g, 9.59 mmol), 4-methoxylphenylboronic acid (1.604 g, 10.55 mmol) and 1,1′-bis(di-*tert*-butylphosphino)ferrocene palladium dichloride (0.313 g, 0.480 mmol) in THF (30 mL) was added potassium carbonate (2.0 M in water, 10.1 mL, 20.15 mmol). The mixture was purged with nitrogen and heated at 50 °C for 1 h and at 60 °C for 5 h. The reaction was poured into ethyl acetate and was washed with brine, dried over sodium sulfate, filtered, and concentrated. It was purified by column chromatography to yield methyl 5-(4-methoxyphenyl)-4-methylpyridine-2-carboxylate (2.47 g, 9.59 mmol) as a pink solid. MS ESI calcd for C$_{15}$H$_{16}$NO$_3$ [M + H]$^+$ 258.1, found 258.1.

Step 2. A suspension of iodine (2.45 g, 9.66 mmol), silver sulfate (3.01 g, 9.66 mmol) and methyl 5-(4-methoxyphenyl)-4-methylpyridine-2-carboxylate (2.47 g, 9.59 mmol) in MeOH (20 mL) was stirred

at room temperature for 3.5 h. It was then heated at 36 °C for 4 h and then at room temperature for another 16 h. Additional iodine (0.8 g, 3.15 mmol) and silver sulfate (1 g, 3.2 mmol) were added, and the reaction was heated to 36 °C for 3 h. The volatiles were removed and the reaction was diluted with ethyl acetate and aqueous sodium thiosulfate. The organic was washed with brine, dried over sodium sulfate, filtered and then concentrated. The resultant oil was purified by column chromatography to yield methyl 5-(3-iodo-4-methoxyphenyl)-4-methylpyridine-2-carboxylate (2.35 g, 6.12 mmol) as a white solid. MS ESI calcd for $C_{15}H_{15}INO_3$ [M + H]$^+$ 384.0, found 384.0.

Step 3. A solution of [1,1′-bis(diphenylphosphino)ferrocene]-dichloropalladium(II) (0.368 g, 0.451 mmol), potassium acetate (1.34 g, 13.6 mmol), bis(pinacolato)diboron (1.4 g, 5.50 mmol) and methyl 5-(3-iodo-4-methoxyphenyl)-4-methylpyridine-2-carboxylate (1.73 g, 4.51 mmol) in DMSO (20 mL) was heated at 80 °C for 80 min. The mixture was cooled to room temperature and was poured into ethyl acetate and water. The organic was washed with brine, dried over sodium sulfate, filtered, and concentrated. The crude oil was purified by column chromatography to yield methyl 5-[4-methoxy-3-(4,4,5,5-tetramethyl-1,3,2-dioxaborolan-2-yl)phenyl]-4-methylpyridine-2-car-boxylate (1.73 g, 4.51 mmol). MS ESI calcd for $C_{21}H_{26}BNO_5$ [M + H]$^+$ 384.2, found 384.2.

5-Bromo-2-(dimethylamino)pyrimidine-4-carbaldehyde (Inter-mediate 16). Step 1. To [5-bromo-2-(methylsulfanyl)pyrimidin-4-yl]methanol (20 g, 85 mmol) in DCM (100 mL) was added *m*-CPBA (41.9 g, 187 mmol) portionwise at room temperature. The reaction was stirred for 1 h before dimethylamine (2.0 M, 213 mL, 425 mmol) was added. After 2 h, additional dimethylamine (2.0 M, 40 mL, 80 mmol) was added, and the reaction was stirred overnight. The volatiles were removed and the crude oil was dissolved in ethyl acetate, washed with water and then brine, dried over magnesium sulfate, filtered, and concentrated. [5-Bromo-2-(dimethylamino)pyrimidin-4-yl]methanol (19 g, 82 mmol) was carried forward as a crude oil. ^{1}H NMR (500 MHz, CDCl$_3$) δ 8.29 (s, 1H), 4.60 (s, 2H), 3.22 (s, 6H).

Step 2. To [5-bromo-2-(dimethylamino)pyrimidin-4-yl]methanol (19 g, 82 mmol) in DCM (10 mL) was added Dess–Martin periodinane (41.7 g, 98 mmol) at room temperature. The reaction was stirred overnight and the reaction was diluted with hexanes, filtered, and concentrated before purification by column chromatography to yield 5-bromo-2-(dimethylamino)pyrimidine-4-carbaldehyde (10 g, 43.5 mmol). ^{1}H NMR (500 MHz, CDCl$_3$) δ 9.95 (s, 1H), 8.52 (s, 1H), 3.24 (s, 6H).

Methyl 3-[4-Methoxy-3-(4,4,5,5-tetramethyl-1,3,2-dioxaborolan-2-yl)phenyl]propanoate (Intermediate 17). Step 1. A three-neck 5 L RBF equipped with a mechanical stirrer, a thermometer, and a nitrogen bubbler was charged with 3-(4-methoxyphenyl)propionic acid methyl ester (100 g, 515 mmol), silver sulfate (161 g, 515 mmol), and iodine (131 g, 515 mmol) in methanol (2 L). The reaction mixture was stirred vigorously at room temperature for 1 h. The reaction was filtered through Solka-Floc (ethyl acetate wash). The filtrate was concentrated, and the residue was taken up in ethyl acetate (4 L). The organic was washed with water, saturated aq. NaHSO$_3$ (50 mL), and brine (50 mL) before drying over Na$_2$SO$_4$, filtering, and concentrating to dryness. The crude reaction was purified by column chromatography to yield methyl 3-(3-iodo-4-methoxyphenyl)propanoate (155 g, 484 mmol) as a clear oil. MS ESI calcd for $C_{11}H_{14}IO_3$ [M + H]$^+$ 321.0, found 321.0.

Step 2. A three-neck 12 L RBF equipped with a mechanical stirrer, a thermometer, a nitrogen bubbler, a condenser, and an addition funnel was charged with methyl 3-(3-iodo-4-methoxyphenyl)propanoate (155 g, 484 mmol), bis(pinacolato)diboron (154 g, 605 mmol), and potassium acetate (95 g, 48.4 mmol) in DMSO (3 L) and dioxane (0.9 L). The system was degassed three times with nitrogen gas before the addition of dichloro[1,1′-bis(diphenylphosphino)ferrocene]-palladium(II) dichloromethane adduct (39.5 g, 48.4 mmol). The system was degassed three times and was then heated to 50 °C for 1 h. The temperature was raised to 80 °C and the reaction was stirred overnight. The reaction was diluted with ethyl acetate (4 L) and was partitioned with water and then with brine. The organic was dried over MgSO$_4$, filtered, and concentrated in vacuo. The crude reaction was purified by column chromatography to yield methyl 3-[4-methoxy-3-

(4,4,5,5-tetramethyl-1,3,2-dioxaborolan-2-yl)phenyl]propanoate (108.1 g, 338 mmol) as a tan solid. MS ESI calcd for $C_{17}H_{26}BO_5$ [M + H]$^+$ 321.2, found 321.2.

tert-Butyl 4-[6-methoxy-5-(4,4,5,5-tetramethyl-1,3,2-dioxaboro-lan-2-yl)pyridin-3-yl]-3-methylbenzoate (Intermediate 18). Step 1. To a 250 mL RBF were added 4-bromo-3-methylbenzoic acid (10 g, 46.5 mmol), DMAP (8.52 g, 69.8 mmol), and *tert*-butyl alcohol (100 mL). Di-*tert*-butyl dicarbonate (12.96 mL, 55.8 mmol) was added via a syringe to the solution, which caused vigorous bubbling, foaming and the loss of some material. The remaining reaction mixture was heated at 70 °C overnight. The reaction was cooled to room temperature, and the volatiles were removed under reduced pressure. Crude material was diluted with ethyl acetate:hexanes (1:4, 200 mL) and was washed sequentially with 5% aqueous KOH (200 mL) and saturated aqueous ammonium chloride (2 × 100 mL). The organics were dried over sodium sulfate, filtered, and concentrated before purification by column chromatography. *tert*-Butyl 4-bromo-3-methylbenzoate was isolated as a colorless oil (7.2 g, 26.6 mmol). ^{1}H NMR (500 MHz, CDCl$_3$) δ 7.87 (s, 1H), 7.67 (d, *J* = 8.3 Hz, 1H), 7.60 (d, *J* = 8.2 Hz, 1H), 2.47 (s, 3H), 1.62 (s, 9H).

Step 2. To a 250 mL RBF were added 1,1′-bis(di-*tert*-butylphosphino)ferrocene palladium dichloride (0.317 g, 0.487 mmol), *tert*-butyl 4-bromo-3-methylbenzoate (6.6 g, 24.34 mmol), bis(pinacolato)diboron (7.42 g, 29.2 mmol), potassium acetate (5.97 g, 60.9 mmol), and dioxane (25 mL). The system was flushed with nitrogen and was heated at 125 °C overnight. The reaction was cooled to room temperature and was diluted with ethyl acetate:hexanes (1:9, 120 mL) and then was washed sequentially with water (150 mL) and then brine (50 mL). The organics were dried over sodium sulfate, filtered, and concentrated before purification by column chromatography. *tert*-Butyl 3-methyl-4-(4,4,5,5-tetramethyl-1,3,2-dioxaborolan-2-yl)benzoate was isolated as a crystalline solid (6.6 g, 14.5 mmol). ^{1}H NMR indicated it is about 70% pure. ^{1}H NMR (500 MHz, CDCl$_3$) δ 7.8 (m, 3H), 2.60 (s, 3H), 1.58 (s, 9H), 1.39 (s, 12H).

Step 3. To a 250 mL RBF were added 5-bromo-3-chloro-2-methoxypyridine (1.5 g), tribasic potassium phosphate (2.86 g, 13.5 mmol), bis(diphenylphosphino)ferrocene]palladium(II) dichlorome-thane adduct (0.275 g, 6.74 mmol), *tert*-butyl 3-methyl-4-(4,4,5,5-tetramethyl-1,3,2-dioxaborolan-2-yl)benzoate (2.27 g, 7.13 mmol), dioxane (50 mL), and water (3 mL). The flask was sealed and was stirred at 80 °C overnight. The reaction was cooled to room temperature, diluted with ethyl acetate, washed with water, filtered, and concentrated. The resultant residue was purified by column chromatography to yield *tert*-butyl 4-(5-chloro-6-methoxypyridin-3-yl)-3-methylbenzoate (2.0 g, 5.99 mmol). MS ESI calcd for $C_{18}H_{21}ClNO_3$ [M + H]$^+$ 334.1, found 334.0.

Step 4. To a 250 mL RBF were added *tert*-butyl 4-(5-chloro-6-methoxypyridin-3-yl)-3-methylbenzoate (4.5 g, 13.5 mmol), bis-(pinacolato)diboron (6.85 g, 27.0 mmol), potassium acetate (3.97 g, 40.4 mmol), and chloro(2-dicyclohexylphosphino-2′,4′,6′-triisopropyl-1,1′-biphenyl)[2-(2′-amino-1,1′-biphenyl)]palladium(II) (0.212 g, 0.27 mmol) followed by anhydrous dioxane (50 mL). The system was evacuated and backfilled with nitrogen (3×) and was heated to 120 °C for 2 h. The mixture was cooled, filtered over Celite (ethyl acetate wash), and concentrated. The residue was purified by column chromatography to afford *tert*-butyl 4-[6-methoxy-5-(4,4,5,5-tetra-methyl-1,3,2-dioxaborolan-2-yl)pyridin-3-yl]-3-methylbenzoate as a solid (4.3 g, 10.11 mmol). MS ESI calcd for $C_{24}H_{33}BNO_5$ [M + H]$^+$ 426.2, found 426.0.

(2S,3S,4R)-tert-Butyl 3-(3-chloro-4-methoxyphenyl)-2,4-dimeth-yl-5-oxopyrrolidine-1-carboxylate (Intermediate 18-1). Step 1. To a 100 mL RBF were added (3-chloro-4-methoxyphenyl)boronic acid (1.89 g, 10.14 mmol), (S)-*tert*-butyl 2-methyl-5-oxo-2,5-dihydro-1H-pyrrole-1-carboxylate (1 g, 5.07 mmol), hydroxy(cyclooctadiene)-rhodium(I) dimer (0.116 g, 0.254 mmol), and potassium hydrogen fluoride (1.58 g, 20.28 mmol). The mixture was degassed and filled back with N$_2$. Dioxane (45 mL) and water (5 mL) were then added. The mixture was degassed again and filled with N$_2$. The reaction mixture was heated at 60 °C overnight. It was diluted with EtOAc (200 mL), washed with water, brine. Organic layer was dried over Na$_2$SO$_4$, and

concentrated. The residue was purified by silica gel chromatography, eluted with 30% EtOAc/hexane to give (2S,3S)-tert-butyl 3-(3-chloro-4-methoxyphenyl)-2-methyl-5-oxopyrrolidine-1-carboxylate (intermediate J1, 0.85 g) as a white crystalline solid. ^{1}H NMR (500 MHz, CDCl$_3$): δ 7.20 (s, 1H), 7.05 (d, 1H), 6.87 (d, 1H), 4.08 (m, 1H), 3.86 (s, 3H), 2.95 (m, 2H), 2.53 (m, 1H), 1.52 (s, 9H), 1.41 (d, 3H).

Step 2. To a solution of (2S,3S)-tert-butyl 3-(3-chloro-4-methoxyphenyl)-2-methyl-5-oxopyrrolidine-1-carboxylate (intermediate J1, 0.85 g, 2.5 mmol) in THF (20 mL) was added LiHMDS (2.5 mL, 2.5 mmol) at −78 °C. After 30 min, MeI (0.187 mL, 3.00 mmol) was added. The reaction mixture was stirred at −78 °C for 1.5 h. It was warmed up to 0 °C for 30 min and then warmed up to RT for 30 min. The reaction mixture was quenched with 2 mL of AcOH and 100 mL of NH$_4$Cl. The product was extracted with EtOAc (3 × 100 mL). The organic layer was washed with brine(100 mL), dried over Na$_2$SO$_4$, and concentrated. The residue was purified by silica gel chromatography, eluted with 30% EtOAc/hexane to give (2S,3S,4R)-tert-butyl 3-(3-chloro-4-methoxyphenyl)-2,4-dimethyl-5-oxopyrrolidine-1-carboxylate (intermediate J2, 0.55 g, yield of 62%) as off-white solid. ^{1}H NMR (500 MHz, CDCl$_3$): δ 7.29 (s, 1H), 7.14 (d, 1H), 6.95 (d, 1H), 3.93 (s, 3H), 3.91 (m, 1H), 2.58 (m, 1H), 2.40 (m, 1H), 1.59 (s, 9H), 1.38 (d, 3H), 1.17 (d, 3H).

(4S,5R)-5-(3-Chloro-4-methoxyphenyl)-4-methyloxazolidin-2-one (Intermediate 19). Step 1. A solution of 4-bromo-2-chloroanisole (3 g, 13.55 mmol) and (S)-benzyl (1-(methoxy(methyl)amino)-1-oxopropan-2-yl)carbamate (3.79 g, 14.22 mmol) in THF (33.9 mL) was cooled to −20 °C with dry ice/ acetone. To this solution was added isopropylmagnesium chloride lithium chloride complex (22.9 mL, 29.8 mmol) at −20 °C dropwise under N$_2$. After addition, the reaction mixture was warmed up to rt and stirred overnight. The reaction mixture was cooled to −40 °C and slowly poured into a stirred mixture of crushed ice and 30 mL of 1 N HCl. The resulting mixture was diluted with 30 mL of brine, extracted with EtOAc (3 × 50 mL). The organic layer was dried with Na$_2$SO$_4$ and concentrated. The residue was purified by silica gel chromatography, eluted with 0−100% EtOAc in hexane to give (S)-benzyl (1-(3-chloro-4-methoxyphenyl)-1-oxopropan-2-yl)carbamate (0.82 g) as a white solid. ^{1}H NMR (500 MHz, CDCl$_3$): δ 8.05 (s, 1H), 7.92 (d, 1H), 6.98 (d, 1H), 5.93 (d, 1H), 5.29 (m, 1H), 5.16 (s, 2H), 3.99 (s, 3H), 1.43 (d, 3H).

Step 2. To a solution of (S)-benzyl (1-(3-chloro-4-methoxyphenyl)-1-oxopropan-2-yl)carbamate (0.81 g, 2.456 mmol) in MeOH (10 mL) and THF (10 mL) was added NaBH$_4$ (0.139 g, 3.68 mmol) at 0 °C. The solution was stirred at that temperature for 0.5 h. The reaction was quenched with Saturated NH$_4$Cl aq. solution (20 mL) and water (20 mL). The mixture was extracted three times with EtOAc (100 mL). The organic layer was washed with brine, dried with Na$_2$SO$_4$, and concentrated. The residue was purified by chromatography over silica gel and eluted with 40% EtOAc in hexane to give two isomers. The major isomer is benzyl ((1R,2S)-1-(3-chloro-4-methoxyphenyl)-1-hydroxypropan-2-yl)carbamate (0.41 g). ^{1}H NMR (500 MHz, CDCl$_3$): δ 7.28 (s, 1H), 7.20 (d, 1H), 6.89 (d, 1H), 5.17 (s, 2H), 5.02 (d, 1H), 4.81 (d, 1H), 4.03 (b, 1H), 3.93 (s, 3H), 1.01 (d, 3H).

Step 3. To a solution of benzyl ((1R,2S)-1-(3-chloro-4-methoxyphenyl)-1-hydroxypropan-2-yl)carbamate (0.24 g, 0.686 mmol) in THF (4.6 mL) was added NaH (0.036 g, 0.892 mmol) at 0 °C. The reaction mixture was warmed to RT and stirred overnight. It was then quenched with 1 N HCl (1.5 mL). This mixture was diluted with EtOAc and washed with sat. aqueous NaHCO$_3$, water, and brine. The organic phase was dried with Na$_2$SO$_4$ and concentrated. The residue was purified by silica gel chromatography, eluted with EtOAc to give (4S,5R)-5-(3-chloro-4-methoxyphenyl)-4-methyloxazolidin-2-one (Intermediate 19, 0.13 g). ^{1}H NMR (500 MHz, CDCl$_3$): δ 7.37 (s, 1H), 7.21 (d, 1H), 6.97 (d, 1H), 5.84 (b, 1H), 5.65 (d, 1H), 4.21 (m, 1H), 3.96 (s, 3H), 0.87 (d, 3H).

(3aR,5s,6aS)-5-(3-Bromo-4-methoxyphenyl)-2,2-dimethyltetrahydro-3aH-cyclopenta[d][1,3]dioxole (Intermediate 20). Step 1. To a 250 mL RBF was added methyl 3-bromo-4-methoxybenzoate (4.0 g, 16.3 mmol). The flask was flushed with N$_2$. THF (60 mL) was added, followed by allylmagnesium bromide (39.2 mL, 39.2 mmol, 1.0 M in ether) at 0 °C via a syringe over 10 min. The resulting reaction mixture

was stirred at 0 °C for 2 h. It was quenched by addition of 50 mL of sat. NH$_4$Cl at 0 °C and 100 mL of water. The product was extracted with EtOAc (3 × 100 mL). Organics were washed with 100 mL of brine, dried over sodium sulfate, filtered, and concentrated to give 4-(3-bromo-4-methoxyphenyl)hepta-1,6-dien-4-ol (5.0 g) as a colorless oil. ^{1}H NMR (500 MHz, CDCl$_3$) δ 7.61 (s, 1H), 7.30 (d, 1H), 6.88 (d, 1H), 5.63 (m, 2H), 5.12 (d, 4H), 3.93 (s, 3H), 2.65 (m, 2H), 2.53 (m, 2H).

Step 2. To a 250 mL RBF were added 4-(3-bromo-4-methoxyphenyl)hepta-1,6-dien-4-ol (4.85 g, 16.32 mmol), triethylsilane (5.21 mL, 32.6 mmol), and CH$_2$Cl$_2$ (50 mL). The flask was flushed with N$_2$. BF$_3$·Et$_2$O (2.275 mL, 17.95 mmol) was added via syringe at −78 °C. The resulting reaction mixture was stirred at −78 °C for 1 h and was then allowed to warm to 0 °C briefly. 10% KOH (50 mL) was added at 0 °C and the reaction mixture was extracted with 50 mL of EtOAc/hexane (1:1). The organics were washed with 30 mL of brine, dried over sodium sulfate, filtered, and concentrated. Crude product was purified by silica gel chromatography, eluted with 10% EtOAc/ hexane to give 2-bromo-4-(hepta-1,6-dien-4-yl)-1-methoxybenzene (3.6 g) as a colorless oil. ^{1}H NMR (500 MHz, CDCl$_3$) δ 7.38 (s, 1H), 7.06 (d, 1H), 6.85 (d, 1H), 5.66 (m, 2H), 4.99 (d, 4H), 3.91 (s, 3H), 2.66 (m, 1H), 2.42 (m, 2H), 2.33 (m, 2H).

Step 3. To a solution of 2-bromo-4-(hepta-1,6-dien-4-yl)-1-methoxybenzene (2.0 g, 7.11 mmol) in DCM (36 mL) was added Zhan catalyst (47 mg). The mixture was flushed with N$_2$ and refluxed at 45 °C overnight. The reaction mixture was concentrated, and the residue was purified by silica gel chromatography, eluting with 10% of EtOAc/isohexane to give 2-bromo-4-(cyclopent-3-en-1-yl)-1-methoxybenzene (1.9 g) as a colorless oil. ^{1}H NMR (500 MHz, CDCl$_3$: δ 7.46 (s, 1H), 7.18 (d, 1H), 6.83 (d, 1H), 5.80 (s, 2H), 3.91 (s, 3H), 3.40 (m, 1H), 2.81 (m, 2H), 2.40 (m, 2H).

Step 4. To a 100 mL RBF were added 2-bromo-4-(cyclopent-3-en-1-yl)-1-methoxybenzene (1.9 g, 7.51 mmol), NMO (2.64 g, 22.5 mmol), osmium tetroxide (0.942 mL, 0.075 mmol, 2.5% in t-BuOH), t-butanol (13 mL) and water (13 mL). The resulting reaction mixture was stirred at rt over the weekend. Volatiles were removed. Crude material was dissolved in 100 mL of EtOAc and washed with 50 mL of water. Organics were dried over sodium sulfate, filtered, and concentrated. The residue was purified by silica gel column chromatography, eluting with 80% EtOAc in hexane to give 4-(3-bromo-4-methoxyphenyl)-cyclopentane-1,2-diol (1.7 g) as a white solid. ^{1}H NMR (500 MHz, CDCl$_3$): δ 7.39 (s, 1H), 7.10 (d, 1H), 6.85 (d, 1H), 4.37 (m, 2H), 3.91 (s, 3H), 3.55 (m, 1H), 2.46 (b, 2H), 2.18 (m, 2H), 1.88 (m, 2H).

Step 5. To a solution of 4-(3-bromo-4-methoxyphenyl)-cyclopentane-1,2-diol (2.0 g, 6.97 mmol) in acetone (50 mL) was added 2,2-dimethoxypropane (2.56 mL, 20.90 mmol) at 0 °C followed by adding methanesulfonic acid (0.167 g, 1.74 mmol) dropwise. The reaction mixture was stirred at RT overnight. Volatiles were removed under vacuum. To the residue was added aqueous NaHCO$_3$, and the resulting mixture was extracted with EtOAc. The combined organics were washed with brine, dried over Na$_2$SO$_4$, filtered, and concentrated. Crude product was purified by silica gel column chromatography, eluting with 15% EtOAc in hexane to give intermediate L (1.7 g) as a white solid. ^{1}H NMR (500 MHz, CDCl$_3$): δ 7.43 (s, 1H), 7.15 (d, 1H), 6.85 (d, 1H), 4.76 (d, 2H), 3.88 (s, 3H), 3.34 (m, 1H), 2.20 (dd, 2H), 1.59 (m, 2H), 1.55 (s, 3H), 1.35 (s, 3H).

5-(3-Bromo-4-methoxyphenyl)-6-methylpiperidin-2-one (Intermediate 21). Step 1. To a 100 mL RBF were added 2-bromo-4-iodo-1-methoxybenzene (0.59 g, 1.87 mmol) and 10 mL of THF. iPrMgCl (0.94 mL, 1.89 mmol, 2 M THF solution) was added at 0 °C via syringe. The reaction mixture was stirred at 0 °C for 1 h. A solution of lithium 2-thenyl cyanocuprate (7.5 mL, 1.87 mmol) in THF was added, followed by 2-methylcyclopent-2-enone (150 mg, 1.56 mmol). The resulting reaction mixture was stirred at 0 °C for 1 h and was allowed to warm up and stirred at rt for 1 h. The reaction mixture was diluted with 30 mL of EtOAc/hexane (1:1), washed with 30 mL of 1 N HCl, then 20 mL of brine. Organics were dried over sodium sulfate, filtered, and concentrated. Crude product was purified by silica gel chromatography to give 135 mg of 3-(3-bromo-4-methoxyphenyl)-2-methylcyclopentanone as a mixture of two diastereomers at 1.6:1 ratio. ^{1}H NMR for the major diastereomer (500 MHz, CDCl$_3$): δ 7.35 (d, J =

2.2 Hz, 1H), 7.05 (dd, J = 2.2, 8.4 Hz, 1H), 6.89 (d, J = 8.4 Hz, 1H), 3.92 (s, 3H), 3.55 (m, 1H), 2.2−2.6 (m, 5H), 0.83 (d, J = 7.6 Hz, 3H). ^{1}H NMR for the minor diastereomer (500 MHz, CDCl$_3$): δ 7.48 (d, J = 2.1 Hz, 1H), 7.19 (dd, J = 2.2, 8.3 Hz, 1H), 6.93 (d, J = 8.3 Hz, 1H), 3.94 (s, 3H), 2.75 (m, 1H), 2.2−2.6 (m, 5H), 1.07 (d, J = 6.8 Hz, 3H).

Step 2. To a vial were added 3-(3-bromo-4-methoxyphenyl)-2-methylcyclopentanone (135 mg, 0.57 mmol), NH$_2$OH (94 mg, 1.43 mmol), and 3 mL of EtOH. The resulting reaction mixture was stirred at 75 °C for 2 h. Volatiles were removed and the resulting residue was diluted with 20 mL of EtOAc, washed with 20 mL of sat. Na$_2$CO$_3$ aqueous solution, and then 10 mL of brine. The organics were dried over sodium sulfate, filtered, and concentrated. The residue was dissolved in 3 mL of DCM and was transferred to a vial. To this vial were added tosyl-Cl (109 mg, 0.57 mmol), DMAP (catalytic) and TEA (0.13 mL, 0.95 mmol). The resulting reaction mixture was stirred at rt for 2 h. Volatiles were removed. To the remaining material was added acetic acid (3.0 mL). The resulting reaction mixture was stirred at rt overnight. Volatiles were removed. Crude material was diluted with 20 mL of EtOAc, washed with 20 mL of sat. Na$_2$CO$_3$ aqueous solution, then 10 mL of brine. Organics were dried over sodium sulfate, filtered, and concentrated. The crude product was purified on reversed-phase HPLC eluted with acetonitrile/water (modified with 0.05% TFA) gradient solvents to give 72 mg of 3-(3-bromo-4-methoxyphenyl)-2-methylcyclopentanone (**Intermediate 21**) as a mixture of cis and trans isomers. MS ESI calcd for C$_{13}$H$_{16}$BrNO$_2$ [M + H]$^+$ 298.0 and 300.20, found 298.1 and 300.1.

(S)-5-(3-Bromo-4-methoxyphenyl)-6,6-dimethyl-1,3-oxazinan-2-one (Intermediate 22). Step 1. To a stirred solution of 2-(3-bromo-4-methoxyphenyl)acetic acid (5 g, 20.40 mmol) in 60 mL of THF was added TEA (3.13 mL, 22.44 mmol), and then pivaloyl chloride (2.64 mL, 21.42 mmol) at 0 °C. The resulting reaction mixture was stirred at 0 °C for 30 min. Ice bath was replaced with dry ice acetone bath. To a separate round-bottom flask was added (S)-4-benzyl-2-oxazolidinone (3.62 g, 20.4 mmol) and 50 mL of THF. To this solution was added n-BuLi (12.8 mL, 20.4 mmol, 1.6 M in hexane) dropwise via a syringe at −78 °C. The resulting reaction mixture was stirred −78 °C for 5 min. This solution was transferred to the previous flask via channular transferring. After transferring, the reaction mixture was stirred at −78 °C for 30 min and was allowed to warm up to rt. It was quenched by addition of 100 mL of brine and 100 mL of water. The reaction mixture was extracted with 200 mL of 30% EtOAc in hexane. The organics were dried over sodium sulfate, filtered, and concentrated. Crude product was purified on a Combiflash prepacked silica gel column eluted with 5 to 35% EtOAc in hexane to give 5.7 g desired product as a colorless viscous material. ^{1}H NMR (500 MHz, CDCl$_3$): δ 7.57 (s, 1H), 7.3 (m, 4H), 7.18 (d, J = 7.3 Hz, 1H), 6.92 (d, J = 8.5 Hz, 1H), 4.71 (br, 1H), 4.1−4.3 (m, 4H), 3.93 (s, 3H), 3.31 (d, J = 12.9 Hz, 1H), 2.81 (dd, J = 9.8, 13.2 Hz, 1H).

Step 2. To a round-bottom flask were added 10 mL of DCM and (S)-4-benzyl-3-(2-(3-bromo-4-methoxyphenyl)acetyl)oxazolidin-2-one (1.0 g, 2.47 mmol). TiCl$_4$ (2.6 mL, 2.60 mmol, 1 M DCM solution) was added at 0 °C. After stirring at 0 °C for 5 min, DIEA (0.45 mL, 2.6 mmol) was added via syringe. The reaction mixture was stirred at 0 °C for 30 min. Acetone (0.27 mL, 3.71 mmol) was added followed by more of TiCl$_4$ (2.6 mL, 2.6 mmol, 1 M DCM solution). The reaction mixture was stirred at 0 °C for 2 h. It was quenched by addition of 80 mL of sat. NH$_4$Cl aqueous solution. The resulting reaction mixture was extracted with 120 mL of EtOAc/hexane (1:1). Organics were dried over sodium sulfate, filtered, and concentrated. Crude product was purified on Combiflash prepacked silica gel column, eluted with 5−40% EtOAc in hexane to give 1.1 g desired product as viscous material. ^{1}H NMR (500 MHz, CDCl$_3$): δ 7.70 (s, 1H), 7.1−7.4 (m, 6H), 6.88 (d, J = 8.5 Hz, 1H), 4.68 (m, 1H), 4.1 (m, 2H), 3.93 (s, 3H), 3.83 (s, 1H), 3.43 (dd, J = 3.4, 13.3 Hz, 1H), 2.82 (dd, J = 9.9, 13.3 Hz, 1H), 1.46 (s, 3H), 1.09 (s, 3H).

Step 3. To a solution of (S)-4-benzyl-3-((R)-2-(3-bromo-4-methoxyphenyl)-3-hydroxy-3-methylbutanoyl)oxazolidin-2-one (540 mg, 1.17 mmol) in 10 mL of THF was added a solution of DIBAL-H (3.5 mL, 3.50 mmol, 1 M toluene solution) via a syringe at 0 °C. After stirring at 0 °C for 20 min, more DIBAL-H (1.0 mL, 1.0 mmol) was

added. After stirring at 0 °C for 10 min, the reaction mixture was quenched by addition of 10 mL of EtOAc and then 10 mL of 3 N HCl. After stirring at 0 °C for 15 min, the reaction was diluted with 30 mL of EtOAc/hexane (1:1) and 30 mL of water. The layers were separated. The organics were washed with 20 mL of 10% KOH aqueous solution, dried over sodium sulfate, filtered, and concentrated. Crude product was purified on prepacked Combiflash column and eluted with 5−40% EtOAc in hexane to give 185 mg of viscous material. NMR indicated it is a mixture of desired product and the chiral auxiliary. ^{1}H NMR (500 MHz, CDCl$_3$): δ 7.49 (d, J = 2.1 Hz, 1H), 7.23 (dd, J = 2.1, 8.3 Hz, 1H), 6.88 (d, J = 8.3 Hz, 1H), 4.05 (m, 2H), 3.92 (s, 3H), 2.85 (m, 1H), 1.27 (s, 3H), 1.24 (s, 3H).

Step 4. To a solution of (S)-2-(3-bromo-4-methoxyphenyl)-3-methylbutane-1,3-diol (115 mg, 0.40 mmol) in 2 mL of DCM were added DMAP (catalytic), DIEA (0.21 mL, 1.29 mmol) and tosyl chloride (106 mg, 0.57 mmol). The resulting reaction mixture was stirred at 40 °C overnight. It was diluted with 20 mL of EtOAc and washed with 20 mL of water. The organics were dried over sodium sulfate, filtered, and concentrated. Crude product was purified by chromatography to give 132 mg of tosylate product. ^{1}H NMR (500 MHz, CDCl$_3$): δ 7.63 (d, J = 8.1 Hz, 2H), 7.31 (d, J = 8.1 Hz, 2H), 7.22 (d, J = 2.0 Hz, 1H), 7.07 (dd, J = 2.0, 8.6 Hz, 1H), 6.82 (d, J = 8.4 Hz, 1H), 4.65 (dd, J = 4.9, 10.0 Hz, 1H), 4.31 (t, J = 9.9 Hz, 1H), 3.92 (s, 3H), 2.9 (m, 1H), 2.48 (s, 3H), 1.28 (s, 3H), 1.10 (s, 3H).

Step 5. To a solution of (S)-2-(3-bromo-4-methoxyphenyl)-3-hydroxy-3-methylbutyl 4-methylbenzenesulfonate (58 mg, 0.13 mmol) in 2 mL of DMF was added NaN$_3$ (34 mg, 0.52 mmol). The resulting reaction mixture was heated at 60 °C overnight and was then diluted with 10 mL of EtOAc/hexane (1:1) and 10 mL of water. The layers were separated. The organics were dried over sodium sulfate, filtered, and concentrated. Crude product was purified on Combiflash prepacked silica gel column, eluted with hexane to 40% EtOAc in hexane to give 38 mg of desired product. ^{1}H NMR (500 MHz, CDCl$_3$): δ 7.49 (d, J = 1.9 Hz, 1H), 7.22 (dd, J = 2.1, 8.5 Hz, 1H), 6.91 (d, J = 8.4 Hz, 1H), 3.93 (s, 3H), 3.9 (m, 1H), 3.71 (m, 1H), 2.82 (m, 1H), 1.28 (s, 3H), 1.17 (s, 3H).

Step 6. To a 25 mL round-bottom flask containing (S)-4-azido-3-(3-bromo-4-methoxyphenyl)-2-methylbutan-2-ol (38 mg, 0.12 mmol) were added PPh$_3$ (48 mg, 0.18 mmol), THF (2 mL) and water (0.2 mL). The resulting reaction mixture was heated to reflux for 2 h. Volatiles were removed under vacuum. To the residue was added 2 mL of THF, DIEA (0.063 mL, 0.36 mmol), and CDI (39 mg, 0.24 mmol). The resulting reaction mixture was heated at 60 °C for 3 h. It was then diluted with 10 mL of saturated NH$_4$Cl and extracted with 15 mL of EtOAc. The organics were dried over sodium sulfate, filtered, and concentrated. Crude product was purified on a Combiflash prepacked silica gel column which was eluted with EtOAc to give 30 mg of the desired product (**Intermediate 22**). ^{1}H NMR (500 MHz, CDCl$_3$): δ 7.41 (s, 1H), 7.16 (d, J = 7.8 Hz, 1H), 6.88 (d, J = 8.5 Hz, 1H), 6.76 (s, 1H), 3.90 (s, 3H), 3.65 (t, J = 11.4 Hz, 1H), 3.46 (br, 1H), 3.0 (br, 1H), 1.34 (s, 3H), 1.32 (s, 3H).

3'-[2-{(1R,5S,7aS)-1-[3,5-Bis(trifluoromethyl)phenyl]-3-oxotetrahydro-1H-pyrrolo[1,2-c][1,3]oxazol-5-yl}-6-(dimethylamino)-5-(propan-2-yl)pyridin-3-yl]-4'-methoxy-2-methylbiphenyl-4-carboxylic Acid (77). Step 1. To a slurry of (1R,5S,7aS)-1-[3,5-bis-(trifluoromethyl)phenyl]-5-[3-bromo-6-(dimethylamino)pyridin-2-yl]tetrahydro-1H-pyrrolo[1,2-c][1,3]oxazol-3-one (200 mg, 0.372 mmol) in MeOH (7.25 mL) under nitrogen at room temperature was added silver sulfate (116 mg, 0.372 mmol), followed by iodine (94 mg, 0.372 mmol). The resulting mixture was stirred for 1 h. The reaction was partitioned with ethyl acetate and aqueous sodium hydroxide (1.0 M). The organic was then washed with aqueous saturated sodium thiosulfate and the combined aqueous layers were extracted with ethyl acetate. The combined organics were washed with brine, dried over magnesium sulfate, filtered, and concentrated in vacuo. The residue was purified by flash column chromatography to yield (1R,5S,7aS)-1-[3,5-bis(trifluoromethyl)phenyl]-5-[3-bromo-6-(dimethylamino)-5-iodopyridin-2-yl]tetrahydro-1H-pyrrolo[1,2-c]-[1,3]oxazol-3-one (180 mg, 0.271 mmol). MS ESI calcd for C$_{21}$H$_{18}$BrF$_6$N$_3$O$_2$ [M + H]$^+$ 666.0, found 666.1.

Step 2. To (1*R*,5*S*,7a*S*)-1-[3,5-bis(trifluoromethyl)phenyl]-5-[3-bromo-6-(dimethylamino)-5-iodopyridin-2-yl]tetrahydro-1*H*-pyrrolo-[1,2-*c*][1,3]oxazol-3-one (50 mg, 0.075 mmol) in DMF (1 mL) were added isopropenylboronic acid pinacol ester (13.9 mg, 0.083 mmol), dichloro[1,1′-bis(diphenylphosphino)ferrocene]palladium(II) dichloromethane adduct (1.84 mg, 2.26 *μ*mol), and potassium carbonate (0.5 M in water, 0.30 mL, 0.151 mmol). The system was stirred at 50 °C overnight before cooling and partitioning with water and ethyl acetate. The organic layer was washed with brine, dried over sodium sulfate, and concentrated before purifying by column chromatography to yield (1*R*,5*S*,7a*S*)-1-[3,5-bis(trifluoromethyl)phenyl]-5-[3-bromo-6-(dimethylamino)-5-(prop-1-en-2-yl)pyridin-2-yl]tetrahydro-1*H*-pyrrolo[1,2-*c*][1,3]oxazol-3-one (19 mg, 0.033 mmol). MS ESI calcd for $C_{24}H_{23}BrF_6N_3O_2$ [M + H]+ 580.1, found 580.2.

Step 3. To (1*R*,5*S*,7a*S*)-1-[3,5-bis(trifluoromethyl)phenyl]-5-[3-bromo-6-(dimethylamino)-5-(prop-1-en-2-yl)pyridin-2-yl]tetrahydro-1*H*-pyrrolo[1,2-*c*][1,3]oxazol-3-one (19 mg, 0.033 mmol) in THF (0.5 mL) were added methyl 4′-methoxy-2-methyl-3′-(4,4,5,5-tetramethyl-1,3,2-dioxaborolan-2-yl)biphenyl-4-carboxylate (18.8 mg, 0.049 mmol), dichloro[1,1′-bis(diphenylphosphino)ferrocene]palladium(II) (2.14 mg, 3.29 *μ*mol), and potassium carbonate (2.0 M in water, 0.049 mL, 0.100 mmol). The system was stirred at room temperature overnight. The reaction was directly purified by column chromatography to yield (1*R*,5*S*,7a*S*)-1-[3,5-bis(trifluoromethyl)phenyl]-5-[3-bromo-6-(dimethylamino)-5-(prop-1-en-2-yl)pyridin-2-yl]tetrahydro-1*H*-pyrrolo[1,2-*c*][1,3]oxazol-3-one (24 mg, 0.033 mmol). MS ESI calcd for $C_{40}H_{38}F_6N_3O_5$ [M + H]+ 754.3, found 754.4.

Step 4. To (1*R*,5*S*,7a*S*)-1-[3,5-bis(trifluoromethyl)phenyl]-5-[3-bromo-6-(dimethylamino)-5-(prop-1-en-2-yl)pyridin-2-yl]tetrahydro-1*H*-pyrrolo[1,2-*c*][1,3]oxazol-3-one (24 mg, 0.033 mmol) in ethanol (5 mL) was added palladium on carbon (0.54 mg, 5.04 *μ*mol). The system was stirred at room temperature under a hydrogen atmosphere for 2 days. The reaction was filtered, and the filtrate was concentrated. Crude methyl 3′-[2-{(1*R*,5*S*,7a*S*)-1-[3,5-bis(trifluoromethyl)phenyl]-3-oxotetrahydro-1*H*-pyrrolo[1,2-*c*][1,3]oxazol-5-yl]-6-(dimethylamino)-5-(propan-2-yl)pyridin-3-yl]-4′-methoxy-2-methylbiphenyl-4-carboxylate (24 mg, 0.033 mmol) was carried forward without further purification. MS ESI calcd for $C_{40}H_{40}F_6N_3O_5$ [M + H]+ 756.3, found 756.4.

Step 5. To methyl 3′-[2-{(1*R*,5*S*,7a*S*)-1-[3,5-bis(trifluoromethyl)phenyl]-3-oxotetrahydro-1*H*-pyrrolo[1,2-*c*][1,3]oxazol-5-yl]-6-(dimethylamino)-5-(propan-2-yl)pyridin-3-yl]-4′-methoxy-2-methylbiphenyl-4-carboxylate (24 mg, 0.033 mmol) in THF (1 mL) was added lithium hydroxide (9.51 mg, 0.397 mmol). The reaction was stirred overnight at room temperature. Reaction was incomplete. More lithium hydroxide (4.76 mg, 1.99 mmol) was added, and the reaction was heated to 50 °C for 5 h. The reaction was purified by HPLC to yield 3′-[2-{(1*R*,5*S*,7a*S*)-1-[3,5-bis(trifluoromethyl)phenyl]-3-oxotetrahydro-1*H*-pyrrolo[1,2-*c*][1,3]oxazol-5-yl]-6-(dimethylamino)-5-(propan-2-yl)pyridin-3-yl]-4′-methoxy-2-methylbiphenyl-4-carboxylic acid (10 mg, 0.012 mmol). ¹H NMR indicated that this compound exists as a pair of rotamers at 1.6:1 ratio. ¹H NMR (500 MHz, CDCl₃) δ 7.94−8.10 (m, 2H), 7.90 (s, 1H), 7.84 (s, 2H), 7.48 (m, 2H), 7.42 (dd, *J* = 8.5 Hz, *J* = 2.0 Hz, 1H), 7.37 (d, *J* = 7.5 Hz, 1H, minor rotamer), 7.30 (d, 1H, merged with solvent peak, major rotamer), 7.14 (d, *J* = 8.5 Hz, 1H, minor rotamer),7.07 (d, *J* = 8.5 Hz, 1H, major rotamer), 5.98 (d, *J* = 8.0 Hz, 1H, minor rotamer), 5.93 (d, *J* = 8.0 Hz, 1H, major rotamer), 5.09 (t, *J* = 7.5 Hz, 1H, minor rotamer), 5.01 (t, *J* = 7.5 Hz, 1H, major rotamer), 4.76 (m, 1H), 3.93 (s, 3H, minor rotamer), 3.83 (s, 3H, major rotamer), 3.40 (m, 1H), 3.07 (s, 6H), 2.47 (s, 3H, major rotamer), 2.40 (s, 3H, minor rotamer), 2.35 (m, 1H), 2.05 (m, 1H), 1.60 (m, 1H), 1.29 (t, *J* = 6.5 Hz, 6H), 1.08 (m, 1H). MS ESI calcd for $C_{39}H_{38}F_6N_3O_5$ [M + H]+ 742.3, found 742.5. RTA (95% HS): 182 nM.

4-{5-[2-{(1R,5S,7aS)-1-[3,5-Bis(trifluoromethyl)phenyl]-3-oxotetrahydro-1H-pyrrolo[1,2-c][1,3]oxazol-5-yl]-4-(trifluoromethyl)-phenyl]-6-methoxypyridin-3-yl]-3-methylbenzoic Acid (87). Step 1. To a solution of **Intermediate 11**-2 (4.4 g, 7.83 mmol) in dioxane (50 mL) and water (5 mL) were added Intermediate I (3.66 g, 8.61 mmol), potassium phosphate (4.98 g, 23.5 mmol), and 1,1′-bis(di-*tert*-butylphosphino)ferrocene palladium dichloride (0.255 g, 0.39

mmol). The mixture was purged with nitrogen and heated at 80 °C overnight. The reaction was poured into ethyl acetate and was washed with water, dried over sodium sulfate, filtered, and concentrated. The resultant residue was purified by column chromatography to yield *tert*-butyl 4-{5-[2-{(1*R*,5*S*,7a*S*)-1-[3,5-bis(trifluoromethyl)phenyl]-3-oxotetrahydro-1*H*-pyrrolo[1,2-*c*][1,3]oxazol-5-yl]-4-(trifluoromethyl)-phenyl]-6-methoxypyridin-3-yl]-3-methylbenzoate (4.5 g, 5.77 mmol). MS ESI calcd for $C_{39}H_{33}F_9N_2O_5$ [M + H]+ 781.2, found 781.2.

Step 2. To *tert*-butyl 4-{5-[2-{(1*R*,5*S*,7a*S*)-1-[3,5-bis-(trifluoromethyl)phenyl]-3-oxotetrahydro-1*H*-pyrrolo[1,2-*c*][1,3]-oxazol-5-yl]-4-(trifluoromethyl)phenyl]-6-methoxypyridin-3-yl]-3-methylbenzoate (1 g, 1.28 mmol) was added dichloromethane:TFA (9:1, 10 mL). The reaction was stirred overnight at room temperature. Upon completion, the solvent was removed under reduced pressure and the resultant residue was redissolved in acetonitrile for direct purification by reversed-phase HPLC to yield 4-{5-[2-{(1*R*,5*S*,7a*S*)-1-[3,5-bis(trifluoromethyl)phenyl]-3-oxotetrahydro-1*H*-pyrrolo[1,2-*c*][1,3]oxazol-5-yl]-4-(trifluoromethyl)phenyl]-6-methoxypyridin-3-yl]-3-methylbenzoic acid (0.674 g, 0.931 mmol). ¹H NMR indicated that this compound exists as a pair of rotamers at a 1.2:1 ratio. ¹H NMR (500 MHz, CDCl₃) δ 8.27 (s, 1H), 8.04 (m, 4H, peaks overlap for the two rotamers), 7.90 (s, 1H), 7.84 (s, 2H, minor rotamer), 7.83 (s, 2H, major rotamer), 7.75 (s, 1H, major rotamer), 7.67 (s, 1H, minor rotamer), 7.63 (d, *J* = 8Hz, 1H, major rotamer), 7.42 (m, 2H), 7.38 (d, *J* = 7.9Hz, 1H, major rotamer), 7.36 (d, *J* = 7.9Hz, 1H, minor rotamer), 6.11(d, *J* = 7.9Hz, 1H, minor rotamer), 6.09 (d, *J* = 7.9 Hz, 1H, major rotamer), 5.27 (t, *J* = 7.9 Hz, 1H, major rotamer), 4.95 (t, *J* = 7.9 Hz, 1H, minor rotamer), 4.62 (m, 1H, minor rotamer), 4.51 (m, 1H, major rotamer), 4.12 (s, 3H, minor rotamer), 3.94(s, 3H, minor rotamer), 2.45 (s, 3H, minor rotamer), 2.45 (s, 3H, major rotamer), 2.37 (m, 1H), 2.2 (m, 1H), 2.05 (m, 1H), 1.85 (m, 1H), 1.55 (m, 1H), 1.4 (m, 1H), 1.1 (m, 2H). MS ESI calcd for $C_{35}H_{26}F_9N_2O_5$ [M + H]+ 725.2, found 725.0. RTA (95% HS): 53.18 nM

3-[2′-{(1R,5S,7aS)-1-[3,5-Bis(trifluoromethyl)phenyl]-3-oxotetrahydro-1H-pyrrolo[1,2-c][1,3]oxazol-5-yl]-6-methoxy-4′-(trifluoromethyl)biphenyl-3-yl]propanoic Acid (92). To **Intermediate 11**-2 (30 mg, 0.044 mmol) were added THF (2 mL), water (0.1 mL), tribasic potassium phosphate (45.3 mg, 0.213 mmol), methyl 3-[4-methoxy-3-(4,4,5,5-tetramethyl-1,3,2-dioxaborolan-2-yl)phenyl]-propanoate (51.3 mg, 0.16 mmol) (Intermediate H), palladium(II) acetate (1.2 mg, 5.34 *μ*mol), and 1,1′-bis(di-*tert*-butylphosphino)-ferrocene (2.53 mg, 5.34 *μ*mol). The system was flushed with nitrogen gas and was heated at 62 °C overnight. The reaction was diluted with ethyl acetate:hexanes (1:2, 10 mL) and was partitioned with water (10 mL). The organic was dried over sodium sulfate, filtered, and concentrated. The crude product was purified by reversed-phase HPLC to yield methyl 3-[2′-{(1*R*,5*S*,7a*S*)-1-[3,5-bis(trifluoromethyl)-phenyl]-3-oxotetrahydro-1*H*-pyrrolo[1,2-*c*][1,3]oxazol-5-yl]-6-methoxy-4′-(trifluoromethyl)biphenyl-3-yl]propanoate (27 mg, 0.04 mmol). ¹H NMR indicated that this compound exists as a pair of rotamers at 1.2:1 ratio. ¹H NMR (500 MHz, CDCl₃) δ 7.87 (s, 1H), 7.81 (s, 2H), 7.75 (s, 1H, major rotamer) 7.73 (s, 1H, minor rotamer) 7.6 (m, 1H) 6.8−7.3 (m, 4H), 6.06 (d, *J* = 7.9 Hz, 1H, major rotamer), 6.06 (d, *J* = 7.9 Hz, 1H, minor rotamer), 6.01 (d, 1H, minor rotamer), 5.12 (m, 1H, major rotamer), 4.98 (m, 1H, minor rotamer), 4.1 (m, 1H), 3.84 (s, 3H, major rotamer), 3.68 (s, 3H), 3.67 (s, 3H) 3.62 (s, 3H, minor rotamer), 2.9 (m, 2H), 2.6 (m, 2H), 0.9−1.7 (m, 4H). MS ESI calcd for $C_{32}H_{27}F_9NO_5$ [M + H]+ 676.2, found 676.4. RTA (95% HS): 296 nM.

To methyl 3-[2′-{(1*R*,5*S*,7a*S*)-1-[3,5-bis(trifluoromethyl)phenyl]-3-oxotetrahydro-1*H*-pyrrolo[1,2-*c*][1,3]oxazol-5-yl]-6-methoxy-4′-(trifluoromethyl)biphenyl-3-yl]propanoate (20 mg, 0.03 mmol) in THF (2 mL) and water (0.5 mL) were added lithium hydroxide monohydrate (6.21 mg, 0.148 mmol) and hydrogen peroxide (30%, 33.6 mg, 0.296 mmol). The reaction mixture was stirred at room temperature. Upon completion the reaction was diluted with water (10 mL), and solid Na₂SO₃ was added to quench hydrogen peroxide. The solution was acidified with aqueous HCl (1 M) and was partitioned with ethyl acetate (20 mL). The organic was dried over sodium sulfate, filtered, and concentrated before purification by reversed-phase HPLC

to yield 3-[2′-{(1R,5S,7aS)-1-[3,5-bis(trifluoromethyl)phenyl]-3-oxo-tetrahydro-1H-pyrrolo[1,2-c][1,3]oxazol-5-yl}-6-methoxy-4′-(trifluoromethyl)biphenyl-3-yl]propanoic acid (9 mg, 0.014 mmol). ^{1}H NMR indicated that this compound exists as a pair of rotamers at a 3:1 ratio. ^{1}H NMR (500 MHz, CDCl$_3$) δ 7.87 (s, 1H), 7.82 (s, 2H), 7.75 (s, 1H, minor rotamer), 7.73 (s, 1H, major rotamer) 7.6 (m, 1H) 6.9−7.4 (m, 4H), 6.08 (d, J = 8.1 Hz, 1H, major rotamer), 5.15 (t, 1H, minor rotamer) 5.06 (t, J = 8.2 Hz, 1H, major rotamer), 4.6 (m, 1H, major rotamer) 4.45 (m, 1H, minor rotamer), 4.98 (m, 1H, minor rotamer), 4.1 (m, 1H), 3.85 (s, 3H, minor rotamer), 3.69 (s, 3H, major rotamer), 2.4−3.1 (m, 4H), 0.9−1.9 (m, 4H). MS ESI calcd for C$_{31}$H$_{25}$F$_9$NO$_5$ [M + H]$^+$ 662.2, found 662.3. RTA (95% HS): 128 nM.

(1R,5S,7aS)-1-(3,5-Bis(trifluoromethyl)phenyl)-5-(5′-((2S,3S,4R)-2,4-dimethyl-5-oxopyrrolidin-3-yl)-2′-methoxy-4-(trifluoromethyl)-[1,1′-biphenyl]-2-yl)tetrahydropyrrolo[1,2-c]oxazol-3(1H)one (exemplar compound of 97a-d). To a 10 mL microwave tube was added (1R,5S,7aS)-1-(3,5-bis(trifluoromethyl)phenyl)-5-(2-(4,4,5,5-tetramethyl-1,3,2-dioxaborolan-2-yl)-5-(trifluoromethyl)phenyl)-tetrahydropyrrolo[1,2-c]oxazol-3(1H)-one (**Intermediate 11-3**, 70 mg, 0.115mmol), **Intermediate 18-2** (37 mg, 0.104 mmol), chloro-(2-dicyclohexylphosphino-2′4′6′-triisopropyl-1,1′-biphenyl)[2-(2-amino-1,1′-biphenyl)]palladium(II) (XPhos precatalyst) (9 mg, 0.021 mmol), potassium phosphate (33 mg, 0.157 mmol), dioxane (1 mL) and water (0.1 mL). The reaction mixture was degassed and filled with N$_2$ and heated at 110 °C for 3 h. It was cooled to rt and diluted with EtOAc (3 mL). The mixture was washed with water and brine and then concentrated. The residue was purified by reversed-phase HPLC. The product fraction was concentrated and extracted with EtOAc. The organic layer was washed with brine and concentrated to give the Boc protected product. It was dissolved in 0.5 mL of DCM and treated with 1 mL of TFA at rt for 10 min. Volatiles were removed under vacuum. The residue was purified by reversed-phase HPLC. Fractions contain desired product was lyophilized to give the title compound (40 mg) as a white powder. MS ESI calcd for C$_{34}$H$_{29}$F$_9$N$_2$O$_4$ [M + H]$^+$ 701.0, found 701.2. RTA (95% HS): 398 nM.

(1R,5S,8aS)-5-{5′-[2-(5-Amino-1,3,4-oxadiazol-2-yl)ethyl]-2′-methoxy-4-(trifluoromethyl)biphenyl-2-yl}-1-[3,5-bis(trifluoromethyl)-phenyl]hexahydro[1,3]oxazolo[3,4-a]pyridin-3-one (Exemplar Compound of 100). To 3-[2′-{(1R,5S,8aS)-1-[3,5-bis-(trifluoromethyl)phenyl]-3-oxohexahydro[1,3]oxazolo[3,4-a]pyridin-5-yl}-6-methoxy-4′-(trifluoromethyl)biphenyl-3-yl]propanehydrazide (10 mg, 0.015 mmol) in dioxane (1 mL) was added sodium bicarbonate (2.4 mg, 0.029 mmol) followed by water (0.2 mL). The system was sealed and cyanogen bromide (5.8 μL, 0.029 mmol) was added at room temperature. The reaction was complete in 5 min, and the solvent was removed before the crude material was purified by HPLC to yield.

(1R,5S,8aS)-5-{5′-[2-(5-amino-1,3,4-oxadiazol-2-yl)ethyl]-2′-me-thoxy-4-(trifluoromethyl)biphenyl-2-yl}-1-[3,5-bis(trifluoromethyl)-phenyl]hexahydro[1,3]oxazolo[3,4-a]pyridin-3-one (7 mg, 9.80 μmol). ^{1}H NMR indicated that this compound exists as a pair of rotamers at 1:1 ratio. ^{1}H NMR (500 MHz, CDCl$_3$) δ 8.45 (br s, 1H), 8.3 (br s, 1H), 7.90 (d, J = 9.2 Hz, 1H), 7.75 (m, 5H), 7.38 (t, J = 8.5 Hz) 7.2 (m, 2H), 7.0 (m, 2H), 5.55 (d, J = 8.9 Hz, 1H), 5.40 (d, J = 8.9 Hz, 1H), 5.38 (m, 1H), 5.25 (m, 1H), 4.2 (m, 1H), 3.95 (m, 1H), 3.82 (s, 3H), 3.8 (s, 3H), 3.2−3.1 (br s, 4H), 2.2 (m, 1H), 2.12 (m, 1H), 1.80 (m, 4H). MS ESI calcd for C$_{33}$H$_{28}$F$_9$N$_4$O$_4$ [M + H]$^+$ 715.2, found 715.3. RTA (95% HS): 1319 nM.

(1R,5S,8aS)-1-[3,5-Bis(trifluoromethyl)phenyl]-5-{2′-methoxy-5′-[2-(5-oxo-4,5-dihydro-1,3,4-oxadiazol-2-yl)ethyl]-4-(trifluoromethyl)biphenyl-2-yl}hexahydro[1,3]oxazolo[3,4-a]-pyridin-3-one (Exemplar Compound of 101). Step 1. To methyl 3-[2′-{(1R,5S,8aS)-1-[3,5-bis(trifluoromethyl)phenyl]-3-oxohexahydro-[1,3]oxazolo[3,4-a]pyridin-5-yl}-6-methoxy-4′-(trifluoromethyl)-biphenyl-3-yl]propanoate (30 mg, 0.044 mmol) was added ethanol (2 mL) followed by hydrazine hydrate (21.8 mg, 0.435 mmol). The mixture was heated for 150 °C by microwave irradiation for an hour. The crude reaction was concentrated and 3-[2′-{(1R,5S,8aS)-1-[3,5-bis(trifluoromethyl)phenyl]-3-oxohexahydro[1,3]oxazolo[3,4-a]-pyridin-5-yl}-6-methoxy-4′-(trifluoromethyl)biphenyl-3-yl]-propanehydrazide (27 mg, 0.039 mmol) was carried forward without

further purification. MS ESI calcd for C$_{32}$H$_{29}$F$_9$N$_3$O$_4$ [M + H]$^+$ 690.2, found 690.2.

Step 2. To 3-[2′-{(1R,5S,8aS)-1-[3,5-bis(trifluoromethyl)phenyl]-3-oxohexahydro[1,3]oxazolo[3,4-a]pyridin-5-yl}-6-methoxy-4′-(trifluoromethyl)biphenyl-3-yl]propanehydrazide (10 mg, 0.015 mmol) in DCM (2 mL) were added DIPEA (5.6 mg, 0.044 mmol) and phosgene (4.30 mg, 0.44 mmol). The reaction was stirred at room temperature for 30 min before the reaction was directly purified by column chromatography to yield (1R,5S,8aS)-1-[3,5-bis-(trifluoromethyl)phenyl]-5-{2′-methoxy-5′-[2-(5-oxo-4,5-dihydro-1,3,4-oxadiazol-2-yl)ethyl]-4-(trifluoromethyl)biphenyl-2-yl}-hexahydro[1,3]oxazolo[3,4-a]pyridin-3-one (5 mg, 6.99 μmol). ^{1}H NMR indicated that this compound exists as a pair of rotamers at 3:1 ratio: ^{1}H NMR (500 MHz, CDCl$_3$) δ 9.23 (s, 1H), 7.88 (s, 1H), 7.80 (s, 2H), 7.79 (s, 1H, minor rotamer), 7.65 (s, 2H, major rotamer) 7.62 (m, 1H) 7.4 (d, J = 7.8 Hz, 1H, major rotamer), 7.25 (d, J = 7.8 Hz, 1H, minor rotamer), 7.09 (s, 1H), 7.02 (m, 1H), 5.58 (m, 1H, minor rotamer) 5.42 (m, 1H, major rotamer), 4.19 (m, 1H), 3.85 (s, 3H, minor rotamer), 3.80 (s, 3H, major rotamer), 3.0−2.85 (m, 4H), 1.98 (m, 2H), 1.5−1.6 (m, 4H). MS ESI calcd for C$_{33}$H$_{27}$F$_9$N$_3$O$_5$ [M + H]$^+$ 716.2, found 716.3. RTA (95% HS): 942 nM.

Preparation of MK-8262 (87) via Optimized Synthesis. *(2S)-1-tert-Butyl 2-Ethyl 5-methoxypyrrolidine-1,2-dicarboxylate (109).* A solution of (S)-1-tert-butyl 2-ethyl 5-oxopyrrolidine-1,2-dicarboxylate (**108**) (40.0 g, 0.155 mol) in toluene (400 mL) was stirred at approximately 25 °C for 30 min and purged with nitrogen three times. The reaction solution was cooled to −35 to −25 °C, and LiBHEt$_3$ (1.0 M in THF, 186 mL, 186 mmol) was added dropwise while maintaining the internal temperature between −35 and −25 °C. The reaction solution was stirred at −35 to −25 °C for 1 h and was quenched with 5 wt % aqueous acetic acid solution between −35 and −25 °C to a pH of 7−8. The reaction mixture was diluted with MTBE (400 mL) and washed with 25 wt % NaCl aqueous solution (2 × 400 mL). The organic layer was solvent switched to MeOH to provide A1 as a MeOH solution (final volume, 200 mL). To the solution was added p-TsOH (2.76 g, 0.016 mol) while maintaining the internal temperature at 15−25 °C. The reaction was stirred at 15−25 °C for 20 h and was quenched with 7 wt % aqueous NaHCO$_3$ at −5 to 5 °C (pH 7−8). The solution was diluted with MTBE (1000 mL) and washed with 25 wt % NaCl aqueous solution (2 × 200 mL). The organic layer was solvent switch to THF to give **109** as a THF solution (assay A: 38 g, 90% yield, 99.4 LCAP%). An analytically pure sample was prepared by silica gel chromatography (ethyl acetate:heptane, 1:200) to provide a mixture of diastereomers of A as a colorless liquid: ^{1}H NMR (CDCl$_3$, 400 MHz) δ 5.11−5.30 (m, 1H), 4.15−4.26 (m, 3H), 3.35−3.43 (m, 3H), 1.75−2.50 (m, 4H), 1.45 (m, 9H), 1.26 (m, 3H); ^{13}C NMR (CDCl$_3$, 100 MHz) δ 172.6, 154.0, 89.2, 88.4, 80.5, 60.8, 59.2, 55.1, 30.9, 28.0, 14.1; HR-MS calcd for C$_{13}$H$_{23}$NO$_5$Na$^+$ [M + Na]$^+$ 296.1468, found 296.1471.

(2S,5S)-1-tert-Butyl 2-ethyl 5-(2-chloro-5-(trifluoromethyl)-phenyl)pyrrolidine-1,2-dicarboxylate (110). A solution of 2-bromo-1-chloro-4-(trifluoromethyl)benzene (142 g, 0.55 mol) in THF (400 mL) was purged with nitrogen three times. The reaction was cooled to −35 to −25 °C, and i-PrMgCl (1.0 M in THF, 586 mL, 586 mmol) was added dropwise followed by CuBr·Me$_2$O (120 g, 586 mmol), maintaining the temperature below −25 °C. BF$_3$·Et$_2$O (156 g, 1.098 mol) was then added dropwise at −35 to −25 °C and the reaction was maintained at −35 to −25 °C for 2 h. (2S)-1-tert-butyl 2-ethyl 5-methoxypyrrolidine-1,2-dicarboxylate (**109**) (100.0 g, 0.366 mol) was added dropwise while maintaining the internal temperature at −35 to −25 °C. The reaction suspension was stirred at −35 to −25 °C for 3 h. Water (100 mL) was added over 30 min and the solution was warmed to 15 and 25 °C. The solution was washed with 25 wt % Na$_2$SO$_4$ aqueous solution (2 × 500 mL). The organic layer was solvent switched to MTBE to afford **110** as an MTBE solution (final volume: 300 mL, assay B: 108 g, 70% yield, 99.9 LCAP%). An analytically pure sample was prepared by silica gel chromatography (ethyl acetate:heptane, 1:200) to provide B as a colorless liquid: ^{1}H NMR (CDCl$_3$, 400 MHz) δ 7.28−7.51 (m, 3H), 5.41 (dd, J = 8.4 Hz, J = 7.2 Hz, 1H), 4.67 (dd, J = 8.4 Hz, J = 8.8 Hz, 1H), 4.25 (m, 2H), 2.56 (m, 1H), 2.19 (m, 1H), 2.02

(m, 1H), 1.84 (m, 1H), 1.42 (s, 4.5H), 1.33 (m, 3H), 1.19 (s, 4.5H); ^{13}C NMR (CDCl$_3$, 100 MHz) δ 172.5, 153.8, 142.7, 141.6, 135.5, 130.1, 128.9, 123.1, 80.8, 61.2, 60.1, 58.8, 31.4, 28.1, 27.0, 14.1; HR-MS calcd for C$_{19}$H$_{23}$ClF$_3$NO$_4$Na$^+$ [M + Na]$^+$ 444.1160, found 444.1165.

(2S,5S)-tert-Butyl 2-(3,5-bis(trifluoromethyl)benzoyl)-5-(2-chloro-5-(trifluoromethyl)phenyl)pyrrolidine-1-carboxylate (111). A solution of 1-bromo-3,5-bis(trifluoromethyl)benzene (257 g, 0.877 mol) in MTBE (500 mL) was cooled to −70 to −60 °C, and *n*-BuLi (2.5 M in *n*-hexane, 350 mL, 877 mmol) was added dropwise while maintaining the internal temperature below −60 °C. After 2 h, the reaction solution was added into a solution of (2*S*,5*S*)-1-*tert*-butyl 2-ethyl 5-(2-chloro-5-(trifluoromethyl)phenyl)pyrrolidine-1,2-dicarboxylate (110) (100 g, 0.237 mol) in MTBE (500 mL) at −70 to −60 °C and stirred for 2 h. The reaction was quenched with a 50 wt % H$_3$PO$_4$ solution in MTBE at −70 to −60 °C to a pH of 7−8. Water (1000 mL) was added over 30 min and the reaction was warmed to 15 and 25 °C. The organic layer was solvent switched to THF to afford 111 as a THF solution (final volume: 300 mL, assay C: 101 g, 72.5% yield, 98.0 LCAP%). An analytically pure sample was prepared by silica gel chromatography (ethyl acetate:heptane, 1:5) to provide C as an off-white solid: mp: 135.7 °C; ^{1}H NMR (CDCl$_3$, 400 MHz) δ 8.50 (d, *J* = 12 Hz, 2H), 8.16 (d, *J* = 15.2 Hz, 1H), 7.53 (m, 3H), 5.56−5.74 (m, 2H), 2.59 (m, 1H), 2.38 (m, 1H), 1.93 (m, 2H), 1.30 (s, 3H), 1.22 (s, 6H); ^{13}C NMR (CDCl$_3$, 100 MHz) δ 195.4, 153.9, 153.0, 142.4, 141.4, 136.3, 132.4, 130.3, 128.5, 126.7, 124.9, 123.1, 81.0, 62.2, 59.1, 31.3, 30.1, 28.1, 27.3, 26.4; HR-MS calcd for C$_{21}$H$_{14}$ClF$_9$NO$_3^+$ [M−56+H]$^+$ 534.0440, found 534.0533.

(2S,5S)-tert-Butyl 2-((R)-(3,5-bis(trifluoromethyl)phenyl)-(hydroxy)methyl)-5-(2-chloro-5-(trifluoromethyl)phenyl)-pyrrolidine-1-carboxylate (112). (2*S*,5*S*)-*tert*-Butyl 2-(3,5-(trifluoromethyl)benzoyl)-5-(2-chloro-5-(trifluoromethyl)phenyl)-pyrrolidine-1-carboxylate (111) (100 g, 169.5 mmol) was added into THF (700 mL) and stirred until to make a solution. The solution was cooled to approximately −5 to 0 °C, and DIBAL-H (1.0 M, 339 mL, 339 mmol) was added dropwise while maintaining the internal temperature below 0 °C. The reaction solution was stirred for 30 min between −5 and 0 °C and was quenched with a 5 wt % aqueous acetic acid solution at −5 to 0 °C. The solution was warmed to 20 and 25 °C. Water (400 mL) was added, the solution was stirred for a further 30 min and then two layers were separated. The organic layer was solvent switched to THF (final volume 150 mL). *n*-Heptane (500 mL) was added dropwise, keeping the temperature between 20 and 30 °C, and the resulting slurry was cooled to 0−10 °C, and was stirred for a further 3 h before filtered. The cake was washed with Heptane (2 × 200 mL) and dried under reduced pressure between 40 and 50 °C to afford 112 as an off-white solid (93 g, 93% yield, 99.4 LCAP%) to provide D as an off-white solid: mp: 223.6 °C; ^{1}H NMR (DMSO-*d$_6$*, 400 MHz) δ 8.03 (m, 2H), 8.16 (d, *J* = 15.2 Hz, 1H), 7.53 (m, 3H), 5.56−5.74 (m, 2H), 2.59 (m, 1H), 2.38 (m, 1H), 1.93 (m, 2H), 1.30 (s, 3H), 1.22 (s, 6H); ^{13}C NMR (DMSO-*d$_6$*, 100 MHz) δ 153.0, 147.2, 144.3, 142.9, 135.5, 131.1, 130.8, 130.5, 130.4, 130.2, 128.2, 127.1, 125.2, 122.5, 120.9, 80.0, 72.2, 64.4, 59.5, 32.0, 28.7, 22.6; HR-MS calcd for C$_{21}$H$_{16}$ClF$_9$NO$_3^+$ [M−56+H]$^+$ 536.0597, found 536.0686.

(R)-(3,5-Bis(trifluoromethyl)phenyl)((2S,5S)-5-(2-chloro-5-(trifluoromethyl)phenyl)pyrrolidin-2-yl)methanol (113). To a stirred solution of (2*S*,5*S*)-*tert*-butyl 2-((*R*)-(3,5-bis(trifluoromethyl)phenyl)-(hydroxy)methyl)-5-(2-chloro-5-(trifluoromethyl)phenyl)pyrrolidine-1-carboxylate (112) (100 g, 169 mmol) in EtOAc (200 mL) was added HCl/EtOAc solution (4 M, 350 mL, 1.4 mol) while maintaining the internal temperature at 20−25 °C. The reaction solution was stirred for 1 h between 20 and 25 °C. The solution was concentrated to 200 mL and then *n*-heptane (400 mL) was added dropwise in 8 h while maintaining the internal temperature at 20−25 °C. The resulting slurry was stirred for a further 5 h before filtered. The cake was washed with *n*-heptane (2 × 200 mL) and dried under reduced pressure at 40−50 °C to afford 113 as an off-white solid (70 g, 84% yield, 99.4 LCAP%): mp: 258.0 °C; ^{1}H NMR (DMSO-*d$_6$*, 400 MHz) δ 9.95 (s, 2H), 8.33 (s, 1H), 8.18 (s, 2H), 8.10 (s, 1H), 7.82 (s, 2H), 6.73 (s, 1H), 5.42 (s, 1H), 5.13 (s, 1H), 4.30 (s, 1H), 2.42 (m, 1H), 2.20 (m, 2H), 1.83 (s, 1H); ^{13}C NMR (DMSO-*d$_6$*, 100 MHz) δ 145.1, 138.0, 134.7, 131.4, 130.9, 130.5,

129.0, 127.7, 127.5, 126.7, 125.4, 125.1, 122.6, 122.4, 69.4, 63.6, 59.5, 31.5, 24.0; HR-MS calcd for C$_{20}$H$_{16}$ClF$_9$NO$^+$ [M + H]$^+$ 492.0771, found 492.0792.

(1R,5S,7aS)-1-(3,5-Bis(trifluoromethyl)phenyl)-5-(2-chloro-5-(trifluoromethyl)phenyl)tetrahydropyrrolo[1,2-c]oxazol-3(1H)-one (114). To a stirred solution of (*R*)-(3,5-bis(trifluoromethyl)phenyl)-((2*S*,5*S*)-5-(2-chloro-5-(trifluoromethyl)phenyl)pyrrolidin-2-yl)-methanol (113) (37.4 g, 76 mmol) and DIPEA (35 g, 274 mmol) in DCM (400 mL) was added triphosgene (22.6 g, 76 mmol), and the reaction solution was stirred at 30−40 °C for 15 h. The solution was cooled to 0−5 °C. An aqueous solution of NaHCO$_3$ (7 wt %, 187 mL) was added dropwise while maintaining the internal temperature between 0 and 5 °C. The solution was warmed to 10−20 °C and stirred for 30 min. The two layers were separated, and the organic layer was washed with water (2 × 200 mL). The solution was concentrated to 75 mL, and heptane (200 mL) was added dropwise in 10 h while maintaining the internal temperature at 10−20 °C. The resulting slurry was stirred for a further 10 h and filtered. The cake was washed with *n*-heptane (2 × 50 mL) and dried under reduced pressure between 40 and 50 °C to afford 114 as an off-white solid (37 g, 95% yield, 98.0 LCAP %): mp: 189.66 °C; ^{1}H NMR (CDCl$_3$, 400 MHz) δ 7.84 (s, 1H), 7.78 (s, 2H), 7.65 (s, 1H), 7.43 (s, 2H), 6.05 (d, *J* = 8.0 Hz, 1H), 5.28 (t, *J* = 8.0 Hz, 1H), 4.50 (m, 1H), 2.85 (m, 1H), 1.58 (m, 1H), 1.46 (m, 1H), 1.16 (m, 1H); ^{13}C NMR (CDCl$_3$, 100 MHz) δ 160.0, 141.0, 138.2, 135.7, 132.6, 132.3, 130.5, 129.6, 125.5, 125.4, 125.3, 124.3, 122.6, 122.5, 75.3, 64.3, 60.9, 34.3, 28.3; HR-MS calcd for C$_{21}$H$_{14}$ClF$_9$NO$_2^+$ [M + H]$^+$ 518.0564, found 518.0563.

tert-Butyl 4-Bromo-3-methylbenzoate (116). To a stirred solution of 4-bromo-3-methylbenzoic acid (115) (40 g, 186 mmol) and Boc$_2$O (203 g, 930 mmol) in t-BuOH and MTBE (v:v = 2:8) (200 mL) was added DMAP (45.4 g, 372 mmol) in portions while maintaining the internal temperature at 20−30 °C. The reaction solution was warmed to 40−50 °C and stirred for 20 h. The reaction was cooled to 0−10 °C. An aqueous solution of NaHCO$_3$ (3 wt %, 200 mL) was added dropwise while maintaining the internal temperature between 0 and 10 °C. The two layers were separated, and the organic layer was concentrated under reduced pressure. The crude residue was subjected to silica gel chromatography eluting with Heptane in EtOAc (200:1) to afford 116 as a yellow oil (46 g, 92% yield, 99.7 LCAP%): ^{1}H NMR (CDCl$_3$, 400 MHz) δ 7.75 (s, 1H), 7.56 (d, *J* = 8.0 Hz, 1H), 7.49 (d, *J* = 8.0 Hz, 1H), 2.35 (s, 3H), 1.51 (s, 9H); ^{13}C NMR (CDCl$_3$, 100 MHz) δ 165.2, 137.9, 132.2, 131.5, 131.1, 129.8, 128.1, 81.2, 28.1, 22.8; HR-MS calcd for C$_{12}$H$_{15}$BrO$_2$Na$^+$ [M + Na]$^+$ 293.0148, found 293.0144.

tert-Butyl 3-Methyl-4-(4,4,5,5-tetramethyl-1,3,2-dioxaborolan-2-yl)benzoate (117). A solution of *tert*-butyl 4-bromo-3-methylbenzoate (116) (300 g, 1.11 mol), B$_2$Pin$_2$ (268.8 g, 1.06 mol) and KOAc (327.7 g, 2.34 mol) in Dioxane (3740 mL) was added Pd(dppf)Cl$_2$.DCM (25.94 g, 0.032 mol) and purged with nitrogen three times. The reaction solution was heated to 120−130 °C and stirred for 16 h. The reaction was cooled to 20−30 °C, filtered, and the cake was washed with EtOAc (100 mL) to remove inorganics. The filtrate was washed with water (2 × 500 mL) and concentrated under reduced pressure. The crude residue was subjected to silica gel chromatography eluting with Heptane in EtOAc (20:1) to afford 117 as a brown solid (282 g, 80% yield, 98.4 LCAP%): mp: 116.9 °C; ^{1}H NMR (CDCl$_3$, 400 MHz) δ 7.67−7.71 (m, 3H), 2.49 (s, 3H), 1.51 (s, 9H), 1.28 (s, 12H); ^{13}C NMR (CDCl$_3$, 100 MHz) δ 166.0, 144.7, 135.6, 133.7, 130.2, 125.4, 83.7, 80.9, 28.2, 24.8, 22.0; HR-MS calcd for C$_{14}$H$_{20}$BO$_4^+$ [M−56+H]$^+$ 263.1376, found 263.1453.

tert-Butyl 4-(5-Chloro-6-methoxypyridin-3-yl)-3-methylbenzoate (118). *tert*-Butyl 3-methyl-4-(4,4,5,5-tetramethyl-1,3,2-dioxaborolan-2-yl)benzoate (117) (145.5 g, 457 mmol), 5-bromo-3-chloro-2-methoxypyridine (101.1 g, 457 mmol), and K$_3$PO$_4$.3H$_2$O (243.4 g, 915 mmol) were added into a mixture of Dioxane (2500 mL) and water (150 mL). Pd(dppf)Cl$_2$.DCM (18.69 g, 23 mmol) was then added followed by nitrogen purge (30 min). The reaction solution was heated to 75−85 °C and stirred for 16 h. The reaction was cooled to 20−30 °C. The two layers were separated, and the organic layer was washed with water (2 × 500 mL) and concentrated under reduced pressure. The crude residue was subjected to silica gel chromatography eluting with

Heptane in EtOAc (20:1) to afford **118** as an off-white solid (120 g, 79% yield, 99.8 LCAP%): mp: 78.91 °C; ^{1}H NMR (CDCl$_3$, 400 MHz) δ 8.03 (s, 1H), 7.92 (s, 1H), 7.88 (d, J = 8.0 Hz, 1H), 7.64 (s, 1H), 7.26 (d, J = 8.0 Hz, 1H), 4.09 (s, 3H), 2.34 (s, 3H), 1.63 (s, 9H); ^{13}C NMR (CDCl3, 100 MHz) δ 165.5, 158.6, 144.2, 140.8, 138.6, 135.8, 131.6, 131.5, 130.8, 129.8, 127.1, 117.7, 81.1, 54.4, 28.2, 20.3; HR-MS calcd for C$_{18}$H$_{21}$ClNO$_3^+$ [M + H]$^+$ 334.1204, found 334.1214.

tert-Butyl 4-(6-Methoxy-5-(4,4,5,5-tetramethyl-1,3,2-dioxaboro-lan-2-yl)pyridin-3-yl)-3-methylbenzoate (119). *tert-*Butyl 4-(5-chloro-6-methoxypyridin-3-yl)-3-methylbenzoate (**118**) (80 g, 240.2 mmol), B$_2$Pin$_2$ (122 g, 480.3 mmol), and KOAc (71 g, 720.5 mmol) were added in Dioxane (1600 mL). To the mixture was added XPhos Pd G3 (3.78 g, 4.8 mmol) and the reaction was purged with nitrogen three times. The reaction was warmed until 75 and 85 °C and stirred for 16 h between 75 and 85 °C. The reaction was cooled to 20−30 °C, filtered, and the cake was washed with EtOAc (500 mL). The filtrate was washed with water (2 × 20 mL) and concentrated under reduced pressure. The crude residue was subjected to silica gel chromatography eluting with Heptane in EtOAc (20:1) to afford **119** as an off-white solid (92 g, 90% yield, 99.6 LCAP%): mp: 152.75 °C; ^{1}H NMR (CDCl$_3$, 400 MHz) δ 8.20 (d, J = 2.8 Hz, 1H), 7.95 (m, 3H), 7.28 (m, 1H), 4.04 (s, 3H), 2.32 (s, 3H), 1.63 (s, 9H), 1.37 (s, 12H); ^{13}C NMR (CDCl$_3$, 100 MHz) δ166.6, 165.8, 149.1, 146.9, 142.4, 135.9, 131.1, 129.4, 127.0, 84.0, 81.0, 54.0, 28.2, 24.8, 20.5; HR-MS calcd for C$_{24}$H$_{33}$BNO$_5^+$ [M + H]$^+$ 425.2483, found 425.2488.

tert-Butyl 4-(5-(2-((1R,5S,7aS)-1-(3,5-Bis(trifluoromethyl)phenyl)-3-oxohexahydropyrrolo[1,2-c]oxazol-5-yl)-4-(trifluoromethyl)-phenyl)-6-methoxypyridin-3-yl)-3-methylbenzoate (120). (1*R*,5*S*,7a*S*)-1-(3,5-Bis(trifluoromethyl)phenyl)-5-(2-chloro-5-(trifluoromethyl)phenyl)tetrahydropyrrolo[1,2-*c*]oxazol-3(1*H*)-one (**114**) (100 g, 0.193 mol), *tert*-butyl 4-(6-methoxy-5-(4,4,5,5-tetramethyl-1,3,2-dioxaborolan-2-yl)pyridin-3-yl)-3-methylbenzoate (**119**) (82 g, 0.193 mol), and K$_3$PO$_4$ (82 g, 0.386 mol) were added into a mixture of THF (500 mL) and H$_2$O (300 mL). The reaction was bubbled with nitrogen for 2 h before XPhos precat. (2.3 g, 3.86 mmol) was added, and the mixture was bubbled with nitrogen for 1 h. The reaction mixture was warmed to 57−62 °C and stirred for 2 h. The mixture was cooled to 20 °C and the two layers were separated. The aqueous layer was extracted with IPAc (2 × 500 mL). The combined organic solutions were washed with 25 wt % NaCl aqueous solution (2 × 500 mL). The crude **120** was dissolved in IPAc (300 mL), and *n*-heptane (500 mL) was added dropwise, keeping the temperature between 20 and 30 °C. The resulting slurry was cooled to 0−10 °C, and was stirred for a further 3 h and filtered. The cake was washed with *n*-heptane (2 × 200 mL) and dried under reduced pressure between 40 and 50 °C to afford **120** as an off-white solid (138.7 g, 92% yield, 99.5 LCAP%): mp: 179.11 °C; ^{1}H NMR (CDCl$_3$, 400 MHz) δ 8.29 (s, 1H), 7.78−7.95 (m, 6H), 7.27−7.67 (m, 4H), 6.06−6.12 (dd, J = 15.2 Hz, 1H), 4.95−5.30 (m, 1H), 4.48−4.66 (dt, J = 8.0 Hz, J = 8.0 Hz, 1H), 4.51−4.65 (m, 1H), 4.1 (s, 1.5H), 2.43 (s, 1.5H), 2.34 (s, 1.5H), 1.85−2.07 (m, 1H), 1.62 (s, 9H), 1.40−1.59 (m, 2H), 1.03−1.14 (m, 1H); ^{13}C NMR (CDCl$_3$, 100 MHz) 165.5, 160.0, 159.6, 146.8, 142.3, 139.9, 138.5, 135.8, 132.2, 131.2, 129.8, 127.2, 125.3, 124.3, 121.6, 118.9, 81.0, 75.0, 64.2, 60.7, 54.1, 53.6, 35.4, 31.9, 28.4, 22.7, 20.5, 14.1; HR-MS calcd for C$_{39}$H$_{34}$F$_9$N$_2$O$_5^+$ [M + H]$^+$ 781.2319, found 781.2311.

4-(5-(2-((1R,5S,7aS)-1-(3,5-Bis(trifluoromethyl)phenyl)-3-oxohexahydropyrrolo[1,2-c]oxazol-5-yl)-4-(trifluoromethyl)-phenyl)-6-methoxypyridin-3-yl)-3-methylbenzoic Acid (87, MK-8262). A solution of *tert*-butyl 4-(5-(2-((1*R*,5*S*,7a*S*)-1-(3,5-bis-(trifluoromethyl)phenyl)-3-oxohexahydropyrrolo[1,2-*c*]oxazol-5-yl)-4-(trifluoromethyl)phenyl)-6-methoxypyridin-3-yl)-3-methylbenzoate (**120**) (100 g, 0.128 mol) in toluene (500 mL) was added TFA (312.7 g, 2.74 mmol) and purged with nitrogen three times. The reaction was warmed to 50−60 °C and stirred for 5 h. The reaction was cooled to 15−25 °C and washed with water (5 × 500 mL). The reaction was concentrated to around 200 mL and *n*-heptane (500 mL) were added dropwise, keeping the temperature between 20 and 30 °C. The resulting slurry was cooled to 0−10 °C, stirred for a further 3 h, and filtered. The cake was washed with *n*-heptane (2 × 200 mL) and dried under reduced pressure between 40 and 50 °C to afford **87** (MK-8286)

as an off-white solid (90 g, 97% yield, 99.0 LCAP%): ^{1}H NMR (CDCl$_3$, 400 MHz) δ 8.29 (t, J = 2.6 Hz, 1H), 8.06 (m, 2H), 7.90 (s, 1H), 7.63−7.84 (m, 3H), 7.38−7.47 (m, 4H), 6.06−6.11 (m, 3H), 4.96−5.27 (tt, J = 8.2 Hz, J = 8.2 Hz, 1H), 4.51−4.66 (m, 1H), 3.94−4.11 (s, 3H), 2.32−2.49 (m, 3.5H), 1.86−2.03 (m, 1H), 1.54 (m, 1H), 1.40 (m, 0.5H), 1.10 (m, 1H); ^{13}C NMR (CDCl$_3$, 100 MHz) δ 171.4, 171.3, 160.3, 160.1, 146.8, 146.7, 142.7, 142.6, 139.9, 138.3, 136.2, 132.5, 132.3, 132.2, 131.2, 130.2, 127.9, 125.3, 124.3, 122.4, 121.6, 118.8, 75.3, 75.1, 64.6, 64.2, 60.9, 60.6, 54.2, 53.7, 35.6, 35.4, 28.5, 20.5; HR-MS calcd for C$_{35}$H$_{26}$F$_9$N$_2$O$_5^+$ [M + H]$^+$ 725.1693, found 725.1702.

■ ASSOCIATED CONTENT

Ⓢ Supporting Information

The Supporting Information is available free of charge at https://pubs.acs.org/doi/10.1021/acs.jmedchem.1c00959.

Molecular formula strings (MFS) (CSV)

Full experimental procedures and characterization including illustrative schemes and tables, ^{1}H NMR spectra, equipment used, and experimental and ethical standards followed; Section 1: Chemistry, 1.1. Preparation of monocyclic oxazolidinone derivatives **1**−**37**, 1.2. Preparation of **38** via first-generation synthesis (Scheme 1) and second-generation synthesis (Scheme 2b,c), 1.3. Preparation of bicyclic derivatives **46**−**52**, 1.4. Preparation of bicyclic derivatives **38**, **73**−**107**, 1.5. Preparation of **87** via fully optimized synthesis (Scheme 3) and characterization of **87**; Section 2: In vitro and in vivo pharmacology; Section 3: Pharmacokinetics and Metabolism; Section 4: Safety assessment; and Section 5: Pharmaceutical properties of **87** (PDF)

■ AUTHOR INFORMATION

Corresponding Author

    Petr Vachal − *Merck & Co., Inc., Kenilworth, New Jersey, United States*; Phone: +1(908)740-3309; Email: petr_vachal@merck.com

Authors

    Joseph L. Duffy − *Merck & Co., Inc., Kenilworth, New Jersey, United States*

    Louis-Charles Campeau − *Merck & Co., Inc., Kenilworth, New Jersey, United States*

    Rupesh P. Amin − *Merck & Co., Inc., Kenilworth, New Jersey, United States*

    Kaushik Mitra − *Merck & Co., Inc., Kenilworth, New Jersey, United States*

    Beth Ann Murphy − *Merck & Co., Inc., Kenilworth, New Jersey, United States*

    Pengcheng P. Shao − *Merck & Co., Inc., Kenilworth, New Jersey, United States*

    Peter J. Sinclair − *Merck & Co., Inc., Kenilworth, New Jersey, United States*

    Feng Ye − *Merck & Co., Inc., Kenilworth, New Jersey, United States*

    Revathi Katipally − *Merck & Co., Inc., Kenilworth, New Jersey, United States*

    Zhijian Lu − *Merck & Co., Inc., Kenilworth, New Jersey, United States*

    Debra Ondeyka − *Merck & Co., Inc., Kenilworth, New Jersey, United States*

    Yi-Heng Chen − *Merck & Co., Inc., Kenilworth, New Jersey, United States*

Kake Zhao − *Merck & Co., Inc., Kenilworth, New Jersey, United States*

Wanying Sun − *Merck & Co., Inc., Kenilworth, New Jersey, United States*

Sriram Tyagarajan − *Merck & Co., Inc., Kenilworth, New Jersey, United States*

Jianming Bao − *Merck & Co., Inc., Kenilworth, New Jersey, United States*

Sheng-Ping Wang − *Merck & Co., Inc., Kenilworth, New Jersey, United States*

Josee Cote − *Merck & Co., Inc., Kenilworth, New Jersey, United States*

Concetta Lipardi − *Merck & Co., Inc., Kenilworth, New Jersey, United States*

Daniel Metzger − *Merck & Co., Inc., Kenilworth, New Jersey, United States*

Dennis Leung − *Merck & Co., Inc., Kenilworth, New Jersey, United States*

Georgy Hartmann − *Merck & Co., Inc., Kenilworth, New Jersey, United States*

Gordon K. Wollenberg − *Merck & Co., Inc., Kenilworth, New Jersey, United States*

Jian Liu − *Merck & Co., Inc., Kenilworth, New Jersey, United States*

Lushi Tan − *Merck & Co., Inc., Kenilworth, New Jersey, United States*

Yingju Xu − *Merck & Co., Inc., Kenilworth, New Jersey, United States*

Qinghao Chen − *Merck & Co., Inc., Kenilworth, New Jersey, United States*

Guiquan Liu − *WuXi AppTec, Shanghai 200131, China*

Robert O. Blaustein − *Merck & Co., Inc., Kenilworth, New Jersey, United States*

Douglas G. Johns − *Merck & Co., Inc., Kenilworth, New Jersey, United States*

Complete contact information is available at:
https://pubs.acs.org/10.1021/acs.jmedchem.1c00959

Notes

The authors declare the following competing financial interest(s): The authors declare no competing financial interest except for the following: at the time of completion of the work described in this manuscript, all authors were employees of Merck Sharp & Dohme Corp., a subsidiary of Merck & Co., Inc., Kenilworth, NJ, USA, and potentially own stock and/or hold stock options in Merck Sharp & Dohme Corp., a subsidiary of Merck & Co., Inc., Kenilworth, NJ, USA.

ABBREVIATIONS USED

ADME, absorption, distribution, metabolism, and excretion; AE, adverse effect; ALDO margin, aldosterone margin; AUC_N, area under the curve, normalized; BDC, bile-duct-cannulated; Boc$_2$O, di-*tert*-butyl decarbonate; BQL, below quantification limit; CE, cholesteryl ester; CETP, cholesteryl ester transfer protein; CHD, coronary heart disease; CPM, counts per minute; CYP, cytochrome P450; cyno-TG, cynomolgus transgenic mouse; DCM, dichloromethane; DDI, inhibition to avoid drug−drug interaction; DILI, drug-induced liver injury; DIO, diet-induced obese; DIPEA, *N,N*-diisopropylethylamine; DMAP, *N,N*-dimethylamino pyridine; DMF, *N,N*-dimethylformamide; E/H, ethyl acetate hexane ratio; ESI, electrospray ionization; EtOAc, ethyl acetate; HDL, high-density lipoprotein; HDL-C, high-density lipoprotein cholesterol; hERG, human ether-à-go-go-related gene; HPLC, isocratic high-performance liquid chromatography; ICD, Implantable Cardioverter Defibrillator; IVIVC, in vitro in vivo correlation; LDL, low-density lipoprotein; LDL-C, low-density lipoprotein cholesterol; LOQ, limit of quantification; MED, minimum efficacious dose, or minimum dose for maximum efficacy; MS, mass spectrometry; NFR, (natural flanking regions)-CETP mouse; NHP, non-human primate; NOEL, no-effect level; OATP, organic anion transporting polypeptides; PD, pharmacodynamic; PK, pharmacokinetic; PXR, pregnane X receptor; QD, once daily; QW, once weekly; RBF, round-bottom flask; RCM, ring-closing metathesis; ROP, research operating plan; SAR, structure−activity relationship; SI, Supporting Information; TEA, triethylamine; TFA, trifluoroacetic acid; TG, transgenic; THF, tetrahydrofuran; TLC, thin-layer chromatography; TPSA, total polar surface area; WEC, whole embryo culture; WH, Wistar-Han rat; WT, wild-type mouse

REFERENCES

(1) World Health Organization Cardiovascular Fact Sheet. https://www.who.int/news-room/fact-sheets/detail/cardiovascular-diseases-(cvds) (accessed July 4, 2021).

(2) National Cholesterol Education Program (NCEP). Expert Panel on Detection, Evaluation, and Treatment of High Blood Cholesterol in Adults (Adult Treatment Panel III). *Circulation* **2002**, *106*, 3143−3421.

(3) Nordestgaard, B. G.; Chapman, M. J.; Ray, K.; Boren, J.; Andreotti, F.; Watts, G. F.; Ginsberg, H.; Amarenco, P.; Catapano, A.; Descamps, O. S.; Fisher, E.; Kovanen, P. T.; Kuivenhoven, J. A.; Lesnik, P.; Masana, L.; Reiner, Z.; Taskinen, M.-R.; Tokgoezoglu, L.; Tybjaerg-Hansen, A. Lipoprotein(a) as a Cardiovascular Risk Factor: Current Status. *Eur Heart J.* **2010**, *31*, 2844−2853.

(4) Erqou, S.; Kaptoge, S.; Perry, P. L.; Angelantonio, E. D.; Thompson, A.; White, I. R.; Marcovina, S. M.; Collins, R.; Thompson, S. G.; Danesh, J. The Emerging Risk Factors Collaboration: Lipoprotein(a) Concentration and the Risk of Coronary Heart Disease, Stroke, and Nonvascular Mortality. *J. Am. Med. Assoc.* **2009**, *302*, 412.

(5) Boekholdt, S. M.; Arsenault, B. J.; Mora, S.; Pedersen, T. R.; LaRosa, J. C.; Nestel, P. J.; Simes, R. J.; Durrington, P.; Hitman, G. A.; Welch, K. M. A.; DeMicco, D. A.; Zwinderman, A. H.; Clearfield, M. B.; Downs, J. R.; Tonkin, A. M.; Colhoun, H. M.; Gotto, A. M.; Ridker, P. M.; Kastelein, J. J. P. Association of LDL Cholesterol, Non−HDL Cholesterol, and Apolipoprotein B Levels With Risk of Cardiovascular Events Among Patients Treated With Statins, A Meta-analysis. *J. Am. Med. Assoc.* **2012**, *307*, 1302−1309.

(6) Castelli, W. P. Cholesterol and Lipids in the Risk of Coronary Artery Disease–the Framingham Heart Study. *Can. J. Cardiol.* **1988**, *4*, 5A−10A.

(7) Yvan-Charvet, L.; Wang, N.; Tall, A. R. Role of HDL, ABCA1, and ABCG1 Transporters in Cholesterol Efflux and Immune Responses. *Arterioscler., Thromb., Vasc. Biol.* **2010**, *30*, 139−143.

(8) Barter, P. J.; Nicholls, S.; Rye, K.-A.; Anantharamaiah, G. M.; Navab, M.; Fogelman, A. M. Anti-inflammatory Properties of HDL. *Circ. Res.* **2004**, *95*, 764−772.

(9) Tall, A. R.; Yvan-Charvet, L.; Terasaka, N.; Pagler, T.; Wang, N. HDL, ABC Transporters, and Cholesterol Efflux: Implications for the Treatment of Atherosclerosis. *Cell Metab.* **2008**, *7*, 365−375.

(10) Tall, A. R. Cholesterol Efflux Pathways and Other Potential Mechanisms Involved in the Athero-protective Effect of High Density Lipoproteins. *J. Intern. Med.* **2008**, *263*, 256−273.

(11) Barter, P. J.; Puranik, R.; Rye, K.-A. New Insights into the Role of HDL as an Anti-inflammatory Agent in the Prevention of Cardiovascular Disease. *Curr. Cardiol. Rep.* **2007**, *9*, 493−498.

(12) Zhang, M.; Lei, D.; Peng, B.; Yang, M.; Zhang, L.; Charles, M. A.; Rye, K.-A.; Krauss, R. M.; Johns, D. G.; Ren, G. Assessing the Mechanisms of Cholesteryl Ester Transfer Protein Inhibitors. *Biochim. Biophys. Acta, Mol. Cell Biol. Lipids* **2017**, *1862*, 1606−1617.

(13) Banerjee, S.; De, A. Pathophysiology and Inhibition of Cholesteryl Ester Transfer Protein for the Prevention of Cardiovascular Diseases: An Update. *Drug Discovery Today* **2021**, DOI: 10.1016/j.drudis.2021.03.016.

(14) Fruchart, J.-C.; Nierman, M. C.; Stroes, E. S. G.; Kastelein, J. J. P.; Duriez, P. New Risk Factors for Atherosclerosis and Patient risk Assessment *Circulation* **2004**, *109* (suppl III), III-15−III-19 .

(15) For a comprehensive review, see Johns, D. G.; Duffy, J. L.; Fisher, T.; Hubbard, B. K.; Forrest, M. J. On- and Off-target Pharmacology of Torcetrapib: Current Understanding and Implications for the Structure Activity Relationships (SAR), Discovery, and Development of Cholesteryl Ester-Transfer Protein (CETP) Inhibitors. *Drugs* **2012**, *72*, 491−507.

(16) Merck & Co., Inc, Kenilworth, NJ USA. Merck Announces Results of REVEAL Outcomes Study of Anacetrapib, Investigational Medicine for Cardiovascular Disease. Press release, August 29, 2017. https://www.merck.com/news/merck-announces-results-of-reveal-outcomes-study-of-anacetrapib-investigational-medicine-for-cardiovascular-disease/ (accessed July 4, 2021).

(17) Recent follow-up studies of REVEAL trial participants have suggested that CHD risk continues to decrease, extending to 19% proportional risk reduction at a median 2.5 years post-treatment. However, the data therein has not been peer reviewed, hence the rationale for referring in this paper to the more conservative 9% reduction benefit cited in reference 16. https://www.ctsu.ox.ac.uk/files/research/reveal_aha_ptfu_slides_2019_11_12.pdf (accessed August 6, 2021).

(18) For an outstanding review of CETP clinical trials outcomes, see Taheri, H. T.; Filion, K. B.; Windle, S. B.; Reynier, P.; Eisenberg, M. J. Cholesteryl Ester Transfer Protein Inhibitors and Cardiovascular Outcomes: A Systematic Review and Meta-Analysis of Randomized Controlled Trials. *Cardiology* **2020**, *145*, 236−250.

(19) Blasi, E.; Bamberger, M.; Knight, D.; Engwall, M.; Wolk, R.; Winter, S.; Betts, A.; John-Baptiste, A.; Keiser, J. Effects of CP-532,623 and Torcetrapib, Cholesteryl Ester Transfer Protein Inhibitors, on Arterial Blood Pressure. *J. Cardiovasc. Pharmacol.* **2009**, *53*, 507−516.

(20) Schwartz, G. G.; Olsson, A. G.; Abt, M.; Ballantyne, C. M.; Barter, P. J.; Brumm, J.; Chaitman, B. R.; Holme, I. M.; Kallend, D.; Leiter, L. A.; Leitersdorf, E.; McMurray, J. J. V.; Mundl, H.; Nicholls, S. J.; Shah, P. K.; Tardif, J.-C.; Wright, R. S. dal-OUTCOMES Investigators Effects of Dalcetrapib in Patients with a Recent Acute Coronary Syndrome. *N. Engl. J. Med.* **2012**, *367*, 2089−2099.

(21) Niesor, E. J.; Magg, C.; Ogawa, N.; Okamoto, H.; von der Mark, E.; Matile, H.; Schmid, G.; Clerc, R. G.; Chaput, E.; Blum-Kaelin, D.; Huber, W.; Thoma, R.; Pflieger, P.; Kakutani, M.; Takahashi, D.; Dernick, G.; Maugeais, C. Modulating Choesteryl Ester Transfer Protein Activity Maintains Efficient pre-β-HDL Formation and Increases Reverse Cholesterol Transport. *J. Lipid Res.* **2010**, *51*, 3443−3454.

(22) Cannon, C. P.; Shah, S.; Dansky, H. M.; Davidson, M.; Brinton, E. A.; Gotto, A. M.; Stepanavage, M.; Liu, S. X.; Gibbons, P.; Ashraf, T. B.; Zafarino, J.; Mitchel, Y.; Barter, P. Determining the Efficacy, Tolerability and Safety of Anacetrapib in Patients with or at High Risk for Coronary Heart Disease". *N. Engl. J. Med.* **2010**, *363*, 2406−2415.

(23) Bowman, L.; Hopewell, J. C.; Chen, F.; Wallendszus, K.; Stevens, W.; Collins, R.; Wiviott, S. D.; Cannon, C. P.; Braunwald, E.; Sammons, E.; Landray, M. J. HPS3/TIMI55−REVEAL Collaborative Group Effects of Anacetrapib in Patients with Athero-sclerotic Vascular Disease. *N. Engl. J. Med.* **2017**, *377*, 1217−1227.

(24) Dalcor Pharmaceuticals press release Jan. 27, 2020: https://www.dalcorpharma.com/news-cp/dalcor-announces-dal-gene-trial-to-continue-as-planned-following-interim-futility-analysis/ (accessed July 4, 2021).

(25) Lincoff, A. M.; Nicholls, S. J.; Riesmeyer, J. S.; Barter, P. J.; Brewer, H. B.; Fox, K. A. A.; Gibson, C. M.; Granger, C.; Menon, V.; Montalescot, G.; Rader, D.; Tall, A. R.; McErlean, E.; Wolski, K.; Ruotolo, G.; Vangerow, B.; Weerakkody, G.; Goodman, S. G.; Conde, D.; McGuire, D. K.; Nicolau, J. C.; Leiva-Pons, J. L.; Pesant, Y.; Li, W.; Kandath, D.; Kouz, S.; Tahirkheli, N.; Mason, D.; Nissen, S. E. ACCELERATE Investigators. Evacetrapib and Cardiovascular Outcomes in High-Risk Vascular Disease. *N. Engl. J. Med.* **2017**, *376*, 1933−1942.

(26) Hovingh, G. K.; Kastelein, J. J. P.; Van Deventer, S. J. H.; Round, P.; Ford, J.; Saleheen, D.; Rader, D. J.; Brewer, H. B.; Barter, P. J. Cholesterol Ester transfer Protein Inhibition by TA-8995 in Patients with Mild Dyslipidaemia (TULIP): A Randomised, Double-Blind, Placebo-Controlled Phase 2 Trial. *Lancet* **2015**, *386*, 452−460.

(27) New Amsterdam Pharma press release Jan. 14, 2021: https://www.newamsterdampharma.com/new-amsterdam-pharma-completes-196m-series-a-funding (accessed July 4, 2021).

(28) Gotto, A. M., Jr.; Kher, U.; Chatterjee, M. S.; Liu, Y.; Li, X. S.; Vaidya, S.; Cannon, C. P.; Brinton, E. A.; Moon, J. E.; Shah, S.; Dansky, H. M.; Mitchel, Y.; Barter, P. DEFINE Investigators. Lipids, Safety Parameters, and Drug Concentrations after an Additional 2 Years of Treatment with Anacetrapib in the DEFINE Study. *J. Cardiovasc. Pharmacol. Ther.* **2014**, *19*, 543−549.

(29) Gotto, A. M., Jr.; Cannon, C. P.; Li, X. S.; Vaidya, S.; Kher, U.; Brinton, E. A.; Davidson, M.; Moon, J. E.; Shah, S.; Dansky, H. M.; Mitchel, Y.; Barter, P. DEFINE Investigators. Evaluation of Lipids, Drug Concentration, and Safety Parameters Following Cessation of Treatment with the Cholesteryl Ester Transfer Protein Inhibitor Anacetrapib in Patients with or at High Risk for Coronary Heart Disease. *Am. J. Cardiol.* **2014**, *113*, 76−83.

(30) Radeau, T.; Lau, P.; Robb, M.; McDonnell, M.; McPherson, R.; Ailhaud, G. Cholesteryl Ester Transfer Protein (CETP) mRNA Abundance in Human Adipose Tissue: Relationship to Cell Size and Membrane Cholesterol Content. *J. Lipid Res.* **1995**, *36*, 2552−2561.

(31) Hartmann, G.; Kumar, S.; Johns, D.; Giheyas, F.; Gutstein, D.; Shen, X.; Burton, A.; Lederman, H.; Lutz, R.; Jackson, T.; Chavez-Eng, C.; Mitra, K. Disposition into Adipose Tissue Determines Accumulation and Elimination Kinetics of the Cholesteryl Ester Transfer Protein Inhibitor Anacetrapib in Mice. *Drug Metab. Dispos.* **2016**, *44*, 428−434.

(32) Gutstein, D.; Krishna, R.; Johns, D.; Mitra, K.; Hartman, G.; Hamilton, V.; Cote, J.; Giheyas, F.; Shah, S.; Mitchel, Y. Observed Long Plasma Terminal Half-life of Anacetrapib (ANA) is Associated with Adipose Deposition: Characterization of Plasma and Adipose Pharmacokinetics (PK) in Mice and Humans. Abstracts of Papers, ACPT 2015 Annual Meeting, New Orleans, LA, March 3−7, American Society for Clinical Pharmacology and Therapeutics: Alexandria, VA, 2015; PI-050.

(33) Krishna, R.; Garg, A.; Jin, B.; Keshavarz, S. S.; Bieberdorf, F. A.; Chodakewitz, J.; Wagner, J. A.; et al. Assessment of the CYP3A-Mediated Drug Interaction Potential of Anacetrapib, a Potent Cholesteryl Ester Transfer Protein (CETP) Inhibitor, in Healthy Volunteers. *J. Clin. Pharm.* **2009**, *49*, 80−87.

(34) Monroe, J. J.; Tanis, K. Q.; Podtelezhnikov, A. A.; Nguyen, T.; Machotka, S. V.; Lynch, D.; Evers, R.; Palamanda, J.; Miller, R. R.; Pippert, T.; Cabalu, T. D.; Johnson, T. E.; Aslamkhan, A. G.; Kang, W.; Tamburino, A. M.; Mitra, K.; Agrawal, N. G. B.; Sistare, F. D. Application of a Rat Liver Drug Bioactivation Transcriptional Response Assay Early in Drug Development That Informs Chemically Reactive Metabolite Formation and Potential for Drug-induced Liver Injury. *Toxicol. Sci.* **2020**, *177*, 281−299.

(35) Wang, X.; Li, W.; Hao, L.; Xie, H.; Hao, C.; Liu, C.; Li, W.; Xiong, X.; Zhao, D. The Therapeutic Potential of CETP Inhibitors: A Patent Review. *Expert Opin. Ther. Pat.* **2018**, *28*, 331−340.

(36) Wilson, J. E.; Kurukulasuriya, R.; Reibarkh, M.; Reiter, M.; Zwicker, A.; Zhao, K.; Zhang, F.; Anand, R.; Colandrea, V. J.; Cumiskey, A.-M.; Crespo, A.; Duffy, R. A.; Murphy, B. A.; Mitra, K.; Johns, D. G.; Duffy, J. L.; Vachal, P. Discovery of Novel Indoline Cholesterol Ester Transfer Protein Inhibitors (CETP) through a Structure-Guided Approach. *ACS Med. Chem. Lett.* **2016**, *7*, 261−265.

(37) Ertl, P.; Rohde, B.; Selzer, P. Fast Calculations of Molecular Polar Surface Area as a Sum of Fragment-based Contributions and its Application to the Prediction of Drug Transport Properties. *J. Med. Chem.* **2000**, *43*, 3714−3717.

(38) Krishna, R.; Garg, A.; Panebianco, D.; Cote, J.; Bergman, A. J.; Van Hoydonck, P.; Laethem, T.; Van Dyck, K.; Chen, J.; Chavez-Eng, C.; Archer, L.; Lutz, R.; Hilliard, D.; Snyder, K.; Jin, B.; Van Bortel, L.; Lasseter, K. C.; Al-Huniti, N.; Dykstra, K.; Gottesdiener, K.; Wagner, J. A.; et al. Multiple-Dose Pharmacodynamics and Pharmacokinetics of Anacetrapib, a Potent Cholesteryl Ester Transfer Protein (CETP) Inhibitor, in Healthy Subjects. *Clin. Pharmacol. Ther.* **2008**, *84*, 679−683.

(39) Krishna, R.; Bergman, A. J.; Green, M.; Dockendorf, M. F.; Wagner, J. A.; Dykstra, K. Model-Based Development of Anacetrapib, a Novel Cholesteryl Ester Transfer Protein Inhibitor. *AAPS J.* **2011**, *13*, 179−190.

(40) Krishna, R.; Bergman, A. J.; Jin, B.; Garg, A.; Roadcap, B.; Chiou, R.; Dru, J.; Cote, J.; Laethem, T.; Wang, R. W.; Didolkar, V.; Vets, E.; Gottesdiener, K.; Wagner, J. A. Assessment of the CYP3A4-Mediated Drug Interaction Potential of Anacetrapib, a Potent Cholesteryl Ester Transfer Protein (CETP) Inhibitor, in Healthy Volunteers. *J. Clin. Pharmacol.* **2009**, *49*, 80−87.

(41) Luo, G.; Guenthner, T.; Gan, L.-S.; Humphreys, W. G. CYP3A4 Induction by Xenobiotics: Biochemistry, Experimental Methods and Impact on Drug Discovery and Development. *Curr. Drug Metab.* **2004**, *5*, 483−505.

(42) Hartmann, G.; Kumar, S.; Johns, D.; Gheyas, F.; Gutstein, D.; Shen, X.; Burton, A.; Lederman, H.; Lutz, R.; Jackson, T.; Chavez-Eng, C.; Mitra, K. Disposition into Adipose Tissue Determines Accumulation and Elimination Kinetics of the Cholesteryl Ester Transfer Protein Inhibitor Anacetrapib in Mice. *Drug Metab. Dispos.* **2016**, *44*, 428−434.

(43) Krishna, R.; Giheyas, F.; Liu, Y.; Hagen, D. R.; Walker, B.; Chawla, A.; Cote, J.; Blaustein, R. O.; Gutstein, D. E. Chronic Administration of Anacetrapib is Associated with Accumulation in Adipose and Slow Elimination. *Clin. Pharmacol. Ther.* **2017**, *102*, 832−840.

(44) Ali, A.; Duffy, J. L. Case Histories in Recent Drug Discovery: Anacetrapib. In *Comprehensive Medicinal Chemistry III*; Rotella, D.; Chackalamannil, S.; Ward, S., Eds.; Elsevier: NY, 2017; pp 284−307.

(45) Lu, Z.; Napolitano, J. B.; Theberge, A.; Ali, A.; Hammond, M. L.; Tan, E.; Tong, X.; Xu, S. S.; Latham, M. J.; Peterson, L. B.; Anderson, M. S.; Eveland, S. S.; Guo, O.; Hyland, S. A.; Milot, D. P.; Chen, Y.; Sparrow, C. P.; Wright, S. D.; Sinclair, P. J. Design of a Novel Class of Biphenyl CETP Inhibitors. *Bioorg. Med. Chem. Lett.* **2010**, *20*, 7469−7472.

(46) Smith, C. J.; Ali, A.; Hammond, M. L.; Li, H.; Lu, Z.; Napolitano, J.; Taylor, G. E.; Thompson, C. F.; Anderson, M. S.; Chen, Y.; Eveland, S. S.; Guo, O.; Hyland, S. A.; Milot, D. P.; Sparrow, C. P.; Wright, S. D.; Cumiskey, A.-M.; Latham, M.; Peterson, L. B.; Rosa, R.; Pivnichny, J. V.; Tong, X.; Xu, S. S.; Sinclair, P. J. Biphenyl-substituted Oxazolidinones as Cholesteryl Ester Transfer Protein Inhibitors: Modifications of the Oxazolidinone Ring Leading to the Discovery of Anacetrapib. *J. Med. Chem.* **2011**, *54*, 4880−4895.

(47) Eveland, S. S.; Milot, D. P.; Guo, O.; Chen, Y.; Hyland, S. A.; Peterson, L. B.; Jezequel-Sur, S.; O'Donnell, G. T.; Zuck, P. D.; Ferrer, M.; Strulovici, B.; Wagner, J. A.; Tanaka, W. K.; Hilliard, D. A.; Laterza, O.; Wright, S. D.; Sparrow, C. P.; Anderson, M. S. High-Precision Fluorogenic Cholesteryl Ester Transfer Protein Assay Compatible with Animal Serum and 3456-well Assay Technology. *Anal. Biochem.* **2007**, *368*, 239−249.

(48) Inhibition of hERG was measured by binding displacement of 35S-labeled MK-0499, a known hERG blocker, and inhibition of this potassium channel is associated with potentially fatal long QT syndrome: Recanatini, M.; Poluzzi, E.; Masetti, M.; Cavalli, A.; De Ponti, F. QT Prolongation Through hERG K+ Channel Blockade: Current Knowledge and Strategies for the Early Prediction During Drug Development. *Med. Res. Rev.* **2005**, *25*, 133−166.

(49) Forrest, M. J.; Bloomfield, D.; Briscoe, R. J.; Brown, P. N.; Cumiskey, A.-M.; Ehrhart, J.; Hershey, J. C.; Keller, W. J.; Ma, X.; McPherson, H. E.; Messina, E.; Peterson, L. B.; Sharif-Rodriguez, W.; P K S Siegl, P. K. S.; Sinclair, P. J.; Sparrow, C. P.; Stevenson, A. S.; Sun, S.-Y.; Tsai, C.; Vargas, H.; Walker, M., III; West, S. H.; White, V.; Woltmann, R. F. Torcetrapib-Induced Blood Pressure Elevation is Independent of CETP Inhibition and is Accompanied by Increased Circulating Levels of Aldosterone. *Br. J. Pharmacol.* **2008**, *154*, 1465−1473.

(50) McLaren, D. G.; Previs, S. F.; Phair, R. D.; Stout, S. J.; Xie, D.; Chen, Y.; Salituro, G. M.; Xu, S. S.; Castro-Perez, J. M.; Opiteck, G. J.; Akinsanya, K. O.; Cleary, M. A.; Dansky, H. M.; Johns, D. G.; Roddy, T. P. Evaluation of CETP Activity in vivo Under non-Steady-State Conditions: Influence of Anacetrapib on HDL-TG Flux. *J. Lipid Res.* **2016**, *57*, 398−409.

(51) Jiang, X. C.; Agellon, L. B.; Walsh, A.; Breslow, J. L.; Tall, A. Dietary Cholesterol Increases Transcription of the Human Cholesteryl Ester Transfer Protein Gene in Transgenic Mice. Dependence on Natural Flanking Sequences. *J. Clin. Invest.* **1992**, *90*, 1290−1295.

(52) Johns, D. G.; Duffy, J. L.; Fisher, T.; Hubbard, B. K.; Forrest, M. J. On- and Off-Target Pharmacology of Torcetrapib. *Drugs* **2012**, *72*, 491−507.

(53) Kumar, A.; Patel, D. R.; Brennan, D. M.; Wolski, K. E.; Lincoff, A. M.; Ruotolo, G.; McErlean, E.; Weerakkody, G.; Riesmeyer, J. S.; Nicholls, S. J.; Nissen, S. E.; Menon, V. Plasma Aldosterone Levels Are Not Associated with Cardiovascular Events Among Patients with High-Risk Vascular Disease: Insights from the ACCELERATE Trial. *J. Am. Heart Assoc.* **2019**, *8*, No. e13790.

(54) Ranalletta, M.; Bierilo, K. K.; Chen, Y.; Milot, D.; Chen, Q.; Tung, E.; Houde, C.; Elowe, N. H.; Garcia-Calvo, M.; Porter, G.; Eveland, S.; Frantz-Wattley, B.; Kavana, M.; Addona, G.; Sinclair, P.; Sparrow, C.; O'Neill, E. A.; Koblan, K. S.; Sitlani, A.; Hubbard, B.; Fisher, T. S. Biochemical Characterization of Cholesteryl Ester Transfer Protein Inhibitors. *J. Lipid Res.* **2010**, *51*, 2739−2752.

(55) Shitara, Y. Clinical Importance of OATP1B1 and OATP1B3 in DrugDrug Interactions. *Drug Metab. Pharmacokinet.* **2011**, *26*, 220−227.

(56) Liu, J.; Shao, P. P.; Guiadeen, D.; Krikorian, A.; Sun, W.; Deng, Q.; Cumiskey, A.-M.; Duffy, R. A.; Murphy, B. A.; Mitra, K.; Johns, D. G.; Duffy, J. L.; Vachal, P. Cholesteryl Ester Transfer Protein (CETP) Inhibitors Based on Cyclic Urea, Bicyclic Urea and Bicyclic Sulfamide Cores. *Bioorg. Med. Chem. Lett.* **2021**, *32*, 127668−127676.

(57) Liu, G.; Cogan, D. A.; Ellman, J. A. Catalytic Asymmetric Synthesis of tert-Butanesulfinamide. Application to the Asymmetric Synthesis of Amines. *J. Am. Chem. Soc.* **1997**, *119*, 9913−9914.

(58) Tu, Y.; Wang, Z.-X.; Shi, Y. An Efficient Asymmetric Epoxidation Method for Trans-Olefins Mediated by a Fructose-Derived Ketone. *J. Am. Chem. Soc.* **1996**, *118*, 9806−9807.

(59) Stanley, L. M.; Bai, C.; Ueda, M.; Hartwig, J. F. Iridium-Catalyzed Kinetic Asymmetric Transformations of Racemic Allylic Benzoates. *J. Am. Chem. Soc.* **2010**, *132*, 8918−8920.

(60) Raskatov, J. A.; Spiess, S.; Gnamm, C.; Brödner, K.; Rominger, F.; Helmchen, G. Ir-Catalysed Asymmetric Allylic Substitutions with Cyclometalated (Phosphoramidite)Ir Complexes—Resting States, Catalytically Active (π-Allyl)Ir Complexes and Computational Exploration. *Chem. − Eur. J.* **2010**, *16*, 6601−6615.

(61) Schrock, R. R. Multiple Metal−Carbon Bonds for Catalytic Metathesis Reactions (Nobel Lecture). *Angew. Chem., Int. Ed.* **2006**, *45*, 3748−3759.

(62) *Handbook of Metathesis*; Grubbs, R. H., Ed.; Wiley-VCH: Weinheim, 2003.

(63) Zhan, Z.-Y. J. Recyclable Ruthenium Catalysts for Metathesis Reactions. U.S. patent application US2007/0043180A1.

(64) Birch, A.; Williamson, D. H. Homogeneous Hydrogenation Catalysts in Organic Synthesis. *Org. React.* **1976**, *24*, 1−186.

(65) For a detailed discussion of the OATP inhibition by **87** in vitro, refer to preclinical profiling section.

(66) Bruno, N. C.; Tudge, M. T.; Buchwald, S. L. Design and Preparation of New Palladium Precatalysts for C−C and C−N Cross-Coupling Reactions. *Chem. Sci.* **2013**, *4*, 916−920.

(67) For a analogous comprehensive study of anacetrapib, see: Johns, D. G.; LeVoci, L.; Krsmanovic, M.; Lu, M.; Hartmann, G.; Xu, S.; Wang, S.-P.; Chen, Y.; Bateman, T.; Blaustein, R. O. Anacetrapib Distributes into Adipocyte Lipid Droplet. *Drug Metab. Dispos.* **2019**, *47*, 227−233.

(68) Cannady, E. A.; Wang, M.-D.; Friedrich, S.; Rehmel, J. L. F.; Yi, P.; Small, D. S.; Zhang, W.; Suico, J. G. Evacetrapib: In vitro and Clinical Disposition, Metabolism, Excretion, and Assessment of Drug Interaction Potential with Strong CYP3A and CYP2C8 Inhibitors. *Pharmacol. Res. Perspect.* **2015**, *3*, No. e00179.

(69) Dalvie, D.; Chen, W.; Zhang, C.; Vaz, A. D.; Smolarek, T. A.; Cox, L. M.; Lin, J.; Obach, R. S. Pharmacokinetics, Metabolism, and Excretion of Torcetrapib, a Cholesteryl Ester Transfer Protein Inhibitor, in Humans. *Drug Metab. Dispos.* **2008**, *36*, 2185−2198.

(70) Refer to Supporting Information section for a full data set of the CV evaluation of **87** as well as its comparison to key clinical CETP inhibitors.

(71) The genes in this signature were selected previously using model compounds associated with drug-induced liver injury in the clinic. Approximately 40 genes comprise the signature and are primarily involved in oxidative stress and proteasome pathways; an algorithm has been developed to summarize their response: Sistare, F. D.; Mattes, W. B.; Le Cluyse, E. L. The Promise of New Technologies to Reduce, Refine, or Replace Animal Use while Reducing Risks of Drug Induced Liver Injury in Pharmaceutical Development. *ILAR J.* **2016**, *57*, 186−211.

(72) Green, M. L.; Lebron, J. A.; Tanis, K. Q.; Redfern, B. G.; Zhu, L.; Yu, Y.; Wang, E.; Kaczor, A. R.; Wysoczanski, E.; Chen, F.; Raymond, C. S.; Mattson, B.; Sistare, F. D.; DeGeorge, J. J. Use of Alternative Developmental Toxicity Assays to Assess Teratogenicity Potential of Pharmaceuticals. *Appl. In Vitro Toxicol.* **2018**, *4*, 44−53.

(73) Krishna, R.; Garg, A.; Panebianco, D.; Cote, J.; Bergman, A. J.; Van Hoydonck, P.; Laethem, T.; Van Dyck, K.; Chen, J.; Chavez-Eng, C.; Archer, L.; Lutz, R.; Hilliard, D.; Snyder, K.; Jin, B.; Van Bortel, L.; Lasseter, K. C.; Al-Huniti, N.; Dykstra, K.; Gottesdiener, K.; Wagner, J. A. Single-Dose Pharmacokinetics and Pharmacodynamics of Anacetrapib, a Potent Cholesteryl Ester Transfer Protein (CETP) Inhibitor, in Healthy Subjects. *J. Clin. Pharmacol.* **2009**, *68*, 535−545.